

GL01404

M 2

Society of Petroleum Engineers of AIME
Fidelity Union Building
Dallas 1, Texas

SUBJ
GPHYS
Log
NDI

PAPER
NUMBER 1300-G

UNIVERSITY OF UTAH
RESEARCH INSTITUTE
EARTH SCIENCE LAB.

THIS IS A PREPRINT — SUBJECT TO CORRECTIONS

NEW DEVELOPMENTS IN INDUCTION AND SONIC LOGGING

By

M. P. Tixier, Member AIME, Schlumberger Well Surveying Corporation, Houston, Texas
R. P. Alger, Member AIME, Schlumberger Well Surveying Corporation, Houston, Texas
D. R. Tanguy, Schlumberger Well Surveying Corporation, Houston, Texas

SPE-1300-G
1959

Publication Rights Reserved

This paper is to be presented at the 34th Annual Fall Meeting of the Society of Petroleum Engineers of the American Institute of Mining, Metallurgical and Petroleum Engineers in Dallas, October 4-7, 1959, and at the Fall Meeting of the Los Angeles Basin Petroleum Section of the AIME in Pasadena, October 22-23, 1959, and is considered the property of the Society of Petroleum Engineers. Permission to publish is hereby restricted to an abstract of not more than 300 words, with no illustrations, unless the paper is specifically released to the press by the Society Publications Committee Chairman or the Executive Secre-

tary on his behalf. Such abstract should contain appropriate, conspicuous acknowledgment. Publication elsewhere after publication in Journal of Petroleum Technology is granted on request, providing proper credit is given that publication and the original presentation of the paper.

Discussion of this paper is invited. Three copies of any discussion should be sent to the Society of Petroleum Engineers office; it will be presented at the above meetings with the paper and considered for publication in Journal of Petroleum Technology.

ABSTRACT

1) In the combination induction-electrical log used at present in the field, the induction logging tool is appropriate for the investigation of moderately invaded formations. A new induction sonde with a radius of investigation about twice as large has been recently designed for the case of deep invasion; it has the same vertical resolution as the old one, so that thin beds are defined as accurately as before. The characteristics of the new tool are described, the corresponding interpretation charts are given, and field examples are discussed.

2) The design of the sonic logging tool has been modified in order to improve the calibration and the reliability. The fact that porosity can be accurately recorded by means of the sonic log has prompted new interpretation procedures for saturation estimation, wherein the data concerning the various permeable beds in a given well are correlated.

a) One approach consists in plotting transit

time versus true resistivity with an appropriate scale. With this approach saturations can be estimated conveniently, even in cases where formation water resistivity is not well known.

b) In another approach, a comparison is made of the values of the formation waters computed from the resistivity and sonic logs. Using the concept of continuity, this procedure makes possible a quick determination of zones of saturation in shaly sands and/or in case of appreciable variations of formation salinities with depth.

c) It has been found, furthermore, that the comparison of the porosity from the sonic log with the apparent porosity computed from a short investigation resistivity log may reveal in many cases the presence of residual oil and thus detect potentially productive formations; this procedure is valuable when the true formation resistivity and the resistivity of the formation water are in doubt.

INTEGRATED RADIAL GEOMETRICAL FACTOR

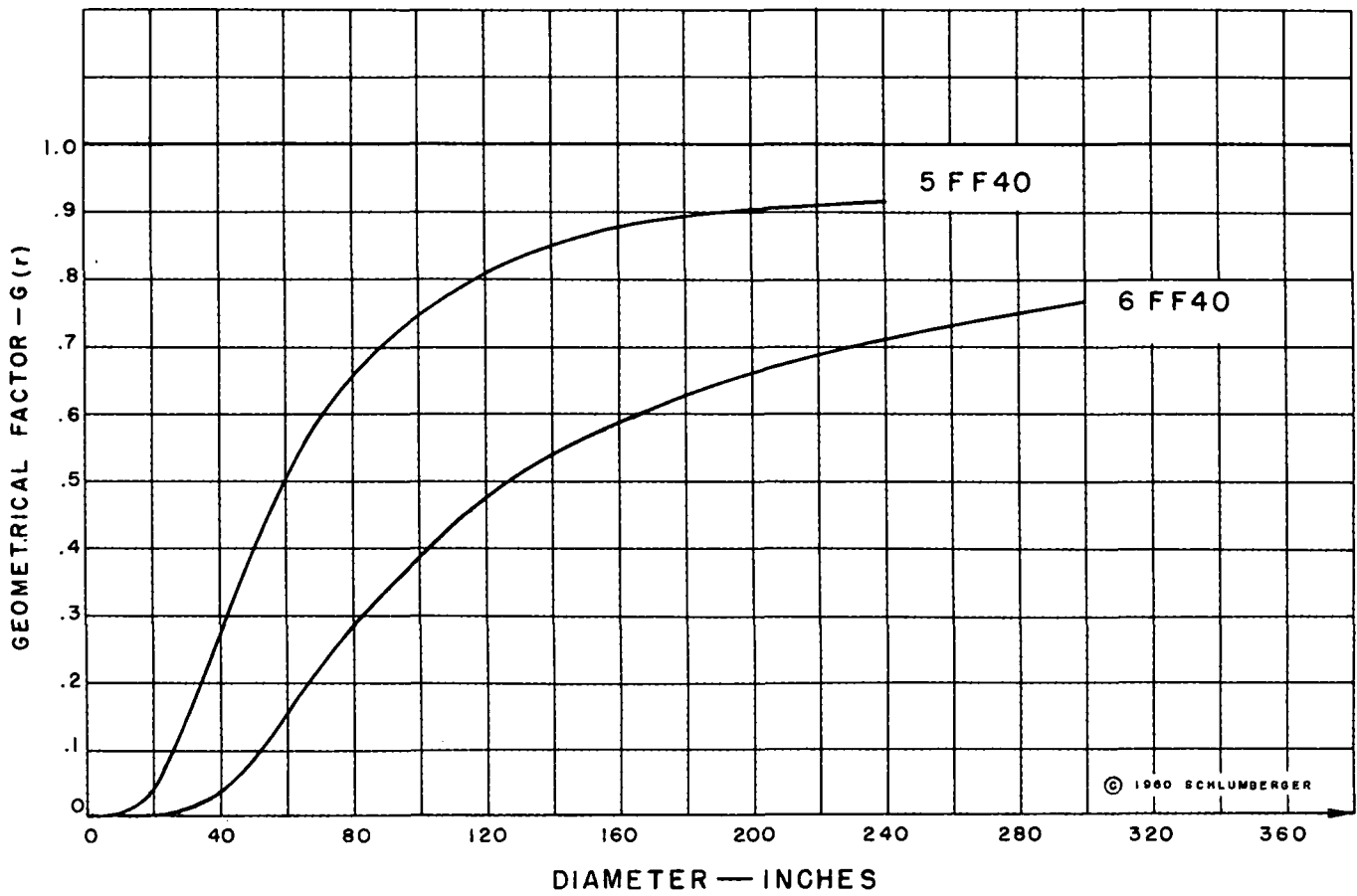


FIG. 1

NEW DEVELOPMENTS IN INDUCTION AND SONIC LOGGING

By

M. P. Tixier*, R. P. Alger**, and D. R. Tanguy***

INTRODUCTION

During the past year the efficiency of log interpretation has been vastly improved. The improvements have largely resulted from the introduction of a deep-investigation induction device, and from the application of new interpretation techniques that utilize sonic versus resistivity readings. Since the new interpretation techniques depend, in part, upon good values of true formation resistivity, we will discuss the new induction log under Part I. The sonic interpretation techniques will be studied under Part II.

PART I — THE DEEP INVESTIGATION INDUCTION LOG

Early this year the 6FF40 induction equipment was introduced in the field. This device was designed for a better approach to true formation resistivities in deeply invaded zones. The greatly improved radial investigation of the 6FF40 equipment has been achieved without any sacrifice of vertical resolution.

The first combination induction-electrical log, the 5FF40, was introduced as a standard tool in 1956 for the logging of wells drilled with fresh muds. The tool has received wide industry acceptance in the United States. The 5FF40 induction log has a radial investigation sufficient to overcome average depths of mud filtrate invasion. As an example, at 5d invasion the 5FF40 induction log will read about $1.4 R_0$ in a water sand where $R_{xo} = 10R_t$. At 10d invasion such induction log would read $2.45 R_0$ in the same water sand. In either case the effects of invasion would not be sufficiently great to cause a water sand to be mistaken for a shale-free oil- or gas-producing zone.

Some formations, however, invade deeply — in excess of 10d. Such water zones can easily be mistaken for oil- or gas-saturated sands unless a porosity balance can clearly make the distinction. It is for these deeply invaded formations that the 6FF40 was developed.

CHARACTERISTICS OF THE 6FF40

A. Investigation Characteristics

In order to describe the comparative responses of the 5FF40 and 6FF40 devices, it is convenient to consider their radial and vertical investigation characteristics.

* Member AIME Schlumberger Well Surveying Corporation, Houston, Texas.
** Member AIME Schlumberger Well Surveying Corporation, Houston, Texas.
*** Schlumberger Well Surveying Corporation, Houston, Texas.

The radial characteristic can be defined as representing the geometrical factor of the medium limited by a coaxial cylinder when the diameter of this cylinder increases from zero to infinity.

Fig. 1 shows the plot of the radial geometrical factor for the standard induction tool (5FF40) and for the deep investigation tool (6FF40).

This figure clearly shows the investigation of the two tools. As an example, 50% of the signal comes from beyond a diameter of 60" for the 5FF40, whereas the same per cent of the signal comes from beyond a diameter of 128" for the 6FF40.

It is interesting to calculate the effect of the invaded zone for the two tools for the case of deep invasion.

1. For $D_i = 10d$ or $D_i = 80''$

$$R_{xo} = 10; R_t = 1. \quad 1/R_a = G_{xo}/R_{xo} + G_t/R_t.$$

$$\text{For the 5FF40, } 1/R_a = .66/10 + .34/1 \text{ or } R_a = 10/4.06 = 2.45.$$

$$\text{For the 6FF40, } 1/R_a = .28/10 + .72/1 \text{ or } R_a = 10/7.48 = 1.34.$$

This shows that for a 10d invasion the deep investigation induction reads within 35% of the true resistivity with a contrast of 10 between the invaded zone and the virgin formation.

2. For $D_i = 20d$ or $D_i = 160''$

$$R_{xo} = 10; R_t = 1.$$

$$\text{For the 5FF40, } 1/R_a = .87/10 + .13/1 \text{ or } R_a = 10/2.17 = 4.6.$$

$$\text{For the 6FF40, } 1/R_a = .58/10 + .42/1 \text{ or } R_a = 10/4.78 = 2.08.$$

Thus, in a very deep invasion, such as 20d, and with a large contrast of 10 between the invaded zone and the virgin formation, the deep induction reads half the resistivity given by the standard induction log. A

HOLE EFFECT

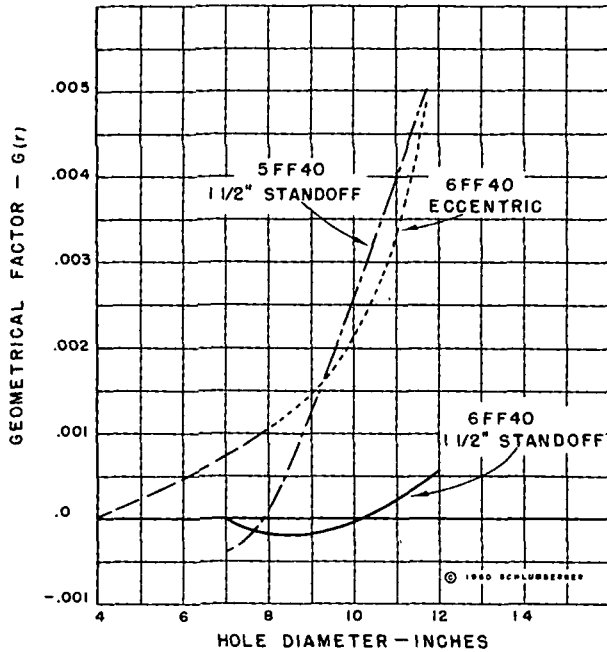


Figure 2

water sand cannot be easily taken as an oil or gas sand with such a tool unless the invasion is much greater than $20d$.

B. Effect of the Mud Column

This effect has been investigated on a full-scale laboratory model. A cylindrical vertical pipe, made of insulating material and filled with water, simulated the borehole. Since the pipe was surrounded by air, the borehole signals were measured under the conditions of an infinitely resistive formation.

On Fig. 2 two curves are given, one corresponding to the tool in an eccentric position in the hole and the other when the tool is maintained $1\frac{1}{2}$ " from the wall of the hole. Characteristics of both the 5FF40 and the 6FF40 are pictured. It is clearly shown that the hole effect for the 6FF40 is less than that for the 5FF40 when the $1\frac{1}{2}$ -inch standoffs are used.

C. Vertical Resolution

The vertical characteristic can be defined as representing the geometrical factor of a horizontal bed with the sonde centered in the bed and the thickness of the bed increasing from zero to infinity.

Fig. 3 shows the plots of the standard induction tool (5FF40) and of the deep investigation tool (6FF40). The thickness of the bed under study is shown on abscissa. The geometrical factors for two different shoulder resistivities (1 ohm and 4 ohms) are illustrated. The contribution of skin effect is incorporated in the measurements for both the

5FF40 and the 6FF40. It is clear that the geometrical factors of the two devices are very similar; consequently, their vertical resolution is the same, and the bed thickness correction published for the 5FF40 is applicable to the 6FF40.

Plots made for other values of shoulder resistivity have led to similar conclusions.

THEORETICAL DEPARTURE CURVES

Like the standard induction, the deep investigation tool is to be run with the short normal in fresh muds. Departure curves have been built for this combination. These curves were determined with the following assumptions:

1. The formations are so thick that the induction log and the 16" normal readings are not affected by adjacent formations.
2. The annulus does not exist, or has a negligible effect. On this point, many studies have been made and will be reported elsewhere.
3. The invaded zone is a homogeneous medium of resistivity R_i and diameter D_i .
4. The hole diameter is equal to 8".

Fig. 4 was calculated in a manner similar to the theoretical chart of the 5FF40.¹ For greater practicability the ordinate is now R_{18c}/R_{1Lc} . Such value should cut the curves R_{x0}/R_t in two points (except for invasion of $7d$ to $8d$), one point corresponding to deep invasion and the other to shallow invasion. It is easy to determine R_{x0}/R_t in a water sand since this ratio is equal to R_{mt}/R_w . The intersections define R_{x0}/R_{18c} in abscissa. Dividing such abscissae values into R_{x0}/R_t determines R_{18c}/R_t and thus R_t .

All the discussion published for the theoretical chart of the 5FF40 applies to Fig. 4.

Further studies of the form of the invasion front and of the annulus may require modification of this chart.

PRACTICAL INTERPRETATION CHART AND APPLICATION

As was done for the 5FF40, a practical interpretation chart was made for the combined short normal, 6FF40, and SP curve. All the discussion made for the practical interpretation of the 5FF40 in Reference 1 applies to Fig. 5. Further studies of the form of the invasion front and of the annulus may require modification of this chart.

FIELD EXAMPLES

Fig. 6 illustrates a comparison between the 5FF40 and the 6FF40 in a water-bearing formation in East Texas. This deeply invaded formation was first surveyed with the 5FF40 and two weeks later with the 6FF40. The invasion in most places is deeper than $20d$, and in those intervals the 6FF40 shows less than half the value read by the 5FF40. For comparison a lateral curve of 24' spacing is also shown; its values are similar to those of the 6FF40 in many intervals.

¹References given at end of paper.

INTEGRATED VERTICAL GEOMETRICAL FACTOR

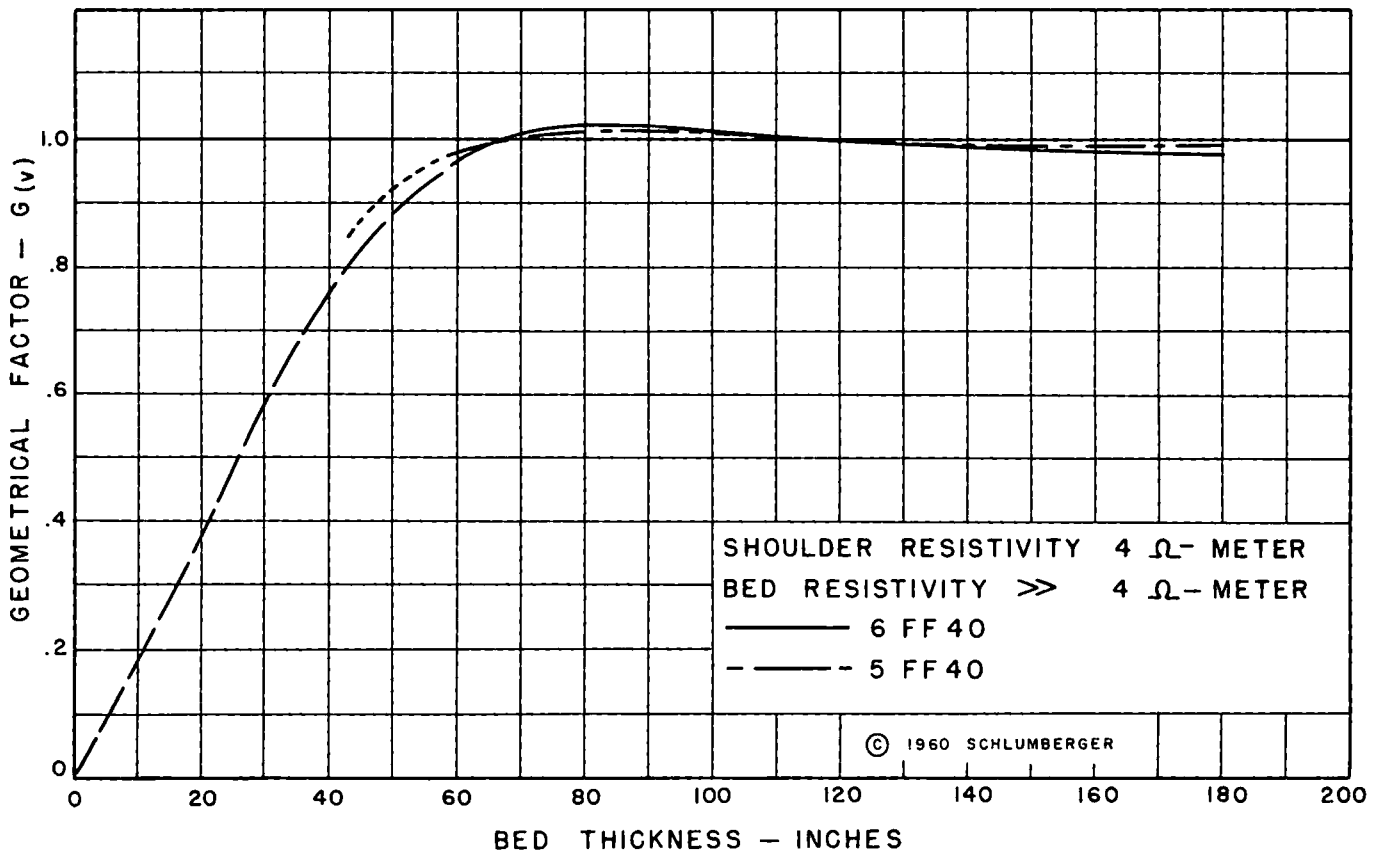
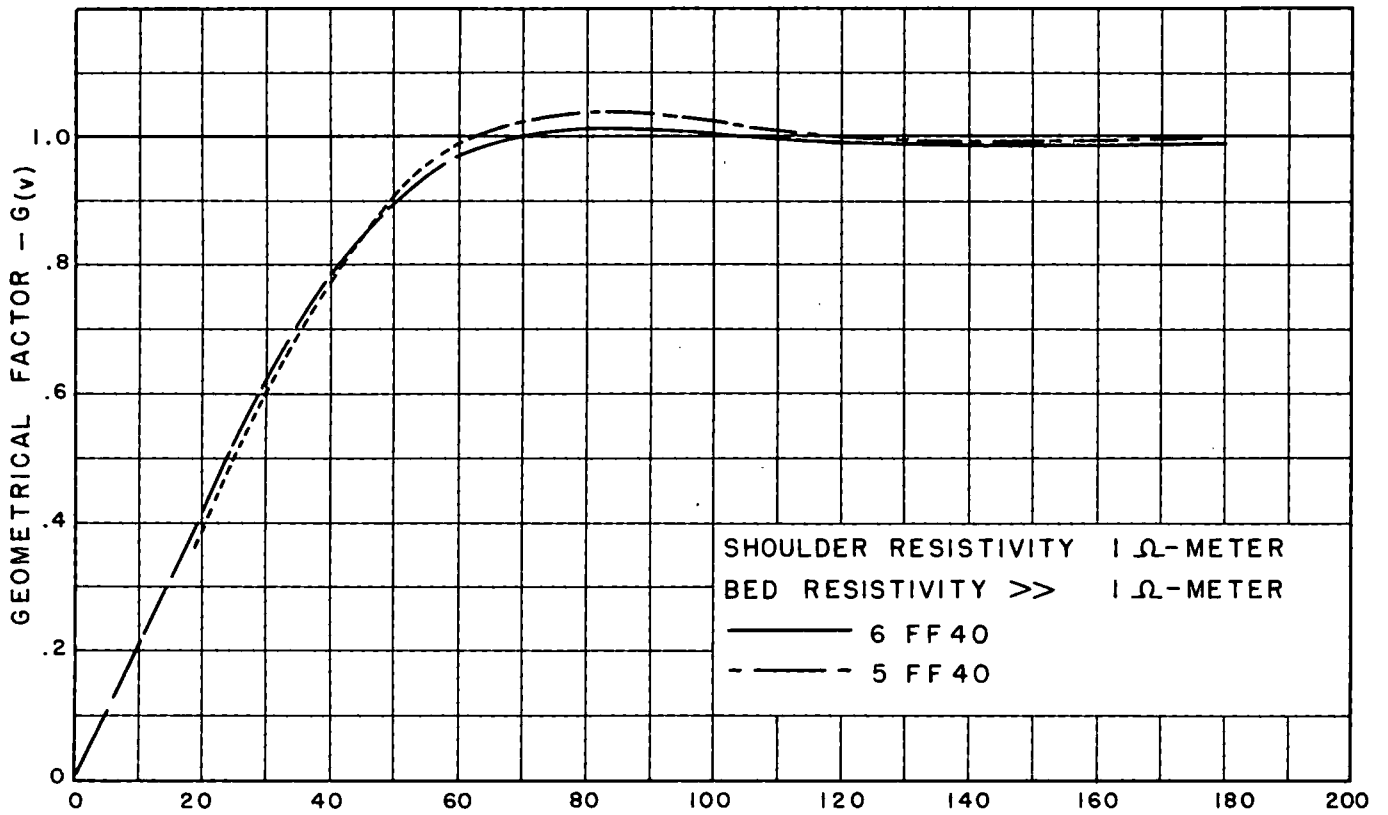


FIG. 3

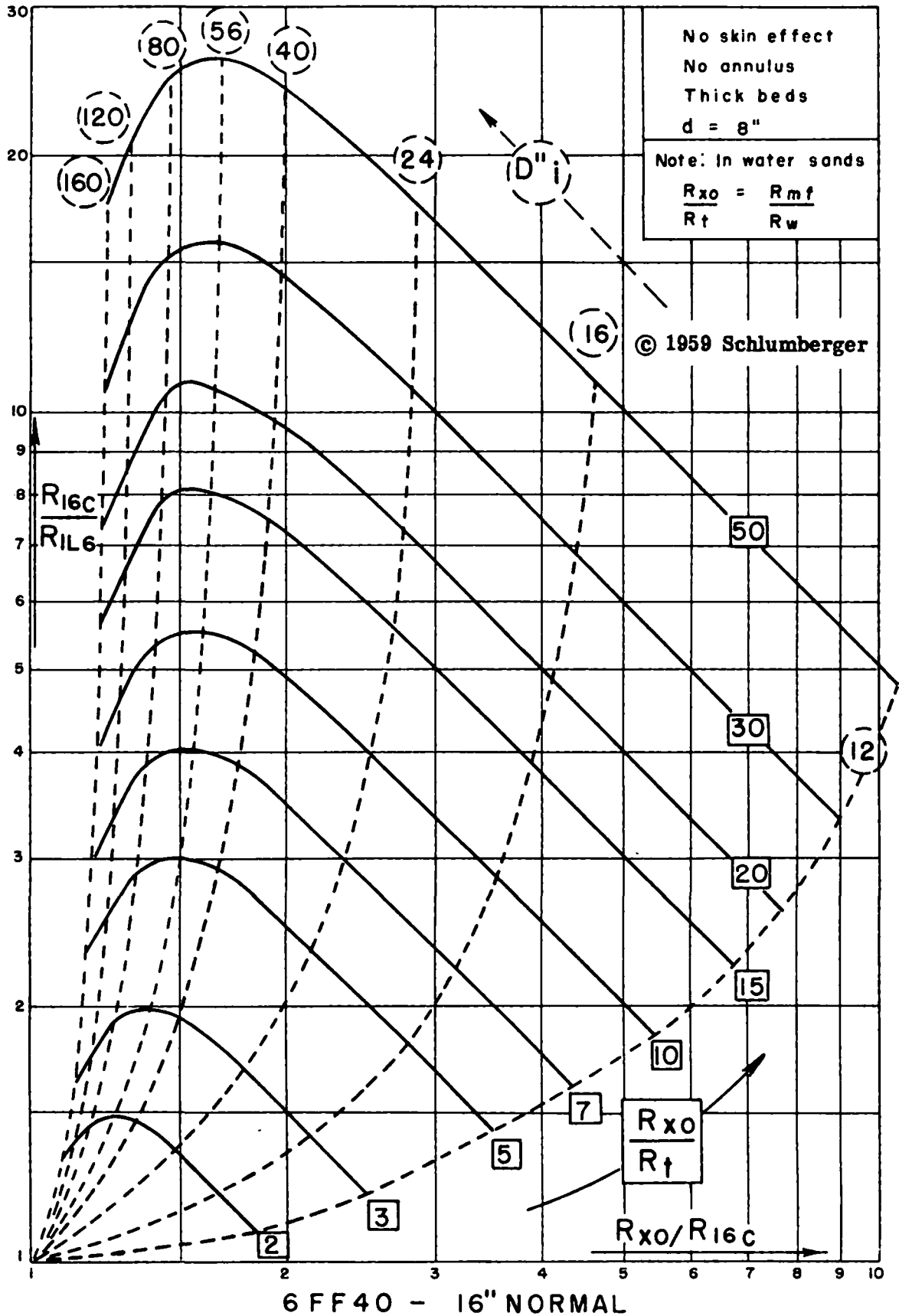


Figure 4

SATURATION DETERMINATION
6 FF40 - 16" NORMAL

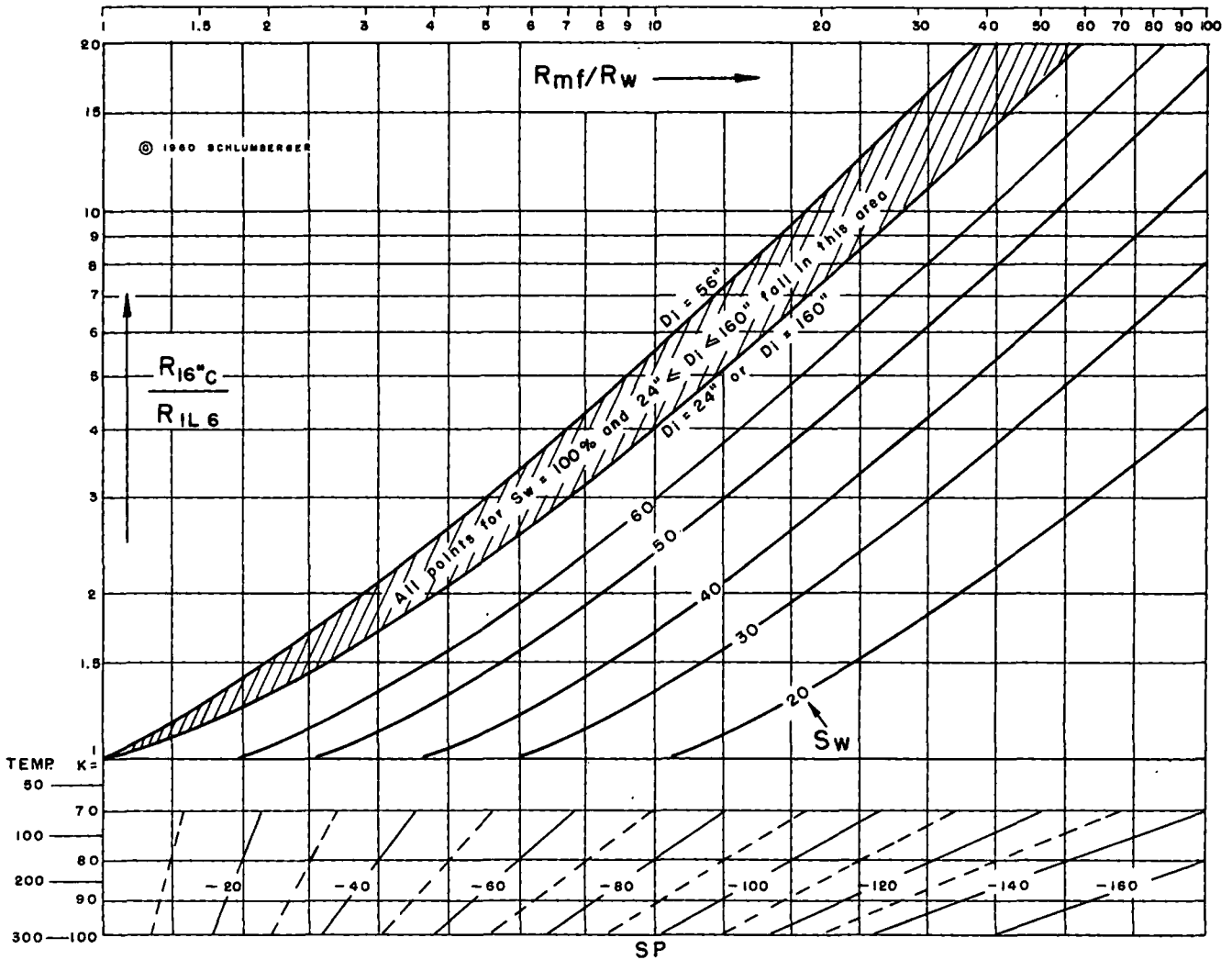


FIG. 5

PART II — NEW DEVELOPMENTS IN SONIC LOGGING

A large number of sonic logs are now being made every month. They have, to a great extent, become the standards for porosity logs.

Better tools are being placed in service in order to improve the reliability of the measurements and to decrease maintenance. In particular, emphasis is being put on good calibration; and steps are being taken to make this foolproof.

Rudiments of sonic log interpretation have been published and are well known. With greater experience, better understanding and interpretation are available. In particular, we will show three techniques that experience has proved to be of wide application and great reliability.

These three techniques permit the use of the sonic log in a more universal fashion. Their headings indicate their

use: *SONIC VS. RESISTIVITY IN HARD AND COMPACTED FORMATIONS, THE SONIC LOG IN SOFT FORMATIONS, and FINDING SATURATION IN INVADED ZONES WITHOUT R_w OR R_t .*

SONIC VS. RESISTIVITY IN HARD AND COMPACTED FORMATIONS

A simple chart, already published², presents a graphical solution of porosity and saturation from sonic and resistivity logs. The key of this chart is the unusual ordinate scale which permits the use of straight lines for the saturation positions.

Mr. A. T. Hingle of the Magnolia Petroleum Company

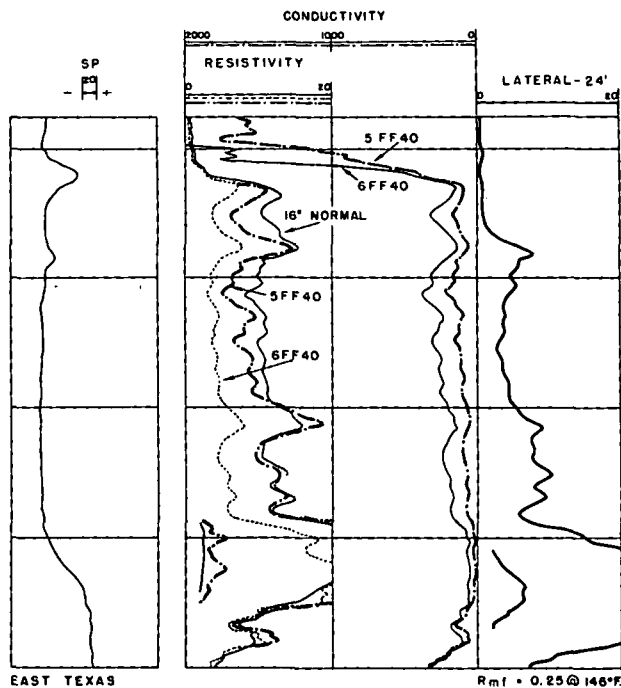


Figure 6

used this chart in a different way. Using the grid as given, the resistivity was plotted in ordinate instead of R_t/R_w . The abscissa, Δt , remained as before; but no attempt was made to choose the matrix velocity. This presentation, together with further refinements, will be the subject of this study. (As an example of the grid, see Fig. 8).

To investigate the use of the method, we will consider separately the wells drilled with salt muds (low R_{mf}/R_w) and those drilled with fresh muds (high R_{mf}/R_w).

A. In Salt Mud

1. Plotting the Points

A good value of resistivity (preferably R_t) is plotted in ordinate. According to conditions, a multiple of R_t (such as R_t , $2 R_t$, $10 R_t$, et cetera) is plotted in order to accommodate the scale already marked on the grid.

The value of Δt is plotted in abscissa. Usually the left origin is 40 microseconds for hard formations but may be greater in softer formations; and each interval on the abscissa is equal to 3, 5, or 10 microseconds, according to conditions.

A shotgun pattern usually exists if a large number of points is plotted.

2. Determining R_o and V_m

A line can be drawn through the points found to the left of the pattern (the most northwestern points if the heading points north). Such a line is presumed to be R_o if the true resistivity has been used to plot the points. The line can be extended to ordinate ∞ ,

and the intersection will determine the Δt of the matrix (porosity zero).

In an ideal situation we can see that prior knowledge of the matrix velocity is unnecessary since it is determined in this fashion. When control from plotted points is not sufficient to establish an R_o line easily, the matrix velocity can be chosen on the basis of experience. Such difficulty might be encountered where porosity values are too uniform to supply a well defined line. Difficulty would also be encountered in the event that R_o was not obtainable from the log, but even then a matrix velocity can be found in many cases. This latter case could be caused by the presence of hydrocarbons throughout the zone under study or deep invasion of fresh filtrate into the water sands making it impossible to read close to R_o on any log.

In compacted formations we already have rather extensive experience indicating that V_m for limestone should be between 21000'/second and 23000'/second; in sandstones V_m should be about 18000'/second. If, because of the lack of R_o control points, the plotted values differ *greatly* from these values, it is advisable to use an experience-dictated V_m versus infinite resistivity as a control point.

3. Porosity and Formation Factor

Having Δt_m (or V_m), it is easy to obtain the porosity according to the time-average formula. This porosity scale can be put on the line marked ϕ . The formation factor can be written on the line below. The charts of Figs. 8 and 10 are made for $m = 2$, and the ϕ, F relation is $F = 1/\phi^2$. The same chart will suffice for any formation if the relation $F = 0.81/\phi^2$ is used.

4. Determining the Line of Complete Invasion

Knowing F and R_{mf} , it is easy to draw a line showing *complete* invasion. As an example, for a formation factor of 100, the complete invasion line must pass through a point of ordinate $100 R_{mf}$. In salty mud such a line is not far from the line R_o , but in fresh mud the complete invasion line will be quite a distance below.

5. Determining R_w

If we are satisfied that the "northwestern line" is indeed R_o , we can obtain R_w simply by dividing the abscissa into the ordinate of any point on the R_o line. It has been found that a plot of points coming from a hydrocarbon-saturated section does not give our R_o line because the most northwestern points still contain some hydrocarbons. Nevertheless, this line, as a rule, should correspond to a water saturation of 70% or more (equal to $2 R_o$).

6. Determining Saturation Lines

Once the R_o is obtained, it is easy to trace any other saturation line. As an example, the line for $S_w = 50\%$ will have ordinate values four times greater than the R_o line.

B. In Fresh Muds

In fresh muds the problem is more complicated because with deep invasion the R_t device may measure R_1 rather than R_t . With a large R_{mf}/R_w , a point would fall well below the R_o line in such a case. To recognize this possibility the steps taken for salt muds are augmented by a plot of R_1 versus Δt .

R_1 can be obtained from a short normal, a limestone curve, a Laterolog 8, or a Proximity Log. However, it should be remembered that obtaining the value of R_1 from the short normal can be very dangerous when resistive shoulders are near the section under study. A Proximity Log or a Laterolog 8 is preferred. In water sands when normal invasion occurs, the value of R_1 should be less than the product $F R_{mf}$ because some formation water remains in the invaded zone. For simplification, the value of R_1 is said to equal $F R_z$, R_z being the resistivity of the mixture of filtrate and formation water. This concept has been explained in *Electric Log Analysis in the Rocky Mountains*³, where the value of z , the proportion of formation water to the total water, has been found to be between 5 and 10% for normal invasion. The plot of R_1 in water sands will fall near an $F R_z$ line when normal invasion occurs; if completely invaded, the values will plot near an $F R_{mf}$ line. The $F R_z$ line is determined in the manner previously described for $F R_{mf}$. In the event that invasion is shallow, the plot will fall above the $F R_z$ line; and, with no invasion at all, such points would determine the line $F R_w$, or R_o . Very shaly water sands will fall below the R_o line because their Δt is too large, and they will be found between the R_o and $2 R_o$ lines.

Sands saturated with hydrocarbons are readily recognized when they lead to an R_t plot clearly below the $F R_{mf}$ line. However, when both the R_t and R_1 plots fall above the $F R_{mf}$ line, no such sweeping assumption can be made. To differentiate between petroliferous sands and deeply invaded water sands we must compare the R_1 with $F R_z$. It now appears that R_1 of a saturated sand should be *at least twice* that of the water sands falling on the $F R_z$ line. This rule can be used only when the contrast between R_{mf} and R_w is not too large. It is possible for the value of z to be higher in oil sands than in water sands, and this may preclude seeing the residual oil clearly when the R_{mf}/R_w ratio is large.

REMARKS

A. Differentiation of Lithology

This plotting has the advantage of showing variations in lithology. As an example, limestone points will usually fall to the left of the sandstone points. Anhydrite and salt are also clearly differentiated because of their high resistivity and characteristic Δt .

B. Advantages of the Plotting Method

1. A value for the matrix does not have to be assumed in many cases; thus, the porosity scale is more trustworthy.
2. The values for full invasion can be easily obtained from the line for $F R_{mf}$.
3. The formation water resistivity can often be computed from the graph.
4. This method gives a visual picture of the petroliferous sections.
5. A minimum of calculation is required.
6. The analyst is forced to look at all the zones, and this decreases the chances of passing an interesting section.
7. This method is well adapted for salt-mud logging.

C. Disadvantages of the Plotting Method

1. It requires a relatively large range of porosities for good plotting.
2. Invasion can be troublesome if not detected properly.
3. Shaly formations and unconsolidated sands do not lend themselves readily to this method.
4. R_w , V_m , and D_i should be fairly constant for the points plotted.

EXAMPLES

Fig. 7 illustrates a limestone section in Kansas surveyed with salt mud.

Fig. 8 shows the plot of Δt vs. Resistivity for the section given in Fig. 7.

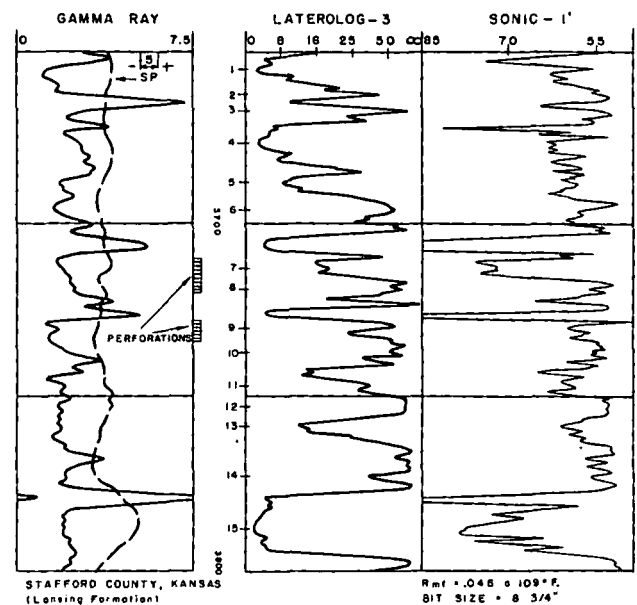


Figure 7

STAFFORD COUNTY, KANSAS
(Lansing Formation)

SONIC vs. RESISTIVITY

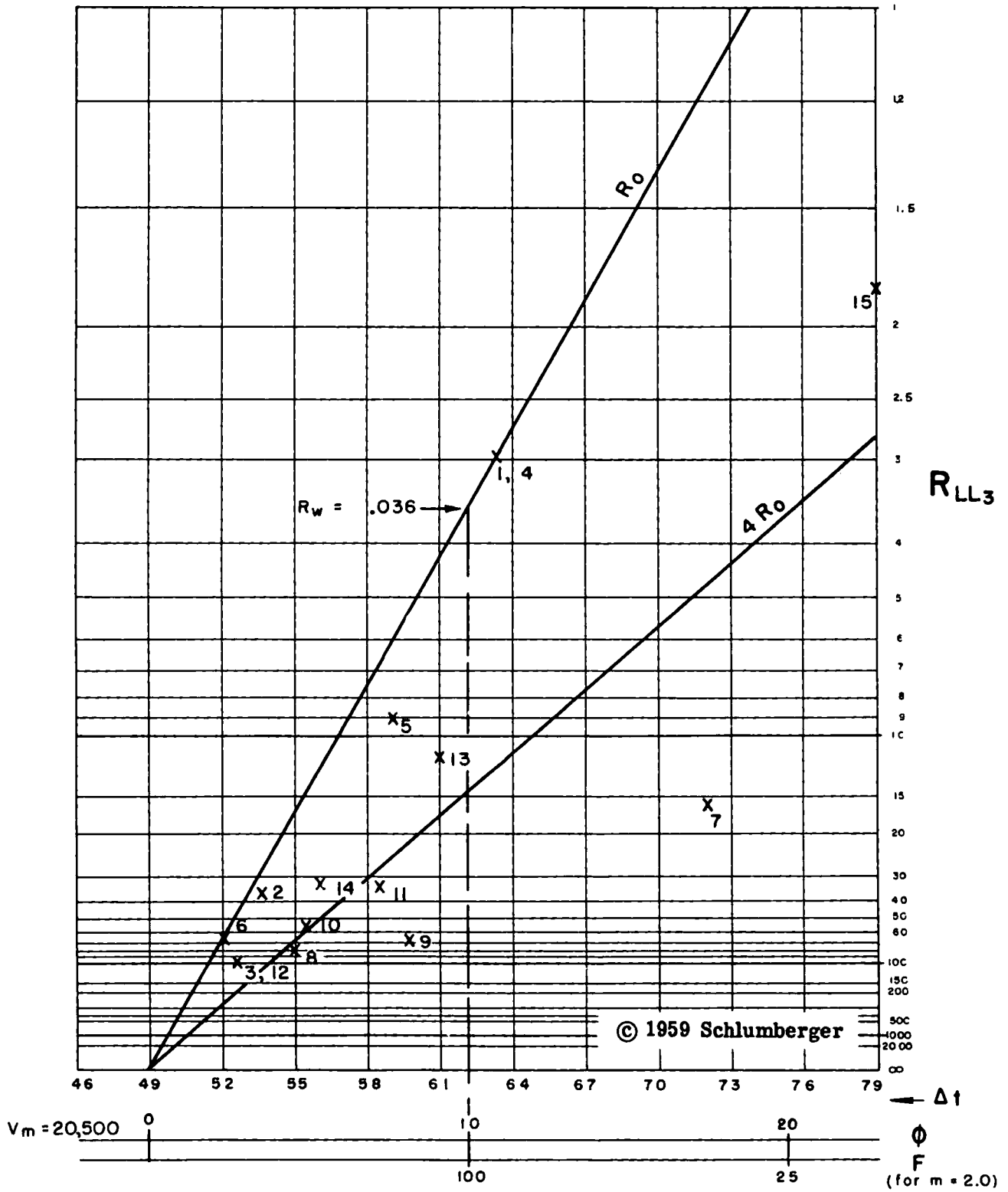
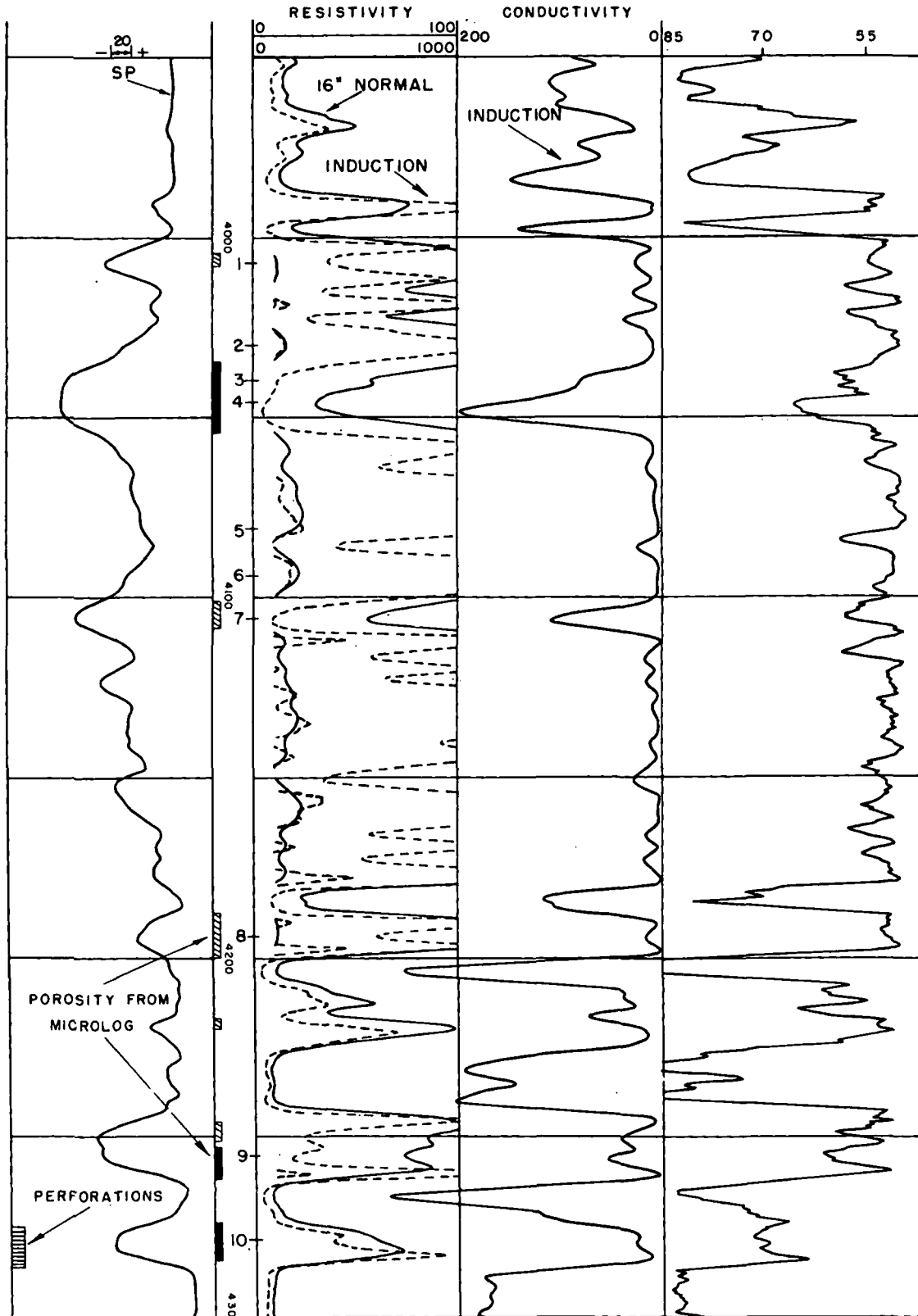


Figure 8

INDUCTION - ELECTRICAL

SONIC



TAYLOR COUNTY, TEXAS

Rmf = 1.35 @ 115° F.
BIT SIZE = 7 7/8"

Figure 9

TAYLOR COUNTY, TEXAS
SONIC vs. RESISTIVITY

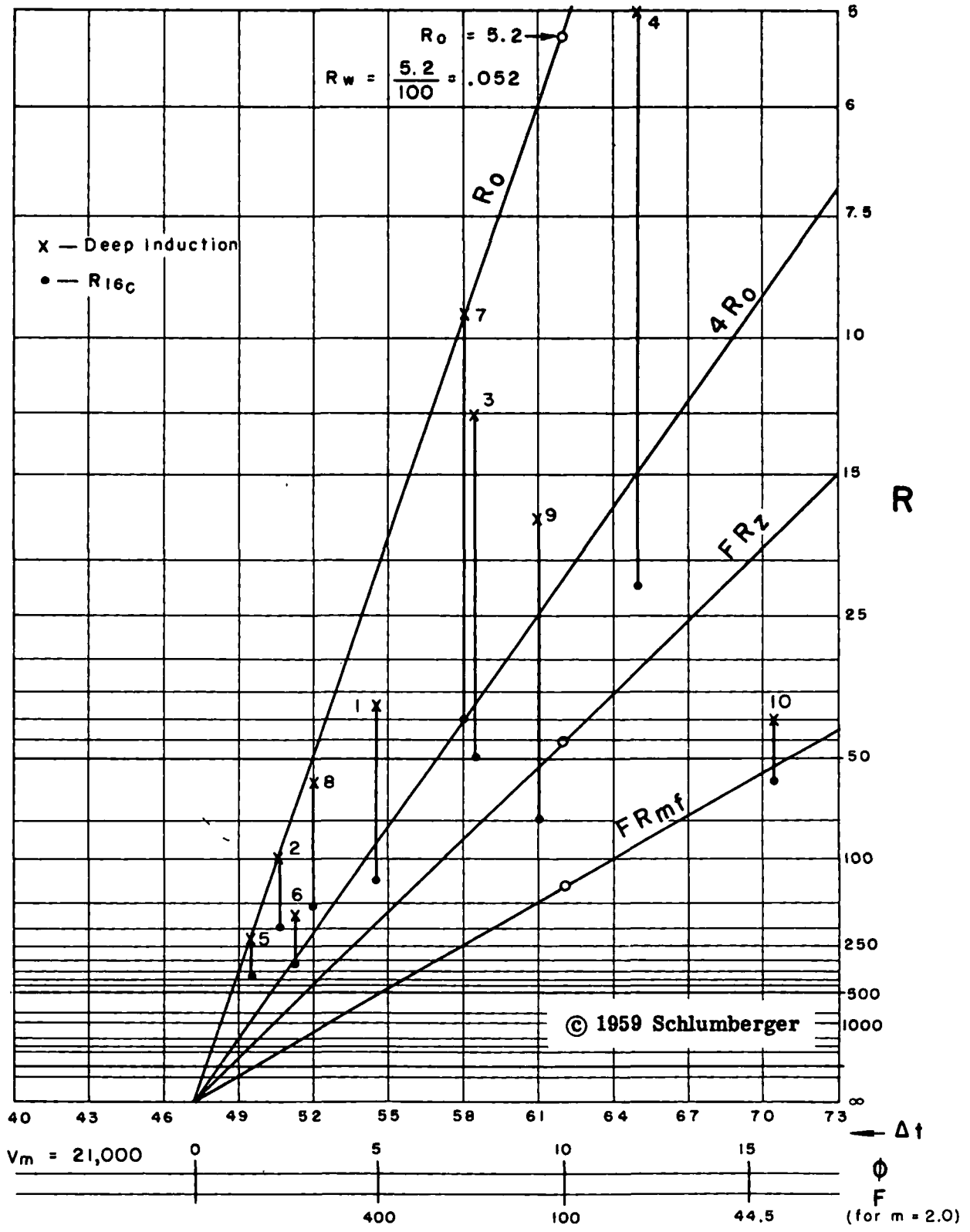


Figure 10

The R_o line is defined by the values given at the level of Points 1, 4, and 6. This line yields a value of 0.036 for R_w and a V_m of 20500'/second. Points 7, 8, and 9 fall below the line representing 4 R_o values. These three points represent the pay sections in the well. Points 10 and 11 also carry oil, but have not been tested.

The perforations marked on the log at the level of Points 7, 8, and 9 yielded, on pump, 130 barrels of oil per day with 11 barrels of water.

Figs. 9 and 10 illustrate the logs and the plots of a well surveyed in fresh mud in the Strawn Section, Taylor County, Texas. A deep investigation induction log was run in this well. The sections showing mud cake on the Microlog are shown in the depth column.

The induction values of Points 2, 5, 7, and 8 permit a good definition of the R_o line. Such line yields a value of .052 for R_w , which checks well with the value obtained from the SP curve (around 0.06). The velocity of the matrix given by the R_o line is 21000'/second. Lines of $F R_{mf}$ and $F R_z$ were calculated and put on the plot.

Only Point 10 shows an induction value greater than 4 R_o . It is interesting to plot R_t obtained from the short normal after correction for hole effect. The R_t value of Point 10 is the only one showing a resistivity greater than $F R_{mf}$. Point 9 is next in interest on both the induction and short normal values.

The perforations shown on the log at the level of Point 10 gave a natural production of 183 barrels of oil daily (40 API gravity and gas-oil ratio of 420 to 1).

THE SONIC LOG IN SOFT FORMATIONS

The method described here provides a quick interpretation by comparing the fluid characteristics of many levels after the porosity variable has been eliminated. In short, the resistivity of the fluid filling the pores is calculated, assuming that such fluid fills all the porosity available.

In final analysis this method is not very different from many others used in the past. It has been found to have a practical usefulness in shaly and unconsolidated formations that cannot be easily studied with the method described under *SONIC VS. RESISTIVITY IN HARD AND COMPACTED FORMATIONS*. In particular, no special graph paper is necessary. Neither do we need to know R_{mf} in any of the simple calculations.

In a sand, the formation factor can be given by one of the two relations:

$$F = 0.62/\phi^{2.15} \quad (\text{Humble Formula})$$

or

$$F = 0.81/\phi^2.$$

The latter is preferred in our work because it is somewhat simpler to use.

In a water sand, $R_o = F R_w$ or $0.81 R_w/\phi^2$. R_w can

be easily determined:

$$R_w = \frac{R_o \phi^2}{0.81} \quad (1)$$

In a sand which contains some hydrocarbons,

$$R_t = \frac{F R_w}{S_w^2} = \frac{0.81 R_w}{\phi^2 S_w^2}$$

In this case,

$$R_w = \frac{R_t \phi^2}{0.81} \times S_w^2 \quad (2)$$

If we do not know that the sand contains oil or gas, and assume it to be wet, we obtain a fictitious value:

$$R_{wa} = \frac{R_t \phi^2}{0.81} = \frac{R_w}{S_w^2} \quad (3)$$

Thus, R_{wa} is too large in oil and gas sands.

It is often difficult to make interpretations where the formation water resistivity varies with depth because the knowledge of R_w is poor. If we systematically check the formation water resistivity according to Relation (3) for all sands, we may have the following picture:

DEPTHS:	1000	1200	1500	1700	1800	2100	2400
R_{wa}	: 0.43	0.37	0.3	1.1	0.28	0.25	0.22

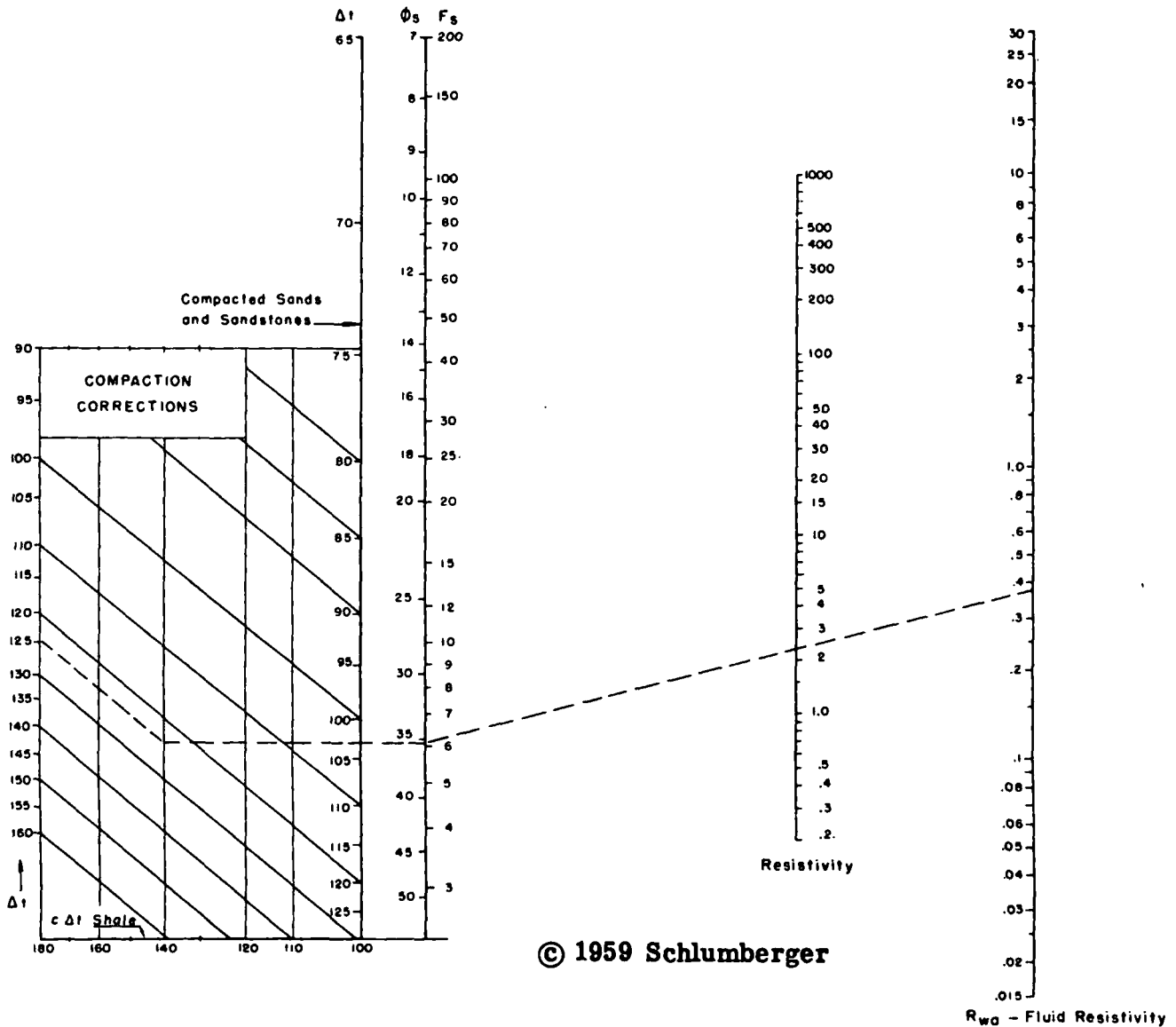
We see that the liquid resistivity is increasing slowly as we go up the hole, but the value at 1700' is clearly much higher than the trend. This section contains oil or gas.

We like to use the sonic log for porosity because only the compaction correction is necessary. No shale or fluid correction is made. Such porosity will be too high in shaly sands, but it is compensated by a low R_t when such sands contain hydrocarbons. In a clean oil and gas sand, the porosity given by the sonic with only the compaction correction will be too high when the transit time is increased by the presence of hydrocarbons. This, in turn, will point out the petroliferous section in an exaggerated manner.

In a water-bearing shaly sand the formation water resistivity calculated in this manner may be as much as 2 R_w because its Δt is too high. For this reason, we believe that oil or gas saturation in shaly sands should be assumed only when R_{wa} is at least 2 R_w , or more. A greater contrast will be found in clean sands.

The attractiveness of this method lies in its rapidity. Fig. 11 shows a nomograph for both compacted and unconsolidated sands. It gives R_{wa} very readily. We can also use this technique in *compacted sands* and where the formation water is salty. We have found this technique as rapid as "eyeballing" and much safer. It is well adapted to the Gulf Coast and California, so long as R_t is available. One can obtain the resistivity index easily since $I = (R_{wa} \text{ in Oil Sand}) / (R_{wa} \text{ in Water Sand})$; and, consequently, quantitative interpretation can be carried out with this approach.

FLUID RESISTIVITY FROM SONIC
AND RESISTIVITY



© 1959 Schlumberger

Figure 11

Calculation of R_{za}

If we apply the same technique but use R_1 instead of R_t , we obtain R_{za} . This value is equal to R_{mf} in completely invaded water sands. It is less than R_{mf} if some formation water remains in the invaded zone of the water sands. (Such invaded water sands are filled with a water of resistivity R_w , as previously explained.) Except for large R_{mf}/R_w contrasts, R_{za} will usually be larger than R_{mf} in oil or gas sands because of residual oil and gas.

In conclusion, calculating R_{wa} and R_{za} is more or less identical to the plotting of R_t and R_1 when the formation water resistivity is constant throughout the section under study. This technique is well adapted to soft formations and, in particular, to shaly sands where the plotting method

is not straightforward because such formations are often unconsolidated.

Figs. 12 and 13, which illustrate this technique, will be discussed after the next section.

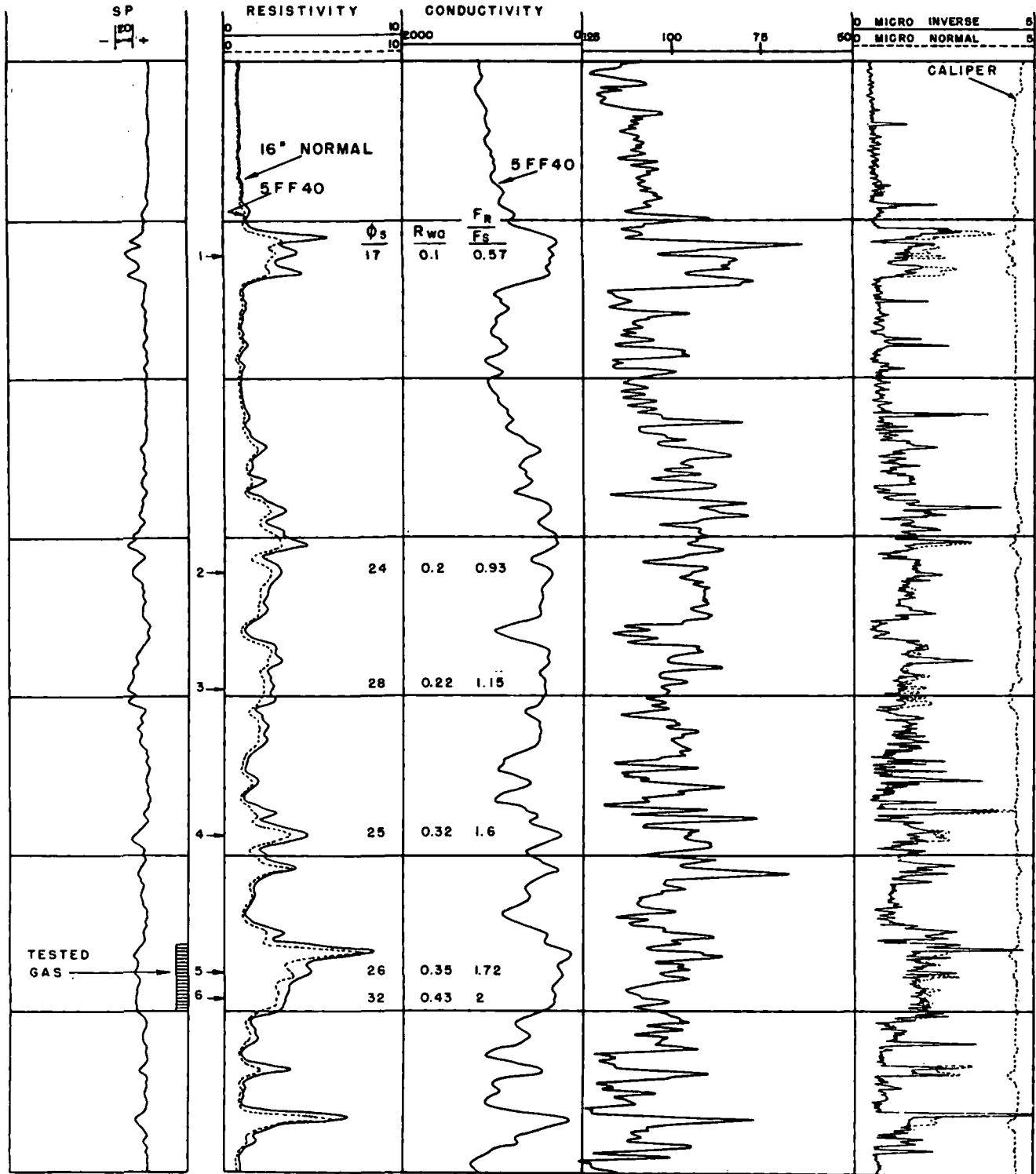
FINDING SATURATION IN INVADIED ZONES WITHOUT R_w AND R_t

In many places R_w and R_t are difficult to obtain for various reasons. The classical methods for finding water saturation require that such parameters, in addition to the formation factor, be known. Great difficulty is encountered when formation water resistivities vary considerably in the formation under study.

INDUCTION - ELECTRICAL

SONIC

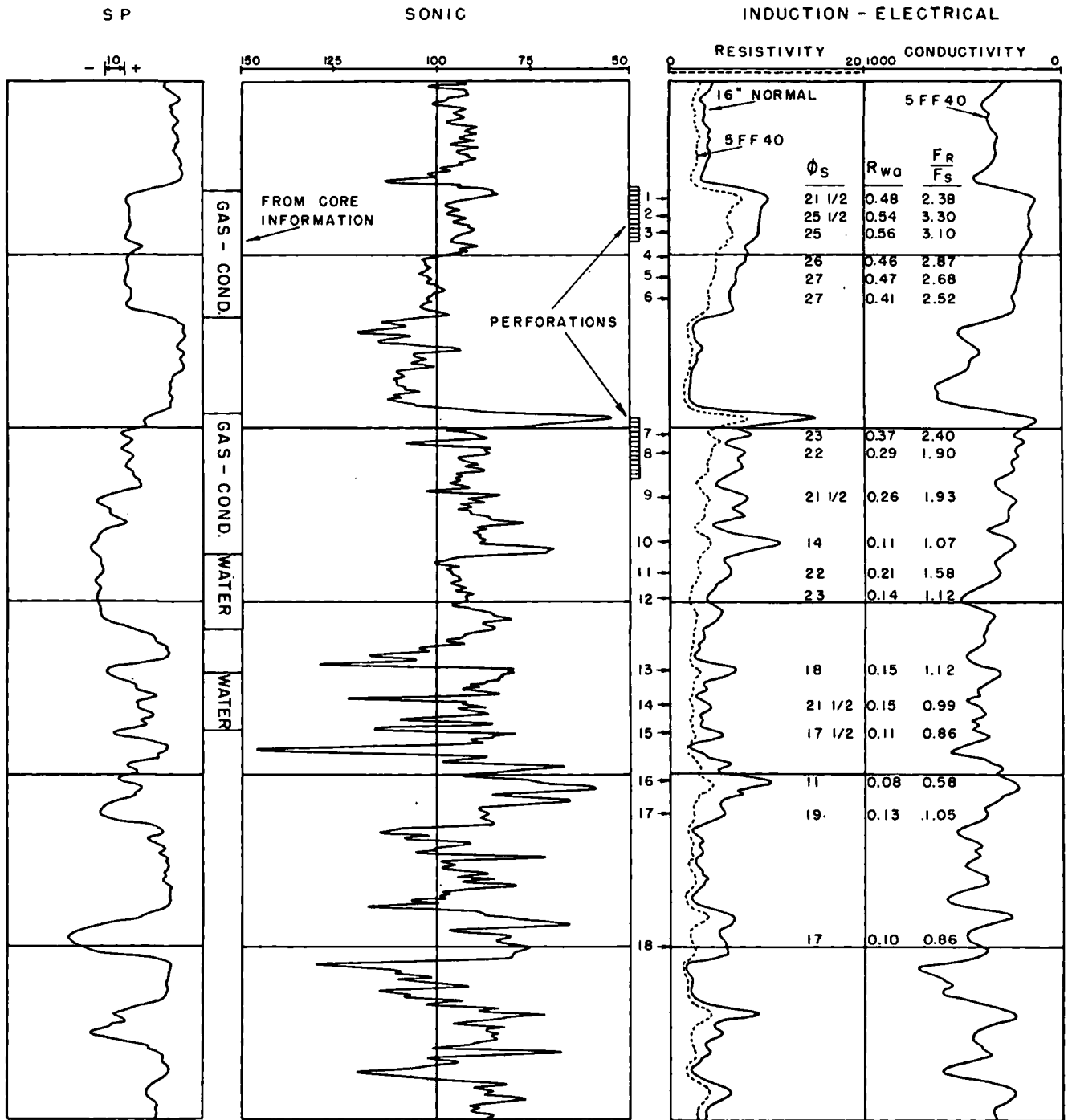
MICROLOG



DEEP FRIO - TEXAS GULF COAST

Rmf = 0.25
 BIT SIZE = 6 3/4"
 R_w ≈ .10
 cΔt_{sh} = 120

Figure 12



WILCOX - SOUTH TEXAS

$R_{mf} = 0.25$
 BIT SIZE = 6 7/8"
 $R_w = 0.06$
 $c \Delta t_{sh} = 100$

Figure 13

We know that if we use small resistivity spacings a value of the formation factor can be obtained under ideal conditions of filtrate invasion. When the formation is saturated with hydrocarbons, the residual oil or gas will increase the resistivity; consequently, the formation water

derived from shallow resistivity measurements will be too high unless a special correction is made to account for the ROS. This is true whether we use the Microlog, the Microlaterolog, the Proximity Log, the limestone curve, or the short normal to obtain the formation factor. As long as in-

vasion has taken place, one fact stands out: The formation factor is too high in oil and gas sands if we do not take the ROS into account.

On the contrary, the formation factor derived by the sonic log will be correct (or too low) in the case of hydrocarbon-saturated formations. We can see that, if we call ϕ_R the porosity and F_R the formation factor derived from a shallow resistivity log (without correction for ROS) and ϕ_S the porosity and F_S the formation factor derived by the sonic log (without correction for fluids or shaliness), we have with normal invasion:

1. In oil or gas formations: $\phi_R < \phi_S$ or $F_R > F_S$; thus, $F_R/F_S > 1$.
2. In water-bearing formations: $\phi_R \geq \phi_S$ or $F_R \leq F_S$; thus $F_R/F_S \leq 1$.

To find F_R it is usually sufficient to divide R_1 (obtained from a short-spacing device) by R_{mf} . More correctly, we should divide by R_2 if there is some formation water mixed with the filtrate; but this is not too important for such qualitative methods so long as a small contrast exists between the mud and formation water resistivity. When the mud is very fresh compared with the formation water, the value of R_2 is very different from R_{mf} ; therefore, this technique is not recommended when the R_{mf}/R_w ratio is large. All the above reasoning applies to shaly sand, as well as to clean sands. The sonic and resistivity logs are affected by the presence of shaliness in a somewhat similar manner.

A word of caution: Shallow invasion must be recognized. If, for instance, the short normal is opposite a non-invaded oil sand, it is very possible that the resistivity value thus obtained might be less than if invasion had occurred. In such a case, an erroneous value of porosity and formation factor would be computed by the R_1/R_{mf} method. The higher the R_{mf}/R_w , the greater would be the error. Of course, the non-invaded water sands would give for $F_R = R_o/R_{mf}$ a value much smaller than those in the non-invaded oil sands; this fact permits the use of the method in such cases if we keep this matter in mind. Of course, shallow invasion allows a good knowledge of R_t , and other types of interpretation, such as described under *THE SONIC LOG IN SOFT FORMATIONS*, can be used.

This qualitative approach to the location of oil or gas saturation should be relied upon only when R_t cannot be reliably obtained. Inability to determine R_t usually occurs in zones of deep invasion. Therefore, the comparison of F_R with F_S is, and should be, a last resort for deeply invaded sections or when R_w (the formation water resistivity) cannot be obtained.

We would like to point out that the Microlog is not recommended for this method because such work is often done in formations of medium and high resistivities, where the Microlog is not efficient.

It must be mentioned that when the oil or gas sands are found in such a qualitative way there should not be much trouble in finishing the interpretation in a quantita-

tive manner. In such saturated sands the long-spacing resistivities are usually not greatly affected by invasion and, consequently, approach R_t . In other words, when the oil and gas sands are separated from the water sands, the rest of the work is usually quite simple. This method gives good qualitative results in low porosity formations ($\phi < 20\%$). The results in high porosity formations ($\phi > 20\%$) should be verified by the R_{wa} method (water comparison) explained previously.

EXAMPLES

Fig. 12 illustrates the logs made in a Deep Frio Section in the Texas Gulf Coast. Because of the brackish mud and shaliness, little SP deflection occurs in the sands. At the level of the sections studied, the values of ϕ_B , R_{wa} , and F_R/F_S have been written on the induction-electrical log.

Level 1 shows a relatively low porosity value and an R_{wa} value equal to the known formation water resistivity. This section is water-bearing. The ratio F_R/F_S is less than unity because insufficient invasion has taken place. It is remarkable that this section shows as good a resistivity and SP as can be found on the induction-electrical log. Points 4, 5, and 6 are the only ones showing an R_{wa} at least three times that of Level 1. The ratio F_R/F_S clearly indicates that hydrocarbons are present in the invaded zone. Tests of Levels 5 and 6 showed gas.

Fig. 13 shows the logs of a Wilcox (Eocene) Section in South Texas. The values of ϕ_B , R_{wa} and F_R/F_S are marked on the log at the levels under study.

In the upper section, Points 1 to 6 show good porosities and values of R_{wa} seven to nine times the known R_w . The ratio F_R/F_S clearly shows that hydrocarbons are present in the invaded zones.

Levels 7, 8, and 9 are also indicative of a section saturated with hydrocarbons. Point 10 shows relatively low porosity, an R_{wa} value less than twice R_w , and a ratio F_R/F_S hardly above unity. This indicates a tight section without an appreciable amount of hydrocarbons. Starting with Point 11, the hydrocarbon saturation decreases rapidly, and no water-free production is possible.

Perforations are indicated on the log. The upper zone produces 23,000 MCF and the lower 12,000 MCF. Each produces 50-60 barrels distillate per MCF.

CONCLUSION

The use of the deep induction log and the application of the new sonic interpretation techniques have greatly helped the evaluation of many formations. In particular, many sandstones in South Texas, Mississippi, and the Rocky Mountains that could not be evaluated in the past can now be easily interpreted. The same is true of various limestones in West Texas and New Mexico.

ACKNOWLEDGEMENT

The authors acknowledge the efficient assistance of M. C. Watson, W. P. Biggs, and R. P. Burton in the preparation of the paper. The courtesy of the oil companies who released log data for the illustration of this paper is appreciated.

REFERENCES

1. Dumanoir, J. L., Tixier, M. P., and Martin, Maurice: "Interpretation of the Induction-Electrical Log in Fresh Muds", *Trans., AIME* (1957) Vol. 210, pp. 202-215.
2. Tixier, M. P., Alger, R. P., and Doh, C. A.: "Sonic Logging", *Journal of Petroleum Technology*, Vol. 11, pp. 106-114, May, 1959 — FIG. 22.
and
Schlumberger Well Surveying Corporation (Editor), *Log Interpretation Charts*, Houston, April, 1959 — CHARTS D-18 and D-20.
3. Tixier, M. P.: "Electric Log Analysis in the Rocky Mountains", *Drilling and Production Practice, API* (1949), pp. 316-328.

A New and More Accurate Method for the Direct Measurement of Earth Temperature Gradients in Deep Boreholes

JAMES N. ALBRIGHT

Los Alamos Scientific Laboratory, University of California, Los Alamos, New Mexico 87544, USA

ABSTRACT

A technique has been developed for the direct determination of bottom-hole equilibrium rock temperatures during economically acceptable interruptions in drilling operations: 12 to 24 hrs, depending on depth and rock type. This technique was developed during the drilling of GT-2, the second deep exploratory test hole in the Los Alamos Scientific Laboratory's (LASL) Dry Hot Rock Geothermal Energy Project.

The major innovative aspect of this technique is a new method of analyzing bottom-hole thermal recovery data, enabling equilibrium rock temperatures to be determined from measurements of substantially shorter term than previously possible. Assuming for an arbitrary time interval, short in comparison with the time required for temperature recovery to be complete, that the rate of temperature relaxation depends only on the difference between the borehole temperature and the undisturbed rock temperature, we can write for the time interval, t :

$$\frac{\theta_{\infty} - \theta(t)}{\theta_{\infty} - \theta_0} = e^{-ct}$$

A linear dependence of c on θ_{∞} enables determinations of equilibrium rock temperature. Relaxation temperatures observed at any specific depth can be treated in this manner giving the same rock temperatures predicted by theory. However, sufficient data can be collected in hours rather than months or years, if direct bottom-hole temperature measurements are used.

Using this technique, the equilibrium rock temperature at the GT-2 terminal depth of 2928 m is 197°C, with a measured temperature gradient of 60°C/km over the bottom 0.8 km.

INTRODUCTION

A 2928-m-deep (9607-ft), 244-mm-diam (9 5/8-in.) borehole recently has been drilled as part of the Los Alamos Scientific Laboratory's Dry Hot Rock Geothermal Energy Project. This borehole, designated Geothermal Test Hole No. 2 (GT-2), is located on the western flank of the Valles Caldera in north-central New Mexico (Pettitt, 1975). Methods

were developed for measurement of rock temperatures during economically acceptable interruptions in drilling operations. Subsequent reduction of these data enabled determination of equilibrium rock temperatures.

Past attempts at inferring equilibrium rock temperatures have concentrated on the analysis of relaxation temperatures measured in a fluid-filled borehole sufficiently distant from the bottom so that end effects could be ignored and data could be reduced using cylindrical heat-flow theory (Lachenbruch and Brewer, 1959; Cooper and Jones, 1959; and Jaeger, 1965). However in GT-2, the time necessary for temperature relaxation to approach theoretical behavior (neglecting convective disturbances) was prohibitively long for these methods to be of practical use.

Rapid determination of equilibrium rock temperatures is possible, however, if bottom-hole measurements are used. Since the rock at the bottom of a borehole is the least disturbed by the drilling process, the time rate of temperature change observed there during relaxation is substantially greater than that observed elsewhere in a borehole. This gives the desirable result of reducing both the precision and the amount of data required for accurate equilibrium rock-temperature determinations. Furthermore, at the bottom of a borehole, temperature sensors easily can be isolated from the cooling effects of convecting borehole fluids.

White et al. (in press), Grisafi, Rieke, and Skidmore (1974), and Summers (1972) approximate equilibrium rock temperature by measuring the bottom-hole temperature with a maximum-reading thermometer. However, the use of maximum-reading thermometers in high-temperature, low-permeability rocks—an environment not encountered by these investigators—is likely to introduce significant error. In the hot and essentially impermeable basement rocks encountered in GT-2, as depth increases the difference between observed temperature and equilibrium temperature increases. This is because the cooling effect of the drilling process is more pronounced at higher rock temperatures and cannot be quickly reduced by fluid exchange between the borehole and surrounding permeable rocks.

A new method is described by which equilibrium rock temperatures are calculated with high precision from an analysis of the thermal recovery of the bottom-hole temperature measured continuously with a thermistor sonde (Dennis and Todd, 1975). The geothermal gradient in GT-2 is the first gradient to be determined by this technique.

DATA REDUCTION

For an arbitrary time interval (short in comparison with the time required for temperature relaxation to be completed) it is assumed that the rate of temperature relaxation depends only on the difference between the bottom-hole temperature and the equilibrium, or undisturbed rock temperature. By allowing the proportionality constant to vary from one interval to another, and by following the change in the proportionality with time, one can calculate equilibrium rock temperature. It will be shown that relaxation temperatures observed at any depth in a borehole can be treated in the same manner to give equilibrium rock temperature. However, sufficient data can be collected in hours rather than months or years, if only bottom-hole temperatures are measured.

Muskat (1937), in an analysis of oil-well production, and Nakaya (1953), in an analysis of the thermal recovery of the South Barrow Well, made the above assumption for relaxation. However, both require that the proportionality be constant throughout the entire period of relaxation. Following Muskat's theoretical development expressed in terms of temperature, we have for the i th time interval beginning at time t_0^i :

$$\theta_{\infty}^i - \theta^i(t) = (\theta_{\infty}^i - \theta_0^i) e^{-c^i(t - t_0^i)} \quad (1)$$

where c^i is a constant for the i th interval, and θ_0^i , $\theta^i(t)$, and θ_{∞}^i temperatures at times t_0^i , t , and t_{∞} , respectively. By knowing the temperature at three specified times, two equations can be written and solved simultaneously for the unknown interval parameters c^i and θ_{∞}^i . Repeating this process n times, new choices are made of t_0^i and new values for c^i and θ_{∞}^i are calculated. Figure 1 shows two such calculations, one at an early time and another at a later time. A unique value of θ_{∞}^i cannot be found such that Equation (1) will adequately describe the observed tempera-

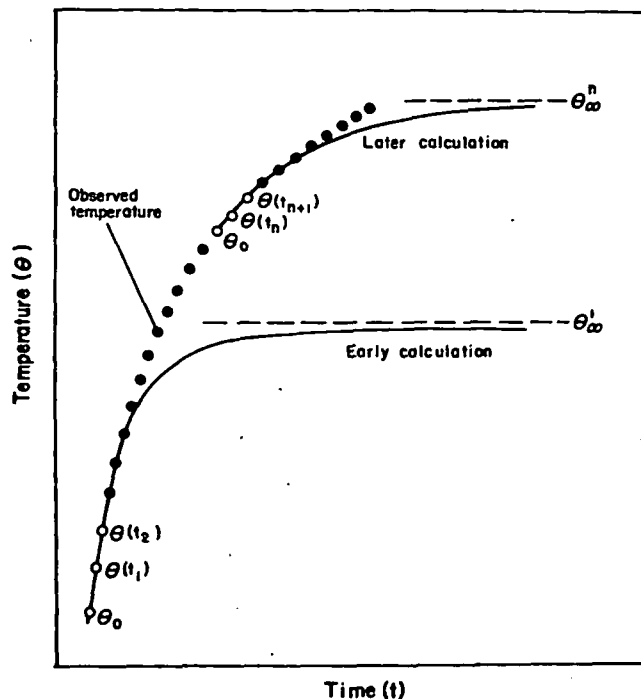


Figure 1. Calculation of c^i/θ_{∞}^i interval parameters.

tures. Thus c^i is varying during relaxation. Only temperature behavior during intervals short in comparison to the time necessary for complete recovery can be modeled by a particular calculated θ_{∞}^i . With successive calculations of θ_{∞}^i , both the curve fit and the extrapolation to the undisturbed rock temperature improve.

The choice of the time interval, $t_2^i - t_0^i$, for successive calculations of c^i and θ_{∞}^i is made which maximizes the range of θ_{∞}^i available from the observed temperature data within limitations imposed by the precision of the temperature measurements. A plot of c^i versus θ_{∞}^i enables the determination of equilibrium rock temperature θ_{∞} since, as $c^i \rightarrow 0$, $\theta_{\infty}^i \rightarrow \theta_{\infty}$ (also since $\theta_0 \rightarrow \theta_{\infty}$ convergence of $\theta_{\infty}^i \rightarrow \theta_{\infty}$ is assured). A regression analysis of the linear portion of each c^i/θ_{∞}^i curve is used to obtain the most likely value of θ_{∞} .

c^i/θ_{∞}^i Plots

Systematic errors have a negligible effect on c^i but substantially affect θ_{∞}^i . For instance, in these analyses a 1% systematic measurement error in the thermistor resistance results in 0.3°C error in θ_{∞}^i . Random measurement errors cause uncertainties in both c^i and θ_{∞}^i , skewed principally in the direction of higher θ_{∞}^i and lower c^i . Both of these latter errors increase with decreasing c^i . Uncertainties at small c^i can be reduced by choice of a greater time interval in computing c^i and θ_{∞}^i , but such a choice has the undesirable consequence of reducing the range of θ_{∞}^i available for extrapolation.

VERIFICATION OF THE LASL METHOD

The dependence of c^i on θ_{∞}^i is demonstrated by the analysis of data reported by Lachenbruch and Brewer, 1959. Figure 2 shows a c^i/θ_{∞}^i plot calculated from temperature measurements made at a depth of 181 m (595 ft) during a 6-yr period after the drilling of a 610-m (2000-ft) well near Barrow, Alaska. θ_{∞}^i approaches θ_{∞} as c^i approaches zero. The equilibrium temperature predicted at $c^i = 0$ corresponds closely to the value of -6.735°C predicted from theory.

Lachenbruch and Brewer, 1959, have shown that the cooling of a well, in which the drilling operation approximates a constant linear heat source persisting throughout the time of drilling, is adequately described by an equation of the form

$$\theta = \theta_{\infty} - \frac{q}{4\pi K} f(t, s) \quad (2)$$

$$\text{where } f = \ln \frac{t}{t-s};$$

θ = relation temperature;

θ_{∞} = equilibrium temperature;

t = time elapsed since the drill bit reached the depth in question;

q = cooling per unit time per unit depth;

K = thermal conductivity of the rocks penetrated by the borehole; and

s = time elapsed since the drill bit first reached the depth in question until the drilling operation ceased.

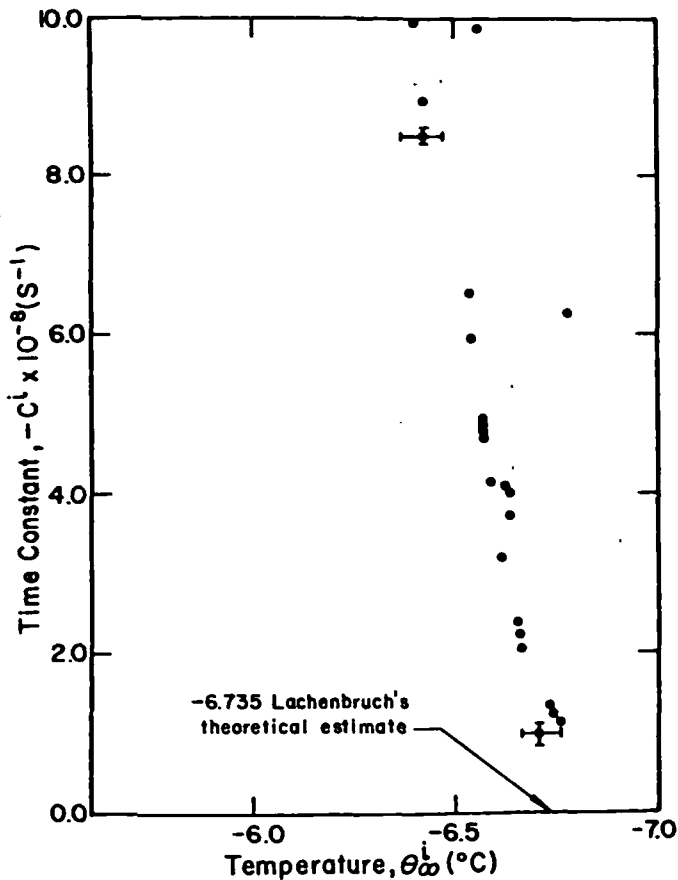


Figure 2. Reduction of temperature recovery data (Lachenbruch and Brewer, 1959) for a depth of 181 m (595 ft) in the South Barrow Well No. 3.

If only radial components of heat flow into a borehole are allowed, an expression identical to Equation (2) describes bottom-hole temperature relaxation. In this case s is the cooling associated with drilling and post-drilling intervals (convection and forced fluid circulation). Because convection continued for an indefinite time in GT-2 subsequent to the cessation of drilling, s is not known.

Likely estimates of s , and hence θ_∞ and $q/2\pi$, however can be derived through iterative calculations of the regression of s on f and its derivative f' (Williams, 1959). Regressions applied to selected bottom-hole temperature data from GT-2 give 0.99 coefficients of determination and θ_∞ estimates within error of the LASL method. The model expressed by Equation (2) is incomplete because it does not account for the axial component of the heat flow into the bottom of the borehole, and thus cannot be used to verify the LASL method. Our calculations, however, do not preclude the possibility that axial effects may in fact be small.

Analysis of thermal recovery data for a laboratory model, reported by Cooper and Jones, 1959, provides experimental verification of the relationship between the interval parameters c^i and θ_∞^i . In their experiment, a cubic meter of sandstone was allowed to come to equilibrium with room temperature. A 4-cm-diam (1.5-in.), 0.6-m-deep (24-in.) borehole was then drilled into the center of the block and filled with a chilled slurry. The temperature in the borehole eight diameters off bottom was measured intermittently during thermal recovery. Figure 3 shows a $c^i \theta_\infty^i$ plot for the recorded temperature

data. Both the $c^i \theta_\infty^i$ extrapolation and the Cooper and Jones theoretical prediction approximate, within measurement error, the equilibrium rock temperature which in this case is known.

EQUILIBRIUM ROCK TEMPERATURES IN GT-2

Estimates of θ_∞ Between 1387 and 2040 m

Figure 4 shows $c^i \theta_\infty^i$ determinations of equilibrium rock temperature at specific depths between 1387 m (4550 ft) and 2040 m (6692 ft) in GT-2 (for original data see Albright, 1975). The standard error in the determination of θ_∞ from regression analysis of the linear portion of each curve in each case is less than 0.1°C. Curvature in the $c^i \theta_\infty^i$ plots at early time probably indicates adjustments in the borehole accentuated by the thermal inertia of the temperature-measuring system. Absence of strong curvature occurring in estimates at 1387 and 1825 m is primarily the result of a long lapse between the time circulation was stopped and the time the first temperature measurements were taken.

Borehole convective instabilities are identified on $c^i \theta_\infty^i$ curves as reversals of direction of time-sequential $c^i \theta_\infty^i$ points. The result of borehole convection is to reset the time reference for conductive heat flow. The reference time is moved ahead when a convectively driven increase in the time rate of temperature change occurs, and is moved back for a decrease. Hence, extrapolated rock temperatures

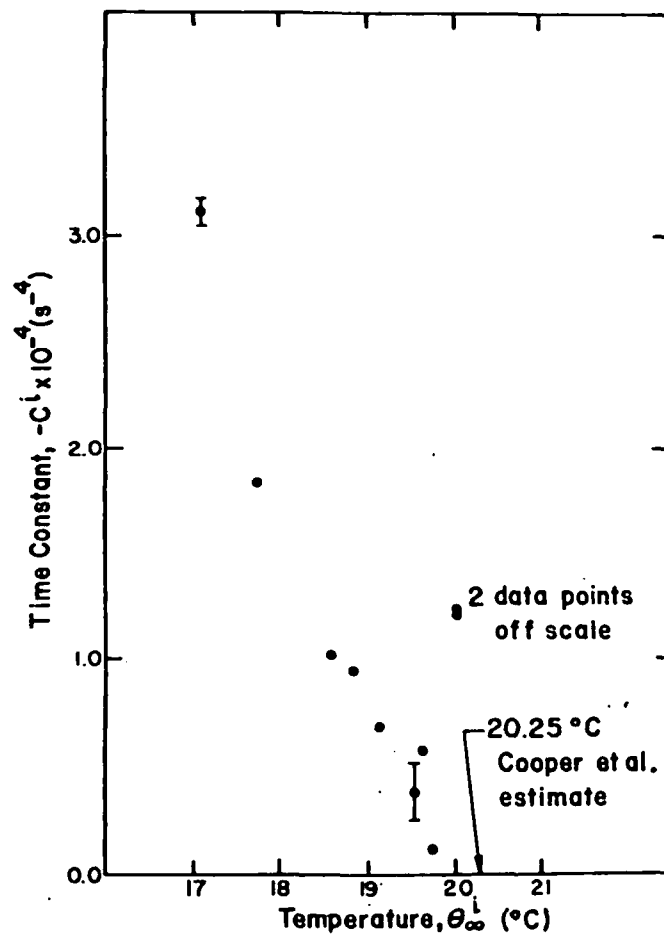


Figure 3. Reduction of temperature recovery data (Cooper and Jones, 1959) for a laboratory experimental model.

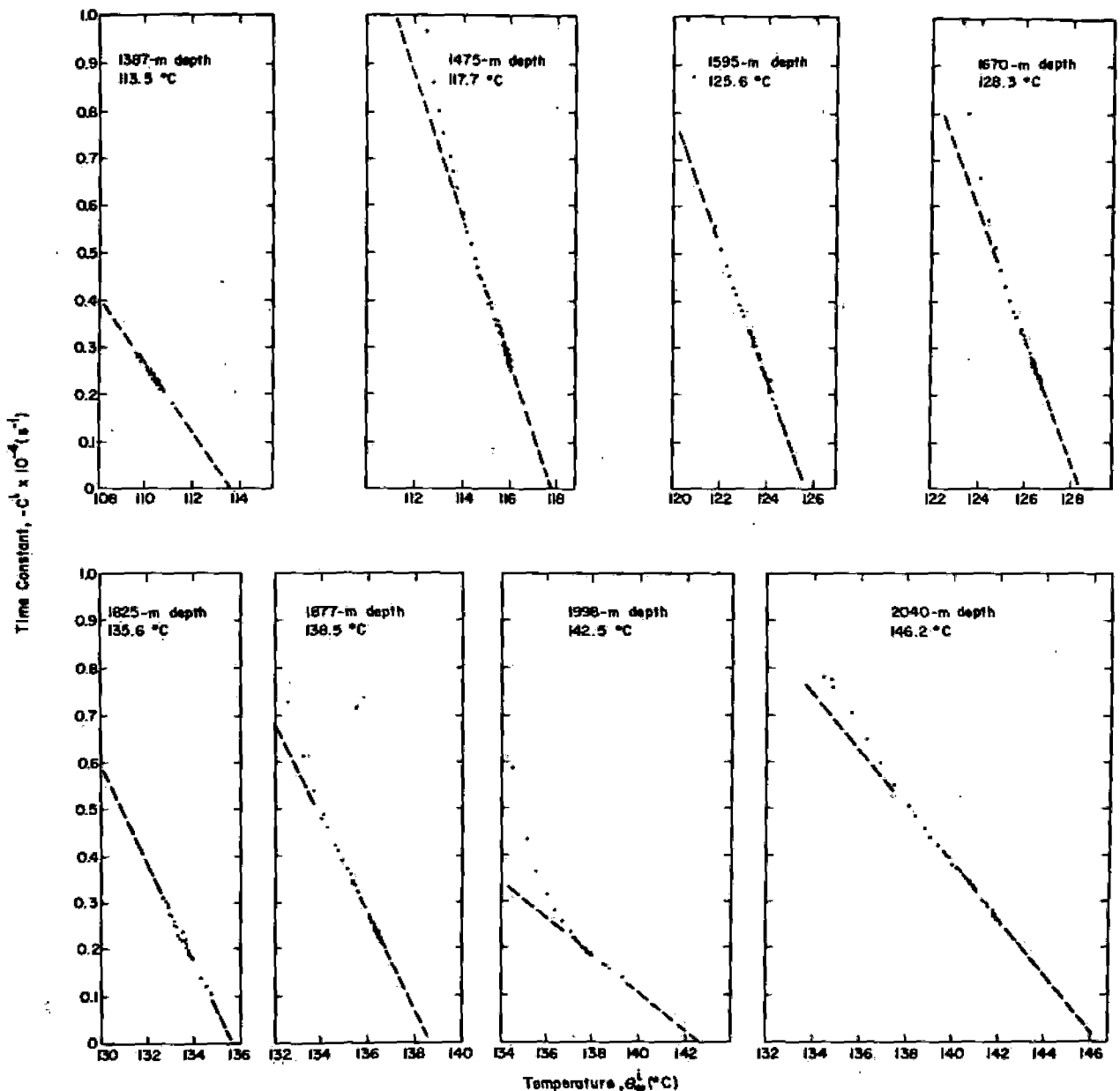


Figure 4. Equilibrium rock temperature determinations for various depths ($t^{+2} - t' \leq 1/2 h$; $t_2 - t_0 = 6 h$).

should not be affected, and the $c^2 \theta_0$ plots are essentially retraced.

Geothermal Gradient—Lower Precambrian Section

The geothermal gradient in the lower Precambrian section of GT-2, which is derived from the previous figure, is shown in Figure 5. The accuracy of each temperature determination is estimated to be $\pm 0.2^\circ C$, with a corresponding precision of better than $0.1^\circ C$ (except for the 2900 m, 9514 ft point). The average gradient throughout the entire section is $54^\circ C/km$, increasing from $50^\circ C/km$ in the 1.2- to 2.1-km (3940- to 6890-ft) interval to $60^\circ C/km$ in the 2.1- to 2.9-km (6890- to 9514-ft) interval.

SUMMARY

An empirical approach for reduction of bottom-hole temperature data can be used for determining equilibrium rock

temperatures. Data sufficient for these calculations can be collected during short interruptions in drilling. Estimates of equilibrium rock temperatures are consistent with theoretical and experimental results of previous investigators.

REFERENCES CITED

- Albright, J. N., 1975, Temperature measurements in the Precambrian section of Geothermal Test Hole No. 2: Los Alamos Scientific Lab. report.
- Cooper, L. R., and Jones, C., 1959, The determination of virgin strata temperature from observations in deep boreholes: *Geophysics*, v. 2, p. 116-131.
- Dennis, B. R., and Todd, B. E., 1975, Transducer technology for deep geothermal environments: 8th Transducer Workshop, Dayton, Ohio.
- Grisafi, T. W., Rieke, H. H., and Skidmore, D. R., 1974, Approximation of geothermal gradients in northern West Virginia using bottom-hole temperatures from electric

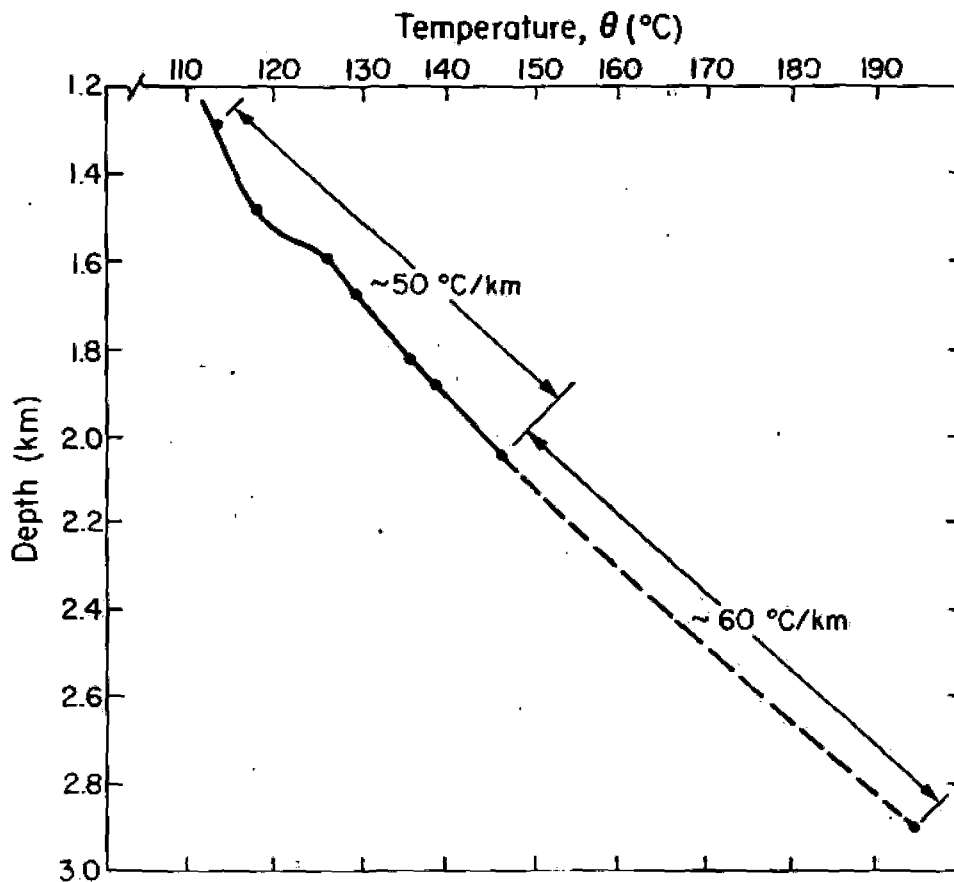


Figure 5. Geothermal gradient in the lower Precambrian section of GT-2 (1387 to 2900 m, 4550 to 9514 ft).

logs: Am. Assoc. Petroleum Geologists Bull. 58, p. 321-323.

Jaeger, J. C., 1965, Application of the theory of heat conduction to geothermal measurements, in Lee, W. H., ed., Terrestrial heat flow: Am. Geophys. Union Geophys. Mon. 8, Series 5.

Lachenbruch, A. H., and Brewer, M. C., 1959, Dissipation of the temperature effect in drilling a well in Arctic Alaska: U.S. Geol. Survey Bull. 1083-C, p. 73-109.

Muskat, M., 1937, Use of data on the buildup of bottom-hole pressures: American Inst. Mechanical Engineers Trans., v. 123, p. 44-48.

Nakaya, U., 1953, A method of analyzing geothermal data

in permafrost: Snow, Ice, and Permafrost Research Establishment Research Paper 5.

Pettitt, R. A., 1975, Planning, drilling, and logging of Geothermal Test Hole GT-2, phase I: Los Alamos Scientific Lab. progress report LA-5819-PR.

Summers, W. K., 1972, Approximation of thermal gradients in southeastern New Mexico using bottom-hole temperatures from electric logs: Am. Assoc. Petroleum Geologists Bull. 56, p. 2072-2074.

White, D., Fournier, R. O., Muffler, L. J. P., and Truesdell, A. H., 1975, Physical results of research drilling in thermal areas of Yellowstone National Park, Wyoming: U.S. Geol. Survey Prof. Paper 892.

Thermal Conductivity Measurement and Prediction from Geophysical Well Log Parameters with Borehole Application

SUBJ
GPHYS
Log
TCM

RONALD GOSS
JIM COMBS

Institute for Geosciences, The University of Texas at Dallas, P.O. Box 688, Richardson, Texas 75080, USA

ABSTRACT

Problems related to thermal conductivity measurements of rocks were examined using the divided-bar method. Thermal contact resistance, measurement pressure, and sample thickness were found to have significant effects on the measured thermal conductivity. For accurate determinations, the effect of pressure on reference standards must be known. Tentative values of K_p (mcal/cm·sec·°C) = $3.30 - 0.18 \times 10^{-3} P$ (bars) for fused silica, and $K_{pq} = 25.3 + 1.2 \times 10^{-3} P$ for Z-cut natural quartz crystals were obtained. Thermal contact resistance obscured these relationships below a uniaxial pressure of 150 bars.

Measurements on each of 50 samples were made for thermal conductivity, bulk density, porosity, permeability, electrical resistivity and conductivity, compressional and shear velocity, and free fluid index. These physical properties were analyzed to derive predictive equations for thermal conductivity. An empirical relationship developed for the Imperial Valley of southern California is $K_{pred} = 2.01 - 0.095 \Phi (\%) + 1.66 V_p$ (km/sec). A standard deviation of ± 0.7 mcg/cm·sec·°C implies a reliability of approximately 10% for the predicted thermal conductivity. Application of this relationship to thoroughly investigated geothermal borehole sections indicates that prediction from standard geophysical well logs may be more reliable than cell measurements in determining the thermal conductivity of unconsolidated sedimentary sequences.

INTRODUCTION

Knowledge of thermal conductivity is an absolute necessity in heat flow studies. It is an important parameter in the detection and development of geothermal fields. Similarly, thermal properties have importance for secondary and tertiary recovery techniques in the petroleum industry. Presently, the most economical and efficient approach to determine thermal conductivity is to collect samples from a borehole for laboratory analysis.

There are many problems in obtaining an accurate thermal conductivity value. The sample collection process is complex. For example, questions arise as to what interval of a borehole should be collected and how the in situ conditions, that is, saturation, pressure, temperature, and so on, should be reproduced. If properly prepared samples are obtained, laboratory measurements are reasonably accurate, although

relatively time consuming and expensive. The most common method for the determination of the thermal conductivity of earth materials is the divided-bar apparatus (Birch, 1950). Bar materials and designs are not standard and therefore each apparatus is subject to its own subtle problems.

Though values of thermal conductivity may be necessary in a particular study, the rock samples and requisite data are often not economically feasible to collect. Alternative approaches to obtaining thermal conductivities of rocks are needed.

In many circumstances, downhole and laboratory methods for measuring thermal conductivity are unsatisfactory. A conductivity logging tool would be ideal, but none exists. Many of the properties which are regularly measured during geophysical logging of boreholes relate to the same physical phenomena that control thermal conductivity; therefore it should be possible to derive thermal conductivity from a correlation with other physical properties.

Theoretical relationships between properties like thermal conductivity and velocity have been derived for specific media (Debye, 1914; Kittel, 1971). These theoretical relationships apply reasonably well only to ideal materials, not to rocks. Thus theoretical work is not likely to predict thermal conductivities in the earth.

Empirical studies have had some success (Karl, 1965; Tikhomirov, 1968; Anand, Somerton, and Goma, 1973). Most empirical studies have been concerned with either correlation of only one physical property at a time, or with suites of rocks from many different environments. Since thermal conductivity can seldom be related closely to rock type, the results of these studies have not been generally applicable.

In this study an attempt was made to find an empirical relationship between thermal conductivity and several physical properties in combination. Each set of physical properties including thermal conductivity was measured with the same sample. Details pertaining to the samples, experimental equipment, and measurement techniques are presented elsewhere (Goss, 1974).

A suite of samples, petrologically similar and obtained from the same geological environment, was chosen. An investigation was then made of possible extensions and limitations over a wider range of rock types. Finally, some use of, and application to, borehole logging data was included.

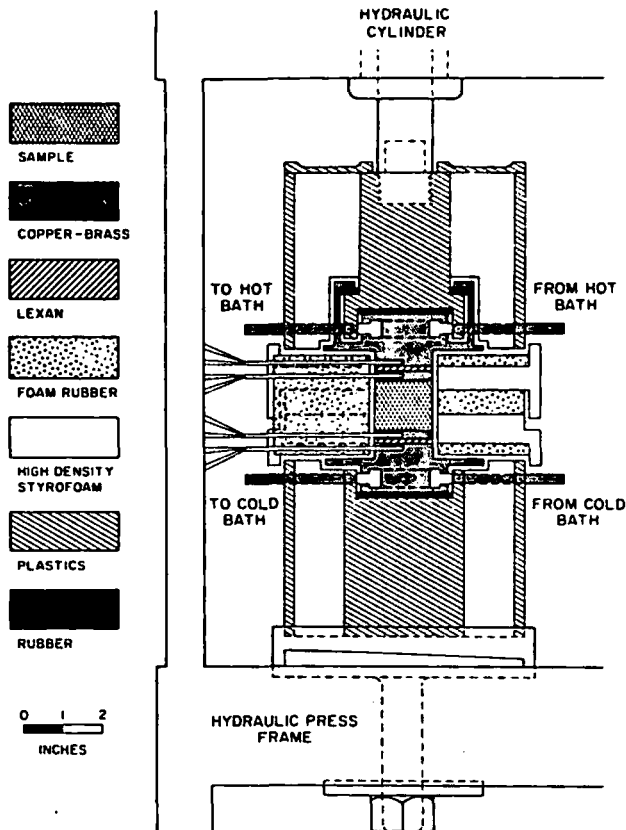


Figure 1. An idealized section for the divided-bar apparatus.

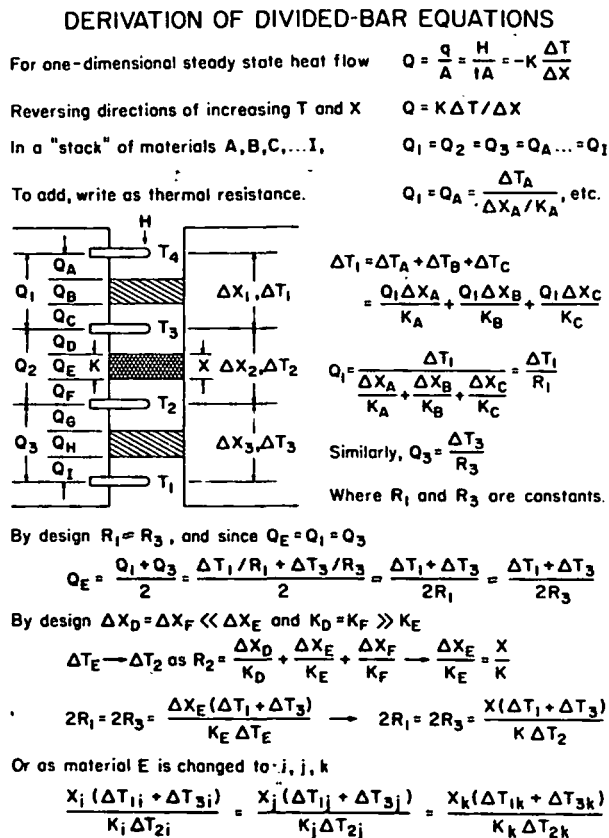


Figure 2. Theoretical derivation with basic assumptions for the steady-state comparative thermal conductivity technique using the divided-bar apparatus.

DIVIDED-BAR APPARATUS

An idealized section of the divided-bar used in the present study is shown in Figure 1. The design is an attempt to incorporate a short bar, having "constant" thermal resistance with a good insulation system capable of accepting a variable length sample. The theory for this design is presented in Figure 2. From Figure 2, it can be seen that any reference thermal conductivity standard gives a comparison factor

$$C^* = K_R^* \Delta T_{2R} / X_R (\Delta T_{1R} + \Delta T_{3R}) \quad (1)$$

In order to determine the thermal conductivity for an unknown sample, the comparison factor C is substituted into the following relationship

$$K = CX (\Delta T_1 + \Delta T_3) / \Delta T_2 \quad (2)$$

The calculation of the comparison factor C is based on the assumption that the thermal conductivity of the reference standard K_R^* is known and constant. However, C^* is found to be a function of pressure. Details of the effect of pressure on the thermal conductivity of reference materials will be published elsewhere (Goss and J. Combs, in preparation, 1975). Nevertheless, a few comments are appropriate.

Since the apparent pressure effect can be in opposite directions for different reference materials, it cannot be

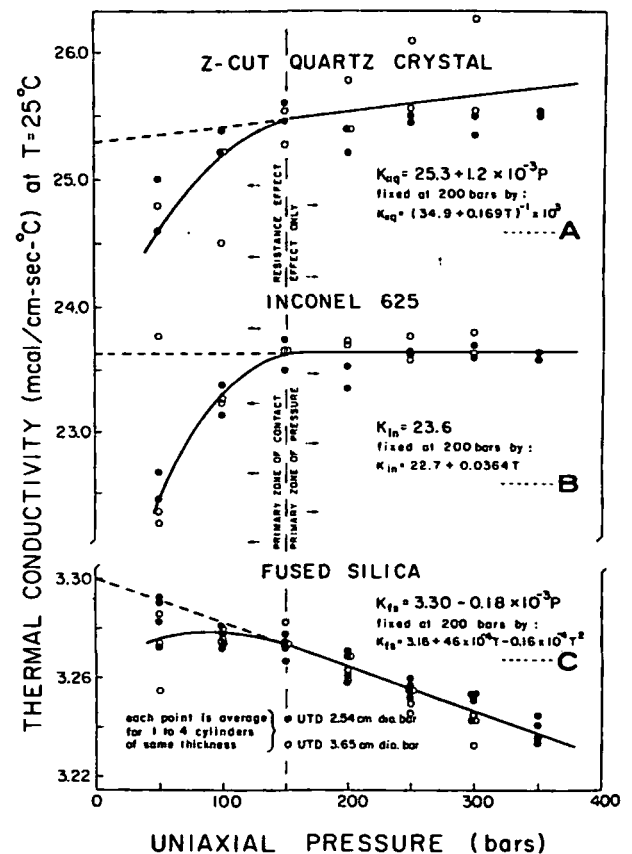


Figure 3. Thermal conductivity of three reference standards as a function of pressure at constant temperature. The curves are fixed to agree at 200 bars with the starting $K = f(T)$ as given by: (A) Mean of two equations given by Horai and Simmons (1969), (B) Linear fit to data between -80 to 80°C as published in Huntington Alloys (1970), (C) Ratcliffe (1959).

primarily an instrument effect. If it is assumed that all of the change is due to the effect of pressure on the reference thermal conductivity K_R^* , then use of the "true" reference conductivity which is a function of pressure, $K_R = f(P)$, would result in a constant comparison factor C .

Careful examination of the mathematical relationships in Figure 2 indicates that $K_R(P) = C_{avg}^* K_R^*/C^*(P)$, where the average measured comparison factor, C_{avg}^* , is used as an approximation to the constant C , should be a good approximation to the curve $K_R = f(P)$. This reduction has been performed for three reference materials and the results are plotted in Figure 3. The result,

$$K_{fs} = 3.30 - 0.18 \times 10^{-3} P \quad (3)$$

in which K_{fs} is in $\text{mcal/cm} \cdot \text{sec} \cdot ^\circ\text{C}$ and P is in bars, has been obtained for fused silica using General Electric (GE) types GE 101, GE 102, and GE 125 fused silica. A more tentative result for Z-cut natural quartz is

$$K_{\parallel q} = 25.3 + 1.2 \times 10^{-3} P \quad (4)$$

Inconel 625 was also investigated as one means of determining whether instrument effects were significant. Because of the elastic properties of this metal alloy, it would not be expected to have a discernible pressure effect over the considered range, 0 to 400 bar. From Figure 3, it can be seen that the assumption of insignificant pressure effects is correct for pressures above 150 bar. Below a pressure of 150 bar for all standards, thermal contact resistance at the bar-reference standard interface produces an apparent decrease in conductivity. Thermal contact resistance can be eliminated by using several thicknesses of a material, assuming the resistance of the bar material is well-known; or it may be successfully eliminated by calibration as

attempted here if all sample ends are similarly prepared and theoretical assumptions are verified.

The above method provides a reliable estimation of the slope for the pressure effects, but each curve (Fig. 3) must be tied to some known point for absolute values. K_R at $P = 200$ bar was chosen to agree with the K_R^* values obtained from the temperature functions of Figure 3 at $T = 25^\circ\text{C}$. This point was chosen since it is well above the contact resistance zone and probably in the range of confining pressures in which studies of the temperature effect on thermal conductivity of the reference materials were conducted.

A question exists as to whether the effect of pressure on the sample length, $X = f(P)$, can be ignored, as has been done. From the respective values of Young's modulus for these materials, $E_{fs} \approx 0.7$, $E_{\parallel q} \approx 1$ and $E_{in} \approx 3.5$ Mb, the maximum changes for the lengths of the standards are $\Delta L_{fs} \approx 0.001$, $\Delta L_{\parallel q} \approx 0.0009$, and $\Delta L_{in} \approx 0.0002$ cm. These changes of length would produce an effect of less than 0.002 for a typical value of $1.200 \text{ mcal/cm}^2 \cdot \text{sec} \cdot ^\circ\text{C}$, and can thus be neglected.

The present bar design (Fig. 1), in conjunction with an exceedingly stable $5\frac{1}{2}$ -digit multimeter manufactured by Systron-Donner, provided repeatability for C of ± 0.005 or about 0.5% for different runs with the same piece of standard material. C has been found to be a function of standard thickness X_R , differing slightly depending on the particular standard (Fig. 4). However, the overall C is essentially the same for either standard, implying that the theoretical assumptions were justified. Until further work with other standards is finished, no meaningful correction for thickness exists, and therefore reductions have been made to the mean curve of Figure 4. Since results may deviate by as much as $\pm 1.0\%$ from the mean curve, allowing for the same magnitude of effects on the unknown rock samples gives

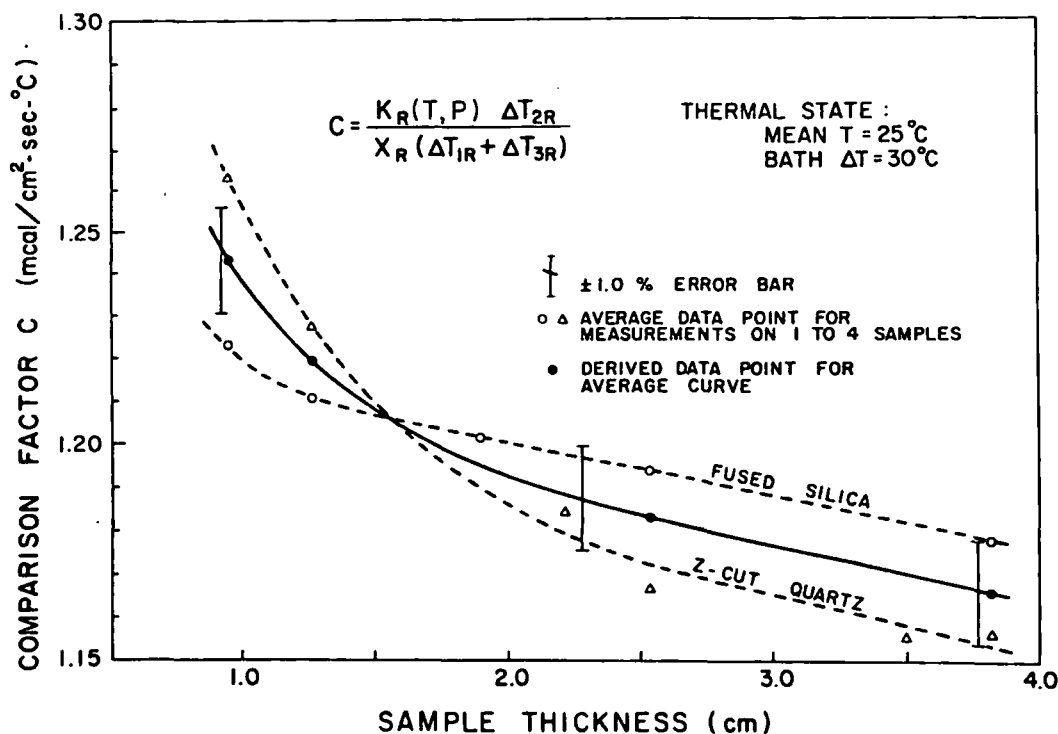


Figure 4. Comparison factor C as a function of sample thickness for two reference standards for the UCR 2.54-cm-diameter-bar.

an expected accuracy of 2% for a measured thermal conductivity value.

For measurements on borehole grab samples of drill chips and unconsolidated sediments, a cell arrangement similar to that described by Sass, Lachenbruch, and Munroe (1971) was used. The cell device essentially constitutes a new divided-bar design. The copper caps of the cell function as an extension of the bar. The cell device, therefore, would be expected to have a somewhat higher comparison factor C_c (that is, equation (1) where ΔT_2 is greater, ΔT_1 and ΔT_3 are the same or less) for its equivalent sample thickness (in the present study, 1.77 cm). This assumption was tested using four materials of known solid conductivity which were crushed and mixed with water. Each material gave a very similar C_c value after reversing the cell reduction calculations, that is, C_c was equal to 1.241 ± 0.006 $\text{mcal/cm}^2 \cdot \text{sec} \cdot ^\circ\text{C}$. The average C_c value was used for all cell reductions. As predicted, this C_c was higher than the equivalent for a fused silica standard, by about 3.5%.

All calculations involving thermal conductivity in aggregates, whether for the solid-liquid in a cell mixture or to convert the solid K_s to an in situ aggregate K_A based on the best estimate of saturated porosity, used the geometric mean equation for liquid volume fraction V

$$K_A = K_s^{1-V} K_L^V, \quad (5)$$

where the thermal conductivity of water is $K_L = 1.45$ $\text{mcal/cm} \cdot \text{sec} \cdot ^\circ\text{C}$. With the reduction estimates implied, cell measurement accuracy is 5 to 6%. However, with the common sampling problems for grab samples, for example, depth determination, drilling mud contamination, and in situ physical state, thermal conductivity values of 10% reliability are the best attainable for the cell technique.

EXPERIMENTAL DATA

Successively more general groups of samples have been collected and analyzed in this investigation. The first 25 core samples are from two exploratory holes at the Dunes geothermal anomaly in the Imperial Valley (Fig. 5). These Dunes samples vary from siltstones through graywackes to pebble sandstones, all having been hydrothermally altered and cemented (Bird, 1975).

An expanded group adds a Mesa core sample, and drill cuttings from boreholes drilled in the Mesa geothermal field. A set of these values represents averages over zones where

the logs and measurements changed conformably with each other. Five sets are from the deep zone (1670 to 1740 m) of the U.S. Bureau of Reclamation (USBR) Mesa No. 5-1 geothermal well, and eight sets of values are from the shallow zone (200 to 800 m) of the USBR Mesa No. 6-1 well. These Mesa samples are representative of the unconsolidated sediments of the Imperial Valley. This group of Dunes and Mesa samples covers most of the range of the Imperial Valley subsurface sedimentary section.

To provide some indication of the potential for generalization, a third suite of samples of Berea, Navajo (quartzite), and Raven Ridge sandstones was added. These samples, like most from areas other than the Imperial Valley, were taken from quarried blocks. They represent rock types or environments to which a sedimentary basin relationship might be expected to apply.

A final miscellaneous group of rock cores included three pieces of two limestones, a dolomite, a shale, and two pieces of a manufactured porcelain. The purpose for these final samples was to determine whether the predictive equations derived for sands and sandstones could be used for other rock types, or to indicate differences which might exist.

Physical properties which were measured include thermal conductivity (K), bulk density (D_B), porosity (Φ), permeability (k), saturated electrical resistivity (ρ) and electrical conductivity (σ), and compressional velocity (V_p). Shear velocity (V_s) and free fluid index (FFI) were also determined for the core samples (see Table 1). The conditions of investigation were 100% saturation with a sodium chloride brine of 160 000 ppm (fluid resistivity $\rho_w = 0.05$ $\text{ohm} \cdot \text{m}$). Temperatures near room condition (24°C) were used with uniaxial pressures of 200 bar.

DATA ANALYSIS AND RESULTS

In any empirical approach, many models are possible. The meager guidance of previous theory and investigations discussed below does not suggest or justify the use of anything beyond linear models. The statistically modest quantity of data indicates that sophisticated analytical methods would not be worthwhile. For these reasons, a straightforward multiple linear regression was considered adequate. For purposes of comparing different combinations of variables, goodness of fit, correlation coefficients, standardized partial regression coefficients, and F-tests were used (Davis, 1973).

Examination of Table 1 shows that the manufactured porcelain is an unusual material to consider as a rock analogue. For example, this porcelain is characterized by both very high porosity and high velocity; in addition, the measured thermal conductivity is twice that of any other sample. In spite of these apparently conflicting data, reasonable correlations could be obtained for a suite of materials including all core samples plus the porcelain, for example, a predicted thermal conductivity $K_{pred} = f(V_s, FFI)$ with a multiple correlation coefficient of $R = 0.91$. This is a forced fit because for the core samples alone, R drops drastically to 0.52. Since the correlations should not depend significantly on one type of sample, the porcelain was eliminated from further multiple regressions. The discussion of porcelain was presented to demonstrate a typical statistical pitfall.

Multiple regression techniques require uncorrelated variables, thus in the stepwise elimination of nonessential

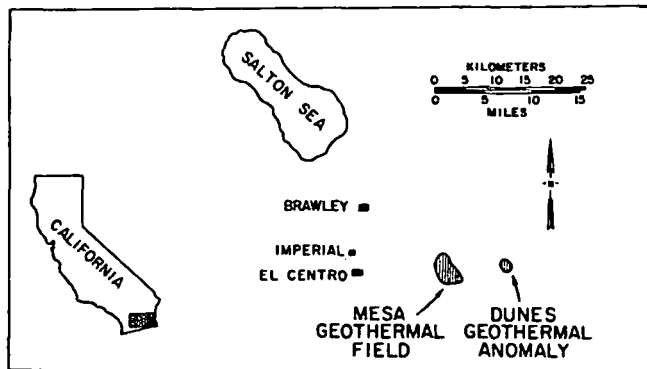


Figure 5. Imperial Valley location map, showing the Mesa geothermal field and the Dunes geothermal anomaly.

Table 1. Data from laboratory measurements of cores.

Identification	$\left(\frac{K}{\text{cm}\cdot\text{sec}\cdot^{\circ}\text{C}}\right)$	$\left(\frac{D_B}{\text{cm}^3}\right)$	Φ (%)	k (mdarc)	ρ (ohm·m)	$\left(\frac{\rightarrow F}{\rho}\right)$ (0.05 ohm·m)	$\left(\frac{\sigma}{\text{mmhos}}\right)$ ($\frac{\text{mmhos}}{\text{m}}$)	$\left(\frac{V_p}{\text{km}}\right)$ ($\frac{\text{km}}{\text{sec}}$)	$\left(\frac{V_s}{\text{km}}\right)$ ($\frac{\text{km}}{\text{sec}}$)	FFI (%)	
Dunes DWR 1 core data from 100 to 300 meters											
UCR-1	10.0	2.47	9.56	0.76	16.7	334	59.9	5.09	3.17	8.33	
UCR-2	10.0	2.49	8.62	0.50	23.6	472	42.4	5.07	3.23	6.52	
UCR-3	7.60	2.35	12.9	350	3.25	65.0	308	4.63	2.60	11.1	
UCR-4	9.99	2.46	10.4	15.0	8.04	161	124	5.03	3.13	8.61	
UCR-5	8.45	2.40	13.1	470	3.24	64.8	309	4.91	2.87	10.0	
UCR-6	9.76	2.44	11.3	7.8	5.32	106	188	4.86	3.01	8.68	
UCR-7	9.00	2.43	12.4	1.3	5.88	118	170	4.33	2.57	9.12	
UCR-8	8.01	2.35	18.5	62.0	2.83	56.6	353	4.01	2.24	11.7	
UCR-9	8.13	2.36	16.3	14.0	2.77	55.4	361	3.98	2.22	4.11	
UCR-10	8.16	2.36	16.5	39.0	2.72	54.4	368	3.88	2.15	11.2	
UCR-11	10.1	2.56	3.93	0.01	193	3860	5.18	5.54	3.49	2.91	
UCR-13	10.2	2.47	9.66	0.56	15.8	316	63.3	4.94	3.03	7.45	
UCR-14	10.0	2.56	4.16	0.08	497	9940	2.01	5.49	3.52	3.53	
UCR-15	10.3	2.55	3.14	0.02	445	8900	2.25	5.54	3.56	2.78	
UCR-16	10.8	2.54	5.32	0.02	154	3080	6.49	5.34	3.49	4.21	
UCR-17	10.0	2.53	5.90	0.02	58.2	1160	17.2	5.34	3.30	4.77	
UCR-18	10.4	2.55	4.64	0.01	90.1	1800	11.1	5.38	3.36	3.23	
UCR-19	10.0	2.51	7.64	0.16	23.8	476	42.0	5.14	3.17	5.97	
UCR-20	10.5	2.53	6.74	0.02	29.7	594	33.7	5.10	3.17	4.60	
UCR-21	10.1	2.53	6.44	0.38	31.7	634	31.5	5.35	3.32	5.07	
UCR-22	10.6	2.53	6.35	0.08	41.8	836	23.9	5.29	3.31	4.92	
UCR 115 core data, a few meters from Dunes hole											
115-A	9.50	2.50	8.09	0.59	21.2	424	47.2	5.09	3.50	6.53	
115-B	10.3	2.53	3.99	0.01	584	11700	1.71	5.25	3.52	3.21	
115-C	9.67	2.53	4.13	0.03	402	8040	2.49	5.31	3.73	3.37	
115-D	10.1	2.60	3.86	0.02	336	6720	2.98	5.31	3.56	2.87	
Core varieties, mostly quarried from reservoir rocks											
Sandstones											
BER	10.1	2.37	17.3	79	1.34	26.8	746	3.79	2.05	15.6	
MESA-2	7.66	2.51	8.39	0.07	4.41	88.2	227	3.94	2.08	6.5	
NAV-1	12.5	2.44	12.1	83	2.55	51.0	392	4.65	2.64	11.0	
NAV-2	12.5	2.44	11.9	100	2.55	51.0	392	4.66	2.65	10.8	
RAV	9.78	2.44	13.5	42	1.89	37.8	529	4.77	2.22	11.3	
Other											
ALH-2	9.33	2.28	21.0	460	1.19	23.8	840	3.81	2.03	18.9	
IND-1	5.75	2.47	13.5	0.55	4.81	96.2	208	4.75	2.42	11.5	
IND-2	5.73	2.47	13.7	0.36	3.94	78.8	254	4.72	2.40	12.0	
DOL	11.0	2.84	0.10	0.02	1940	38800	0.516	6.98	3.76	0.06	
SHA	8.13	2.65	1.20	0.05	54.2	1080	18.4	5.10	2.84	0.52	
POR-1	24.6	3.06	28.1	18.0	1.14	22.8	877	6.92	4.11	28.1	
POR-2	24.7	3.06	28.2	19.0	1.65	33.0	606	6.87	4.07	28.2	
Drill cuttings and borehole logged measurements*											
Mesa borehole	Depth (m)	K cell measure	D_B	Φ	"k" est. by SARABAND	ρ deep reading	$\rightarrow F$	σ	V_p	Temp. (°C)	Salin. (ppm)
MESA 5-1 log data (deep), avg of 3 for 10-meter intervals											
5	1680	4.2	2.25	24.0	90	6.4	7.1	160	3.11	150	1400
5	1690	3.6	2.30	21.0	40	7.1	12	140	3.30	150	2300
5	1700	4.2	2.25	19.6	110	4.0	8.9	290	3.16	150	3000
5	1710	3.8	2.23	22.6	60	4.4	6.8	240	2.83	150	2000
5	1730	4.2	2.30	20.3	32	8.0	6.7	170	3.40	150	1000
MESA 6-1 log data (shallow), avg of 3 for 30-meter intervals											
6	220	3.2	2.05	22.5	800	3.5	15	350	1.85	65	
6	470	4.4	2.10	21.6	80	1.7	17	600	2.27	80	
6	500	3.9	2.17	18.0	100	1.1	25	960	2.15	90	
6	560	3.6	2.15	20.0	70	1.7	20	630	2.28	100	
6	650	3.6	2.20	23.7	100	1.1	14	940	2.17	105	
6	680	3.9	2.17	24.3	200	1.3	14	770	2.32	110	
6	710	4.1	2.20	25.0	200	1.2	12	860	2.29	115	
6	740	3.6	2.20	22.5	100	1.2	15	840	2.26	120	

* D_B obtained from FDC log; Φ from FDC, CNL, and BHC logs; "k" is by SARABAND computer analysis, true k estimate only in a transition zone; ρ and σ from DIL-8 log; F calculated from Φ and ρ using R_w estimate for borehole 5 and the Humble equation for borehole 6; V_p from BHC log, and salinity from SARABAND computer analysis.

physical properties from the regression equations, special attention was given to the cancelling effect of obviously related variables. For example, neither compressional nor shear velocity was highly significant when both were included since each offsets the effect of the other. Each velocity, when taken one at a time, was one of the most significant variables. During the present investigation, electrical resistivity ρ , and $\log \rho$, electrical conductivity σ , formation factor F , $1/F$, and $\log F$ were all examined. The most significant functional forms were commonly ρ , σ and F . Therefore they are used in the present regression analysis. Free fluid index was one of the least significant variables. Final eliminations generally resulted in bulk density or porosity, permeability, or electrical conductivity, in addition to compressional velocity as the meaningful variables.

We obtained predicted thermal conductivity for the most significant variable, $K_{prd} = f(V_p)$, for each of the main groups of samples, and compared linear correlation coefficients, r . For the closely related Dunes core, r was equal to 0.825 ($N = 25$). With the Mesa samples added, r increased to 0.962 ($N = 39$), and the statistical significance improved dramatically. With all sandstones and chips, $r = 0.914$ ($N = 43$) and the significance also dropped, even though only a few samples were added. Finally, consideration of all rock types resulted in a much poorer fit with $r = 0.863$ ($N = 48$), where those types which were not from a similar geological environment fell in an essentially random pattern.

From this brief discussion, it can be seen that the best results were obtained with samples representing a specific geological environment. Three predictive equations for the 39 Imperial Valley samples are:

$$K_{prd} = -1.42 + 2.18 V_p, r = 0.962 \quad (6)$$

$$K_{prd} = 2.01 - 0.095 \Phi + 1.66 V_p, r = 0.966 \quad (7)$$

$$K_{prd} = -0.534 - 0.082 \Phi + 0.0019 \sigma + 2.11 V_p, r = 0.971 \quad (8)$$

where K_{prd} has units of $\text{mcal/cm}\cdot\text{sec}\cdot^\circ\text{C}$, V_p is in km/sec , Φ is in percent, and σ is in mmho .

Some other regression equations had equal or higher correlation coefficients, but were eliminated because they had constants which could conceivably cause unreasonably low or negative predictions; had coefficients an order of magnitude higher or lower than that for which the variable might account, implied that variables were simply canceling each other; or had physically incorrect signs on coefficients. Of the three regression equations above, (6) furnishes an excellent fit for one variable, although the negative constant coefficient is problematic. Equation (7) provides some improvement with no obvious defects. Equation (8) is reasonable and gives a higher multiple regression coefficient than Equations (6) or (7); however, Equation (8) has questionable application in the field because of the dependence of electrical conductivity, σ , on the single salinity saturating fluid used. As a result of these considerations, Equation (7) is deemed the most useful.

An indication of the scatter in the data can be seen in Figure 6, which is a multiple regression plot for Equation (7). A distinct separation exists between core sample data and log data. Although there is no suggestion of forced linearity, it would be desirable to have samples which fell into the intermediate range. The standard deviation for this

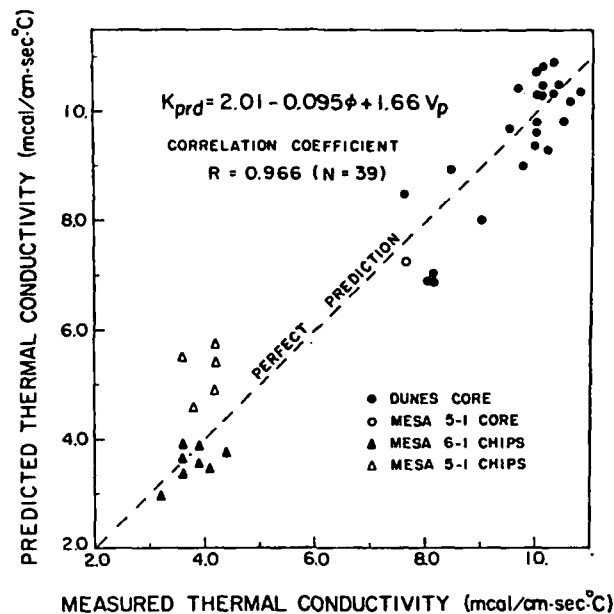


Figure 6. Measured versus predicted thermal conductivity for a multiple linear regression on the Imperial Valley samples, using Equation (7).

regression is $\pm 0.7 \text{ mcal/cm}\cdot\text{sec}\cdot^\circ\text{C}$, which implies a reliability of approximately 10% for the predicted thermal conductivity.

DISCUSSION

Many empirical investigations have involved thermal conductivity, but only a few have been concerned with the derivation of predictive equations from several physical parameters. Since a number of these empirical studies require specific data or constants which are not usually available, they were disregarded. The following are published relationships which did not require additional laboratory measurements beyond an analysis of geophysical borehole logs.

One of the earliest studies (Thornton, 1919), using data on insulators from ice to wood, resulted in the relation

$$K = V_p^2 D_B^2 \times 10^{-4}, \quad (9)$$

where velocity V_p is in cm/sec , the saturated bulk density D_B in g/cm^3 , and thermal conductivity K in $\text{cal/cm}\cdot\text{sec}\cdot^\circ\text{C}$. Dakhnov and Kjakonov (1952) used rock values from the literature to provide

$$K = D_B (3.1/4680) \quad (10)$$

With the same approach, for classes of feldspathic, salt, and other rock types Karl (1965) obtained

$$K = 0.8 \times 10^{-8} V_p \quad (11a)$$

$$K = 2.0 \times 10^{-8} V_p \quad (11b)$$

and

$$K = 1.3 \times 10^{-8} V_p \quad (11c)$$

respectively. Tikhomirov (1968) examined dry and partially saturated individual samples of many rock types, and com-

bined the results into one equation,

$$K = 1.30 \exp(0.58 D_D + 0.40 S_w) \quad (12)$$

where S_w is the fractional water saturation and D_D is the bulk density in the dry state. Using core from a wide region of the Siberian lowlands, Moiseyenko and coworkers (1970) derived the relation

$$K = [1.17 + 0.83(3.42 - 0.55\Phi)] 10^{-3} \quad (13)$$

where the term in parentheses is for the dry conductivity, and Φ is the porosity in percent. For a group of rock-forming silicate minerals, Horai (1971) obtained

$$V_p = 6.07 + 0.15 K \quad (14)$$

and

$$V_s = 3.37 + 0.08 K \quad (15)$$

where the thermal conductivities are in $\text{mcal/cm}\cdot\text{sec}\cdot^\circ\text{C}$, and the compressional and shear velocities in km/sec . If these equations are solved for K in the velocity range of normal rocks, however, they return meaningless negative thermal conductivities. In an experiment with unconsolidated sands, Somerton, Keese, and Chu (1974) found that

$$K' = 0.735 - 0.0130\Phi + 0.363 K'_s \sqrt{S_w} \quad (16)$$

where the prime will imply a result in $\text{Btu/ft}\cdot\text{hr}\cdot^\circ\text{F}$, and K'_s is the thermal conductivity of the solid or component grains. Of most direct interest for the present study is the work by Anand, Somerton, and Gomaa (1973) which yields for dry sandstones

$$K'_D = 0.340 D_D - 0.032\Phi + 0.53k^{0.10} + 0.013 F - 0.031 \quad (17)$$

and for saturated samples,

$$K' = K'_D \left[1.0 + 0.30 \left(\frac{K'_L}{K'_G} - 1.0 \right)^{0.33} + 4.57 \left(\frac{\Phi}{100 - \Phi} \frac{K'_L}{K'_D} \right)^{0.48m} \left(\frac{D_B}{D_D} \right)^{-4.3} \right] \quad (18)$$

where the permeability, k , is in millidarcies; K , Φ , and D are the thermal conductivity, porosity, and density, respectively, with subscripts D , L , and G , for dry rock, saturating liquid, and gas (air), respectively; m , an empirical parameter, is the cementation factor of Archie's formula

$$F = A/\Phi^m \quad (19)$$

with A another empirical parameter.

Most of the relationships presented above are deficient since they are not based on sets of variables measured for the same samples; instead values from the literature which are related by rock type were considered. The investigators have noted this problem and recommend that multiple measurements on the same samples be a future goal. Investigators who have made multiple measurements often note that velocity should have been a useful parameter, but was not available. When correlations are based on values for dry rock, the reductions for saturated samples tend to be involved and are not always effective for prediction. Results using different equations usually do not agree. Finally, there are not enough studies with their initial data published to determine limitations, areas of overlap, or reliability of extension to other samples.

A comparison of the results of the empirical equations described above with our results is listed in Table 2. None of the equations are completely satisfactory although it must be expected that Equation (7), which is partially based on these samples, will give the best fit. Thornton (1919) used many materials besides rock to obtain Equation (9); and as noted in Table 2, values range widely. Equation (10) yields exceedingly low values, probably because Dakhnov and Kjakonov (1952) used bulk densities of nonporous rocks. Of these published relationships, reasonable agreement of trend is provided by Equation (11c) from Karl (1965), although it is consistently low. Equation (12) derived by Tikhomirov (1968) from many consolidated rock types does not appear to allow for unconsolidated material. Equation (13) of Moiseyenko et al. (1970) from core samples smooths out to very low values. Equation (16) of Somerton, Keese, and Chu (1974) with the assumed solid conductivities used, does not differentiate the unconsolidated materials, even though the equation was derived for these. Finally, Equation (18) by Anand, Somerton, and Gomaa (1973) tends to give very high values especially when applied to the nonreservoir type samples.

None of these relations furnishes completely satisfactory predictions over the range of interest, and none is expected

Table 2. Comparison of prediction equations.

Sample Identification	9	Equation numbers for empirical relations					18*†	7	Measurement‡
		11c	12*	13	16*	$F_{\text{mea}}/F_{\text{est}}$			
		Thermal conductivity (mcal/cm·sec·°C)							
UCR-1§ (Dunes)	16	1.6	6.6	7.7	3.6	9.2	42/15	9.6	10
115-A§ (Dunes)	16	1.7	6.6	7.9	3.6	9.3	52/18	9.7	9.5
BER§ (Berea)	8.1	1.6	4.9	6.6	3.2	8.8	11/11	6.7	10
5-1680 (Mesa)	4.9	1.5	4.0	6.2	2.9	7.0	7.8/8.7	4.9	4.2
6-220 (Mesa)	1.4	1.4	2.4	5.6	3.0	7.1	9.1/9.1	2.9	3.2

*Requires assumed-dry density $D_D = D_p - 0.01\Phi$, saturation $S_w = 1.0$, and/or solid conductivity $K_s = 4.5 \text{ Btu/ft}\cdot\text{hr}\cdot^\circ\text{F}$ if sample is predominately quartz and 3.5 if significant clay in sample. Values based on discussion of Somerton, Keese, and Chu, (1974). †Requires an assumption for gas conductivity (air) $K_G = 0.055$, liquid conductivity (sea water) $K_L = 1.4$, and $m = 1.73$; values taken respectively from Ingersoll, Zobel, and Ingersoll (1954), Ratcliffe (1960), and Timur, Hemphkins, and Worthington (1972). Since the measured values of formation factor F_{mea} for the thermally altered samples are quite high, a comparison is also made using F_{est} values estimated from the relation $F = 1.13 V^{-1.73}$, $V = 0.01\Phi$ of Timur, Hemphkins, and Worthington (1972). ‡Thermal conductivity value obtained from measurement of the sample in a divided-bar apparatus. §Core samples. ||Unconsolidated material.

to give satisfactory results in the Imperial Valley geological environment. Therefore, we return to Equation (7), derived herein.

APPLICATION

Our ultimate goal is to determine thermal conductivity from common borehole logging parameters. Empirical relations are of little value unless they can predict reasonable thermal conductivities. We have made an initial attempt to predict thermal conductivities for the 300- to 700-m interval of a borehole from the Mesa geothermal field. Casing at 310 m and a convective thermal regime below 670 m determine the limits of useful investigation. Equation (7) has been applied.

The logs from which hand-digitized versions of Figure 7 were made, and a computer evaluation generated from them, provided the basic data for the predicted thermal conductivities. Measured values were taken from drill chips of the unconsolidated sediments, using a cell apparatus in the divided-bar (Sass, Lachenbruch, and Munroe, 1971). Problems exist in the accuracy of this method, for example, the effect of drilling mud, the uncertainty in depth, and the incompleteness of sampling. An ideal relationship with excellent measurements throughout could not be expected to provide exact agreement. As a minimum, however, both predicted and measured values should reflect similar changes with depth, with reasonable explanations for the differences.

From Figure 8, showing the deviations in repeatability for cell measurements (the line arbitrarily passes through the first measurement) with the differences of sampling

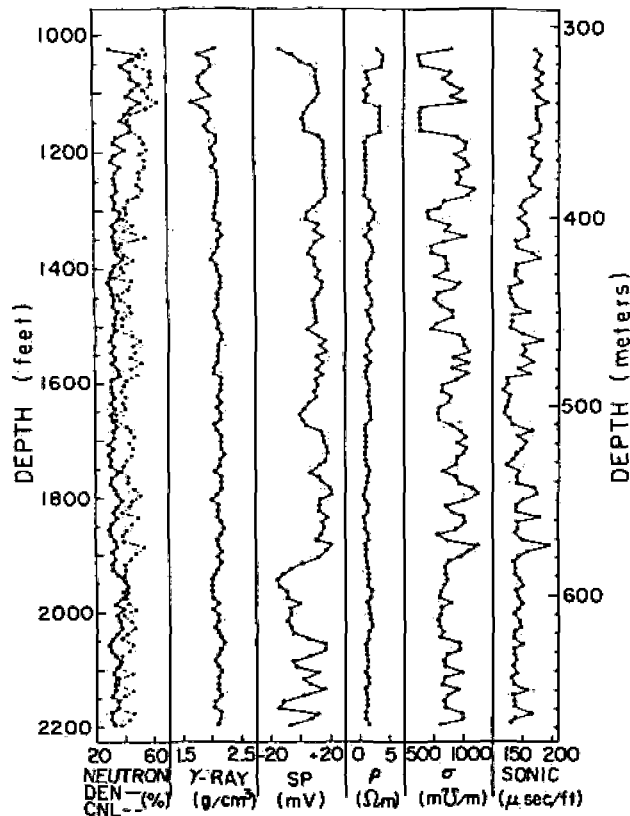


Figure 7. Digitized geophysical logs for the Mesa 5-1 geothermal well. Data points obtained from original logs by averaging over 3-m intervals.

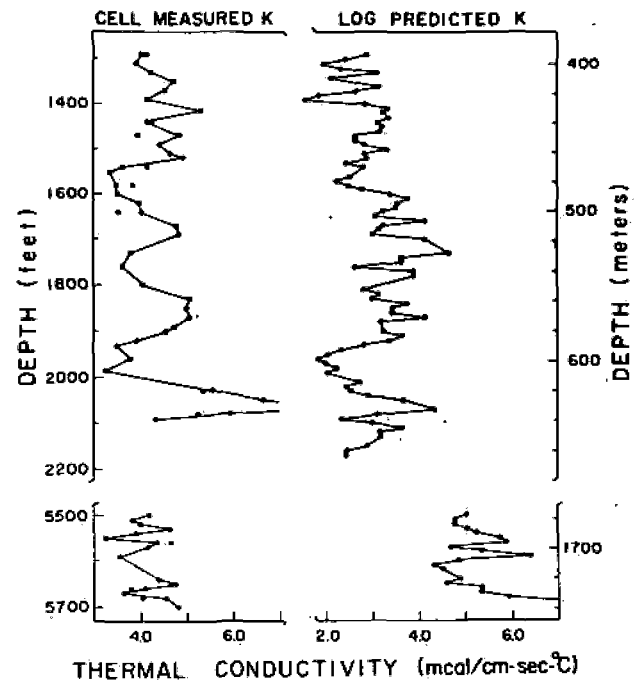


Figure 8. Thermal conductivities for the Mesa 5-1 geothermal well. Two cell data points at the same depth indicate repeated measurements. Log predictions are from Equation (7).

depth, it can be seen that agreement between measured and predicted trends with depth is quite good. However, there is a distinct difference in the mean value using the two methods, from a mean of near 4.5 compared to about 3 $\text{mcal/cm}\cdot\text{sec}\cdot^{\circ}\text{C}$. Field washing of the samples, which is certain to have depleted the clay content, probably caused the shift in the mean value of the two methods. Since computer evaluation of the geophysical logs indicates a relatively high content of clay (about 30%) in this shallow interval, higher measured values are expected.

For the deep zone, the shift is reversed from a mean near 4 to about 5 $\text{mcal/cm}\cdot\text{sec}\cdot^{\circ}\text{C}$. This is partly a cored section from which samples were taken for the prediction analysis and the values measured on the core samples were about 7 $\text{mcal/cm}\cdot\text{sec}\cdot^{\circ}\text{C}$. Deviations in this zone appear to be caused by a relative loss of sand from the drill chips reaching the surface. The core includes sections of clay-cemented sand; computer evaluation of the geophysical logs indicates less clay than in the shallower section, yet the grab samples consist of a considerable amount of shale fragments. There are also shifts with depth of about 10 m in this deep zone, but the gross patterns appear to follow closely. These shifts are almost certainly a result of poor control of sampling and the sampled depth as depth increased.

CONCLUSIONS

A divided-bar design has been developed which is rapid and easy to use. Under test, the design appears to meet or exceed the limits of most divided-bar apparatuses described in the literature. It has been used to estimate the pressure effects on thermal conductivity for three common reference standards and to investigate the effects of sample thickness. The pressure dependence of thermal conductivity for fused silica appears reliably established. Further work

on the two phenomena, pressure effects and sample thickness, are expected to clarify many subtle problems associated with the divided-bar technique.

A study of the possibility of using borehole logging parameters to predict thermal conductivity has been completed. There is every indication that useful empirical relationships can be obtained. Application of a predictive equation to a geological sequence similar to the one from which it was derived may be reliable. Although a relationship might remain useful in comparable environments, limitations must be determined. There seems little hope of more general predictive relationships being successful; however, typical geological settings can probably be characterized.

Experimental data and an empirical equation for the Imperial Valley of southern California have indicated satisfactory prediction of thermal conductivity in an initial application. In fact, we conclude that the indirect method of prediction may be more accurate than direct cell measurements on drill chips. This may well be true for most unconsolidated sedimentary environments.

ACKNOWLEDGMENTS

Part of this research was carried out while the authors were associated with the University of California, Riverside. Among those who have been particularly helpful at various stages of the project are Shawn Biehler, Lewis Cohen, Jean Davidson, Fumiko Goss, Frank Griswold, Ross Hager, Susan Hilton, and Jo Shearer. Financial support was provided by a University of California at Riverside Chancellor's Patent Fund Grant, the Chevron Oil Field Research Company, the U.S. Department of the Interior Bureau of Reclamation contract no. 14-06-300-2390, and by U.S. National Science Foundation-Research Applied to National Needs grants no. GI-36250 and AER 72-03551.

REFERENCES CITED

- Anand, J., Somerton, W. H., and Gomas, E., 1973, Predicting thermal conductivities of formations from other known properties: *Soc. Petroleum Engineers Jour.*, v. 13, p. 267-273.
- Bird, D. K., 1975, Geology and geochemistry of the Dunes hydrothermal system, Imperial Valley of California [M.S. thesis]: University of California, Riverside, 123 p.
- Birch, F., 1950, Flow of heat in the Front Range, Colorado: *Geol. Soc. America Bull.*, v. 61, p. 567-630.
- Dakhnov, V. N., and Kjakonov, D. J., 1952, Thermal investigation of fissures (Russian text): Moscow; cited in Karl, 1965, Sec. 2.1.3.
- Davis, J. C., 1973, Statistics and data analysis in geology: New York, Wiley and Sons, 550 p.
- Debye, P., 1914, Equation of state and quantum hypothesis, with an appendix on thermal conductivity (German text), in Von M. Planck et al., editors, *Lectures on the kinetic theory of matter and electricity*: Leipzig, Teubner, p. 19-60.
- Goss, R. D., 1974, Empirical relationships between thermal conductivity and other physical parameters in rocks [Ph.D. thesis]: University of California, Riverside, 216 p.
- Horai, K., 1971, Thermal conductivity of rock-forming minerals: *Jour. Geophys.*, v. 76, p. 1278-1308.
- Horai, K., and Simmons, G., 1969, Thermal conductivity of rock-forming minerals: *Earth and Planetary Sci. Letters*, v. 6, p. 359-368.
- Huntington Alloys, 1970, Inconel alloy 625 data catalog: Huntington, W. Va., International Nickel Company, 19 p.
- Ingersoll, L. R., Zobel, O. J., and Ingersoll, A. C., 1954, Heat conduction with engineering, geological and other applications: Madison, Wisconsin, University of Wisconsin Press, 325 p.
- Karl, R., 1965, Physical rock parameters, wave velocity, thermal conductivity, (German text): *Freiberger Forschungshefte, Series C*, v. 197, p. 7-76.
- Kittel, C., 1971, Introduction to solid state physics: New York, Wiley and Sons, 4th ed., 766 p.
- Moiseyenko, V. I., Doroginskaya, L. M., Leont'ev, Ye. I., and Sokolova, L. S., 1970, Dependence of the heat conductivity of the clastic rocks of the West Siberian Lowlands on other physical parameters (Russian text), in *Methods of determining the thermal properties of rocks: Akademy Nauk SSR Sibirsk, Otdeleniye Geologiya i Geofizika*, no. 2, p. 106-110.
- Ratcliffe, E. H., 1959, Thermal conductivities of fused and crystalline quartz: *British Jour. Appl. Physics*, v. 10, p. 22-25.
- , 1960, The thermal conductivities of ocean sediments: *Jour. Geophys. Research*, v. 65, p. 1535-1541.
- Sass, J. H., Lachenbruch, A. H., and Munroe, R. J., 1971, Thermal conductivity of rocks from measurements on fragments and its application to heat-flow determinations: *Jour. Geophys. Research*, v. 76, p. 3391-3401.
- Somerton, W. H., Keese, J. A., and Chu, S. L., 1974, Thermal behavior of unconsolidated oil sands: *Soc. Petroleum Engineers Jour.*, v. 14, p. 513-521.
- Thornton, W. M., 1919, The thermal conductivity of solid insulators: cited in Karl, 1965, Sec. 2.2.
- Tikhomirov, V. M., 1968, The thermal conductivity of rocks and its relationship to density, moisture content, and temperature (Russian text): *Neftianoe Khoziaistvo*, v. 46, p. 36-40.
- Timur, A., Hempkins, W. B., and Worthington, A. E., 1972, Porosity and pressure dependence of formation resistivity factor for sandstones: *Canadian Well Logging Society Trans.*, Fourth Formation Evaluation Symposium, Sec. D.

SUBJ
GPHYS
Log
TMDD

UNIVERSITY OF UTAH RESEARCH INSTITUTE

UURI

EARTH SCIENCE LABORATORY
420 CHIPETA WAY, SUITE 120
SALT LAKE CITY, UTAH 84108
TELEPHONE 801-581-5283

June 21, 1979

Research Department
Lynes, Inc.
504 Republic Building
1612 Tremont Place
Denver, Colorado 80202

Gentlemen:

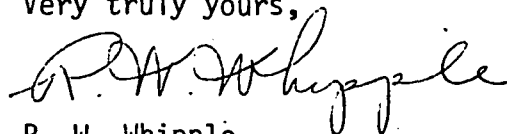
The Earth Sciences Laboratory of the University of Utah Research Institute is engaged in cataloguing temperatures recorded in drill stem tests. This is part of a program of studying sub-surface temperatures which might be of use in locating areas important from a geothermal energy standpoint.

Our first view of DST temperatures suggests that the scatter of values may be even greater than can be attributed to disequilibrium conditions due to the recent circulation of drilling fluids. We would be pleased to hear your comments on the reliability of temperatures measured in DST's. Are they, for example, always measured under approximately the same conditions and with the same instruments by you and other contractors, and with what precision are they measured?

Bottom hole temperatures from electric logs have been widely used for calculating geothermal gradients as in the recent Geothermal Survey of North America by the AAPG. Do you believe that temperatures from DST's are more or less reliable than these?

We appreciate that temperatures from DST's are not taken under laboratory conditions but we need a better understanding of how reliable they really are. Any information or comments from you in this regard would be appreciated.

Very truly yours,



R. W. Whipple
Geophysicist

RWW:ccw

UNIVERSITY OF UTAH RESEARCH INSTITUTE

UURI

EARTH SCIENCE LABORATORY
420 CHIPETA WAY, SUITE 120
SALT LAKE CITY, UTAH 84108
TELEPHONE 801-581-5283

June 21, 1979

Research Department
Schlumberger Well Services
Rocky Mountain Division Office
1450 Metrobank Building
475 - 17th Street
Denver, Colorado 80202

Gentlemen:

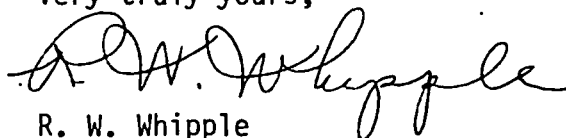
The Earth Sciences Laboratory of the University of Utah Research Institute is engaged in cataloguing temperatures recorded in drill stem tests. This is part of a program of studying subsurface temperatures which might be of use in locating areas important from a geothermal energy standpoint.

Our first view of DST temperatures suggests that the scatter of values may be even greater than can be attributed to disequilibrium conditions due to the recent circulation of drilling fluids. We would be pleased to hear your comments on the reliability of temperatures measured in DST's. Are they, for example, always measured under approximately the same conditions and with the same instruments by you and by other contractors, and with what precision are they measured?

Bottom hole temperatures from electric logs have been widely used for calculating geothermal gradients as in the recent Geothermal Survey of North America by the AAPG. Do you believe that temperatures from DST's are more or less reliable than these?

We appreciate that temperatures from DST's are not taken under laboratory conditions but we need a better understanding of how reliable they really are. Any information or comments from you in this regard would be appreciated.

Very truly yours,



R. W. Whipple
Geophysicist

RWW:ccw

UURI

EARTH SCIENCE LABORATORY
420 CHIPETA WAY, SUITE 120
SALT LAKE CITY, UTAH 84108
TELEPHONE 801-581-5283

June 21, 1979

Research Department
Halliburton Services
Drawer 1431
Duncan, Oklahoma 73533

Gentlemen:

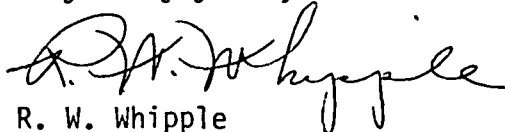
The Earth Sciences Laboratory of the University of Utah Research Institute is engaged in cataloguing temperatures recorded in drill stem tests. This is part of a program of studying sub-surface temperatures which might be of use in locating areas important from a geothermal energy standpoint.

Our first view of DST temperatures suggests that the scatter of values may be even greater than can be attributed to disequilibrium conditions due to the recent circulation of drilling fluids. We would be pleased to hear your comments on the reliability of temperatures measured in DST's. Are they, for example, always measured under approximately the same conditions and with the same instruments by you and other contractors, and with what precision are they measured?

Bottom hole temperatures from electric logs have been widely used for calculating geothermal gradients as in the recent Geothermal Survey of North America by the AAPG. Do you believe that temperatures from DST's are more or less reliable than these?

We appreciate that temperatures from DST's are not taken under laboratory conditions but we need a better understanding of how reliable they really are. Any information or comments from you in this regard would be appreciated.

Very truly yours,



R. W. Whipple
Geophysicist

RWW:ccw

JOHNSTON

Schlumberger

POST OFFICE BOX 36369
HOUSTON, TEXAS 77036
PHONE (713) 494-6161

August 16, 1979

Mr. R. W. Whipple, Geophysicist
University of Utah Research Institute
Earth Science Laboratory
420 Chipeta Way, Suite 120
Salt Lake City, Utah 84108

Dear Mr. Whipple:

With regard to your questions concerning temperatures measured during drillstem tests, I have the following comments. First, Mr. Troxel's comments concerning DST temperatures versus temperatures measured during electric logging are accurate. Temperatures measured during DST's are more representative of true formation temperature than electric log temperatures. However a note of caution is warranted regarding DST temperatures. Most DST's utilize a mechanical thermometer that records the maximum temperature encountered while the DST equipment is in the hole. Thus, if a shallow formation of higher temperature (geothermal gradient anomaly) than a deeper test formation is encountered during test string tripping, the true test formation temperature will not be recorded. In general, we at Johnston believe that DST temperatures usually reflect true formation temperature, because geothermal gradients are rarely negative with depth.

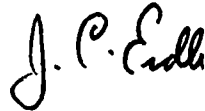
The accuracy of the thermometer used in most DST equipment is quite good (usually accurate to within plus or minus 0.2 degrees Centigrade at any temperature level). Recent DST's run by Johnston using a battery-powered electronic pressure/temperature recorder called the J-300 confirm the accuracy of the maximum recording mercury thermometer. The electronic J-300 recorder measures bottomhole temperature as often as every 30 seconds during the DST, including tripping in and out of the hole. An example of a DST

Mr. R. W. Whipple, Geophysicist
August 16, 1979
Page 2

run with the J-300 is attached for your information. The temperature recorded by the mercury thermometer is included for comparison.

I hope you will find this information useful. Should you have additional questions or comments, please write or phone at your convenience.

Regards,

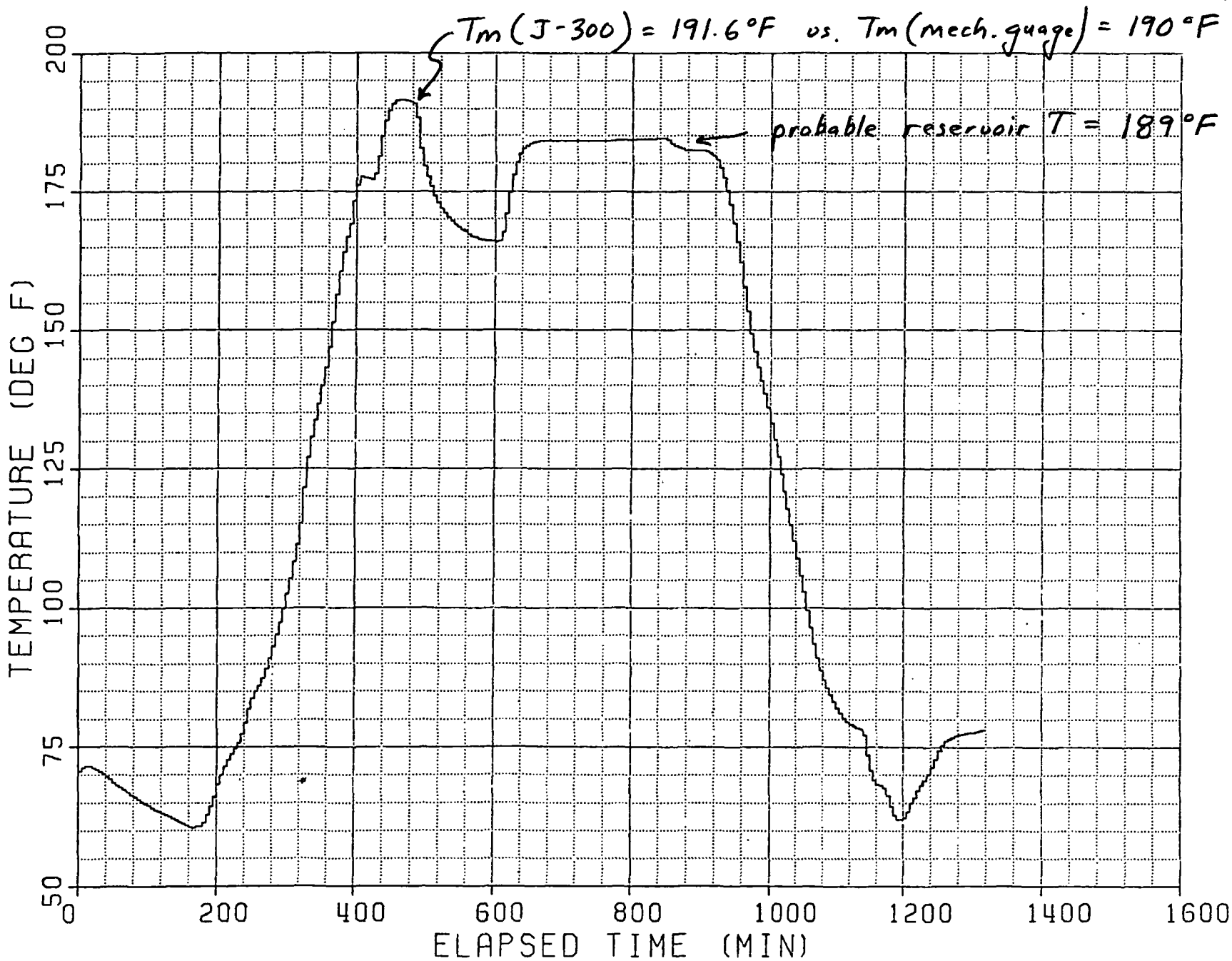
A handwritten signature in cursive script that reads "J. C. Erdle".

J. C. Erdle

JCE:et
cc: ATC
Bill Wiley
PSH

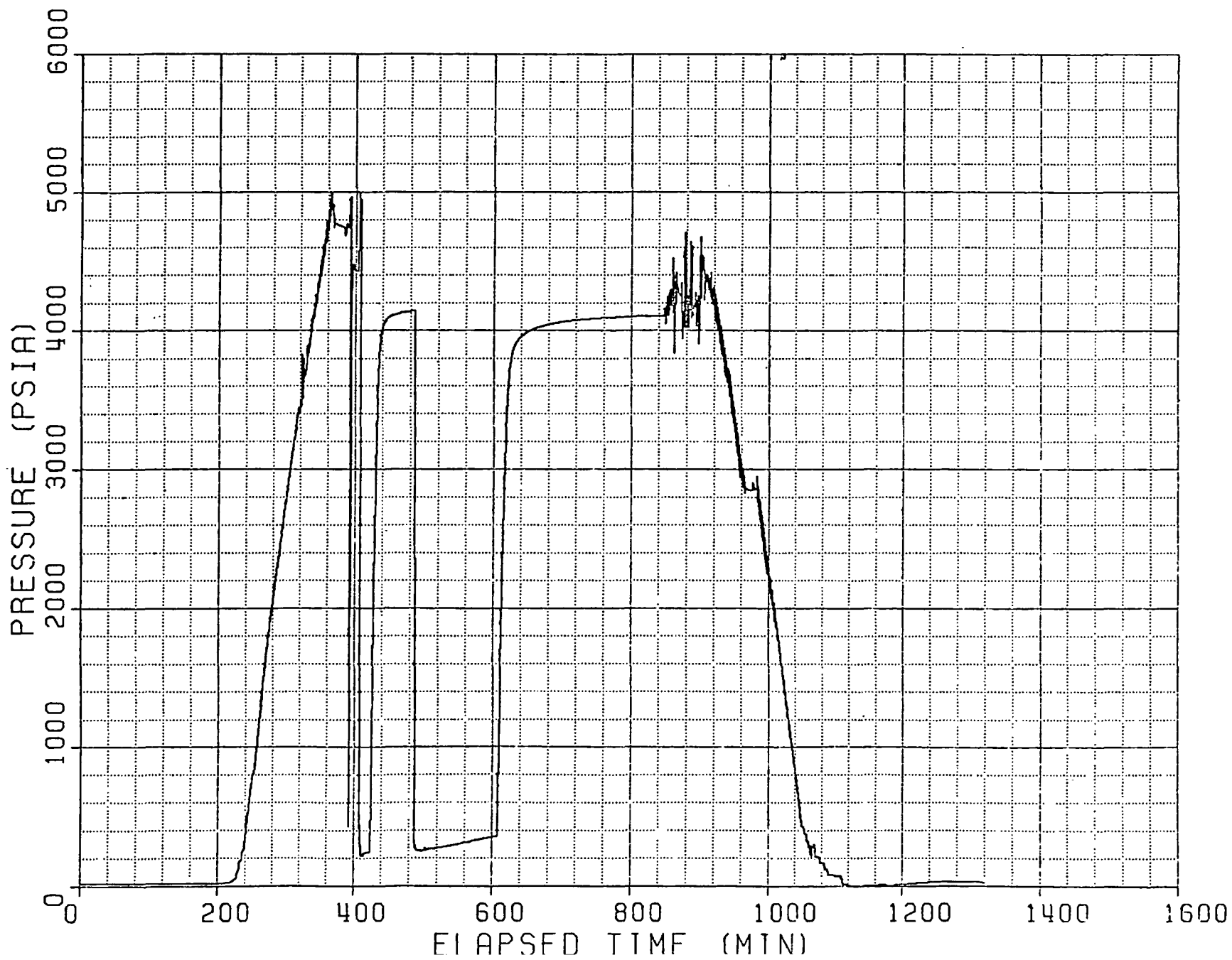
Temperature vs. Elapsed Time (entire test)

J-300 Recorder



Pressure vs. Elapsed Time (entire test)

J-300 Recorder



Field Report No. : ~~██████~~ D

<u>Label Point</u>	<u>Pressure Gauge T-335</u>	<u>Pressure SSDR</u>	<u>Pressure Difference</u>
Initial Hydrostatic	4870.01 psia	4759.15 psia	110.86
Start Flow	316.84	247.06	69.78
End Flow/Start Shut-in	361.11	244.06	117.05
End Shut-in	4268.03	4143.89	124.14
Start Flow	363.76	266.62	97.14
End Flow/Start Shut-in	461.22	360.88	100.34
End Shut-in	4228.05	4109.71	118.34
Final Hydrostatic	4372.10	4263.91	108.19

Comments:

1. Both T-335 and SSDR were inside recorders. T-335 was located 162 feet deeper than the SSDR, so the "Pressure Difference" should be about +80 psi for all points.
2. Temperature from the maximum recording thermometer was 190⁰F. Maximum SSDR temperature was 191.6⁰F.
3. In general, the SSDR and T-335 agree quite well.

CONSULTING

PRODUCING OIL

GRAHAM S. CAMPBELL

LIFE



MEMBER

CERTIFIED PROFESSIONAL GEOLOGIST #832
AND ENGINEER

A. P. G. S.
A. I. M. E.

DRILL STEM TESTERS:

RESEARCH DEPARTMENT

Schlumberger Well Services
Rocky Mountain Division Office
1450 Metrobank Building
475 - 17th Street
Denver, Colorado 80202

(303) 825-5207

RD

Lynes, Inc.
504 Republic Building
1612 Tremont Place
Denver, Colorado 80202

(303) 573-8027

RD

Halliburton Services
Drawer 1431
Duncan, Oklahoma 73533

(405) 251-3760

1600 Broadway, Suite 470
Denver, Colorado 80202

(303) 839-5241

(801) 355-8256 PARK CITY RES. 649-8734

510 WALKER BANK BLDG.
SALT LAKE CITY, UTAH 84111

Schlumberger

SCHLUMBERGER WELL SERVICES
6000 GULF FREEWAY, P.O. BOX 2175
HOUSTON, TEXAS 77001, (713) 926-4000

PLEASE REPLY TO
1450 METROBANK BUILDING
475 SEVENTEENTH STREET
DENVER, COLORADO 80202
(303) 825-5207

June 29, 1979

R.W. Whipple
University of Utah Research Institute
Earth Science Laboratory
420 Chipota Way, Suite 120
Salt Lake City, Utah 84108

Dear Mr. Whipple:

Since Schlumberger Well Services is a well logging company, I am referring your request to Johnston, a division of Schlumberger Technology Corporation. Johnston specializes in formation evaluation by drill-stem testing.

I would comment, though, on your reference to bottom hole temperatures obtained from electric logs versus bottom hole temperatures obtained from DST's. Since the temperature measured with a thermometer attached to a logging tool is greatly influenced by the cooling effect of mud at something near surface temperature being circulated in the borehole, it is obvious that this temperature should normally be considerably less than ambient formation temperature. The BHT obtained from a DST should more nearly represent ambient formation temperature since the DST represents a much longer time in the hole, and large quantities of formation fluid are frequently drawn from the formation. It is important in well logging that the temperature at the time which the measurement is made and in the environment in which the measurement is made be known accurately - hence, the BHT recorded with the logging tool.

I hope this information will be of benefit to you.

Good luck on your project.

Sincerely,



W.L. Troxel
Sales Development Engineer

WLT:m1

cc: Johnston
633 - 17th Street, Suite 1945
Denver, CO 80202

SCHLUMBERGER WELL SERVICES

A DIVISION OF SCHLUMBERGER TECHNOLOGY CORPORATION
1450 METROBANK BLDG. • 475 17TH STREET • DENVER, COLORADO 80202



LYNES

LYNES, INC. Domestic Division 504 Republic Building-1612 Tremont Place Denver, Colorado 80202 Phone: (303) 573-8027

June 28, 1979

Earth Science Laboratory
420 Chipeta Way, Suite 120
Salt Lake City, Utah 84108

ATTN: Mr. R. W. Whipple

In answering your questions as to the reliability of the bottom temperatures noted on drill stem test reports, personally I can not have as much confidence in these reports as in temperatures found from electric logging tools.

On most drill stem test operations, the temperature is taken with a thermometer of the shake down type, where the instrument is whirled down by centrifugal motion. The instrument then stays at the maximum reading reached until it is again whirled down. Again, I do not believe these thermometers are as reliable as those used by electric logging tools.

Occasionally we will use a temperature recorder that uses a chart to record temperature and time. These are precision instruments and are quite accurate. However, these tests are in the minority and the majority of tests are ran using the above instrument.

Thanks for your inquiry and I hope my opinions can be of use to you.

Very truly yours,

Wilber Baumann
SALES MANAGER, DRILL STEM TESTING

WB:s1

UNIVERSITY OF UTAH RESEARCH INSTITUTE

UURI

EARTH SCIENCE LABORATORY
420 CHIPETA WAY, SUITE 120
SALT LAKE CITY, UTAH 84108
TELEPHONE 801-581-5283

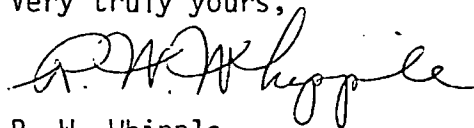
July 5, 1979

Mr. Wilber Baumann
Sales Manager, Drill Stem Testing
Lynes, Inc.
504 Republic Building
1612 Tremont Place
Denver, Colorado 80202

Dear Mr. Baumann:

Thank you for your comments on drill stem test temperatures.
We will give them due consideration in our investigations.

Very truly yours,



R. W. Whipple

RWW:ccw

UNIVERSITY OF UTAH RESEARCH INSTITUTE

UURI

EARTH SCIENCE LABORATORY
420 CHIPETA WAY, SUITE 120
SALT LAKE CITY, UTAH 84108
TELEPHONE 801-581-5283

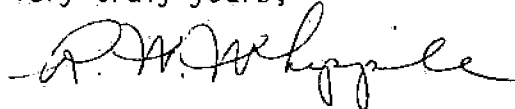
July 5, 1979

Mr. W. L. Troxel
Sales Development Engineer
Schlumberger Well Services
1450 Metro Bank Building
475 17th Street
Denver, Colorado 80202

Dear Mr. Troxel:

Thank you for your prompt reply to my inquiry about temperatures from drill stem tests. I am looking forward to hearing from your Mr. Johnston.

Very truly yours,



R. W. Whipple

RWW:ccw



HALLIBURTON SERVICES

DRAWER 1431, DUNCAN, OKLAHOMA 73533

July 2, 1979

Mr. R. W. Whipple
Geophysicist
University of Utah Research Institute
Earth Science Laboratory
420 Chipeta Way, Suite 120
Salt Lake City, Utah 84108

Dear Mr. Whipple:

The reliability of temperatures on a drill stem test are certainly sometimes questionable as you stated in your letter. This may be due in part to variations in the length of time since circulating the hole (dependent upon both depth and possible operational problems encountered). In the United States most temperatures are measured under basically the same conditions, that is a maximum registering temperature device is run near the bottom of the testing string and records only the maximum temperature observed during the test. These instruments can be either of two types. The most popular has been a maximum registering thermometer. As you can well imagine, these are difficult to shake down but the extreme vibration they are subjected to during a drill stem test always leaves a small doubt as to their reliability. A more positive recorder using a bi-metal temperature element driven by a mechanical clock has proven more accurate in temperatures up to 250°F. The reliability at higher temperatures is questionable as the laboratory tests have shown. They may vary as much as $\pm 10\%$ in the 300 to 400°F range.

We are currently introducing a new continuous recording temperature measuring device that appears to be much more accurate than either of the above mentioned instruments. The new temperature recorder is a modified Bourdon Tube type pressure recorder. The Bourdon Tube in this instrument is filled with a special gas mixture and has proven accurate to $\pm 2^\circ$ at 500°F. The data from these instruments should eventually prove more useful than either the previous drill stem test temperatures or the log temperatures as several people in the oil industry are investigating the possibility of extrapolating the data to static bottom hole temperature.

If you need additional information or we can be of further service, please advise.

Yours truly,

Glen Edwards
Section Supervisor

TRE - Client Services

Jp

UNIVERSITY OF UTAH
RESEARCH INSTITUTE
EARTH SCIENCE LAB.

THE TIME NECESSARY FOR A BORE HOLE TO ATTAIN
TEMPERATURE EQUILIBRIUM

E. C. Bullard, F.R.S.

(Received 1946 June 13)

Summary

The time for which it is necessary to leave a bore hole in order that the disturbance of temperature due to drilling may have disappeared is discussed.

During the drilling of a bore hole the temperature is disturbed by the heat generated by the tool and by the circulation of the drilling fluid. Of these two causes the latter has the larger effect and results in the lower part of the hole being cooled and the upper part heated. If temperatures measured in the hole are to be used for determining the geothermal gradient it is necessary that the well be left long enough for these disturbances to have subsided. This has long been recognized, but little attention seems to have been given to the estimation of the minimum time required.

As the hole approaches a point on its axis the temperature will start to fall, then, as the bottom passes the point, the fall will reach its maximum value. Thereafter it will be warmed by the drilling fluid ascending from the bottom of the bore and if the bore is deep enough the warming may exceed the original cooling. When drilling is finished the temperature distribution will gradually return to its original state by diffusion of heat to the surrounding rock.

The natural way to idealize this process for purposes of calculation is to assume that at any instant the temperature disturbance at the wall of the hole is a linear function of depth and is zero at half the depth reached at that time. If the depth is supposed to increase uniformly from zero to the final depth of the hole the problem can be formally stated, but is hopelessly intractable mathematically. ~~Fortunately, it will be shown below, the disturbance is negligible at distances of more than 5 metres from the hole.~~ The variation of the disturbance with depth can therefore be neglected when investigating its radial diffusion. Even with this simplification a prohibitive amount of arithmetical work would be required to obtain a solution, since the problem of heat conduction in a medium bounded internally by a cylinder has no convenient analytical solutions.* For the purpose of calculating

* H. S. Carslaw, *Introduction to the Mathematical Theory of the Conduction of Heat in Solids*, pp. 127-129, London, 1921; and J. C. Jaeger, *Phil. Mag.* (7), 26, 473-495, 1938.

A simple solution can be obtained for the temperature at the face of a narrow slot-like hole of indefinitely great depth and breadth. If it is cooled by an amount T_0 for a time t_1 , and then left for a further time t_2 , the temperature at the hole is $T_0 \left(1 - \frac{2}{\pi} \tan^{-1} \sqrt{\frac{t_2}{t_1}} \right)$ and reaches 1 per cent. of T_0 only after $t_2 = 4,000 t_1$.

the time necessary for the disturbance to become negligible it is probably sufficient to take the simpler problem of a constant linear source of heat on the axis of the hole. This source is supposed to start at the time the bore reaches the point and to continue till the bore is finished. The intensity of the source is chosen so as to give the correct temperature disturbance at the end of the boring.

This treatment does not deal correctly with the warming of the fluid in the hole after the bore is finished. It can however be shown that its heat capacity is small compared to that of the surrounding cooled rock.

Let the strength of the source be Q cal. sec.⁻¹ cm.⁻¹, and let it persist from time zero to t_1 . Then for times t less than t_1 the temperature T at a distance r from the hole will be

$$T = -\frac{Q}{4\pi k} Ei(-r^2/4kt),$$

where k is the diffusivity of the rock through which the hole is drilled and

$$-Ei(-z) = \int_z^\infty \frac{e^{-z}}{z} dz.$$

The temperature after t_1 may be calculated by adding to this solution that for a source $-Q$ starting at t_1 . The result is

$$T = \frac{Q}{4\pi k} \{Ei(-r^2/4kt_2) - Ei(-r^2/4kt)\},$$

where $t_2 = t - t_1$.

If T_0 be the temperature at the wall of the hole ($r = a$) at $t = t_1$, then

$$T = T_0 \{Ei(-r^2/4kt_2) - Ei(-r^2/4kt)\} / Ei(-a^2/4kt_1).$$

In calculating the temperatures at the wall of the hole the approximation

$$Ei(-z) = \log_e z + 0.577 \dots,$$

valid when z is small may be used giving

$$T/T_0 = \log(1 + t_1/t_2) / (\log 4kt/a^2 - 0.577). \quad (1)$$

A table of $Ei(-z)$ covering small values of the argument is given by Wenzel.*

T = T_0 (2)

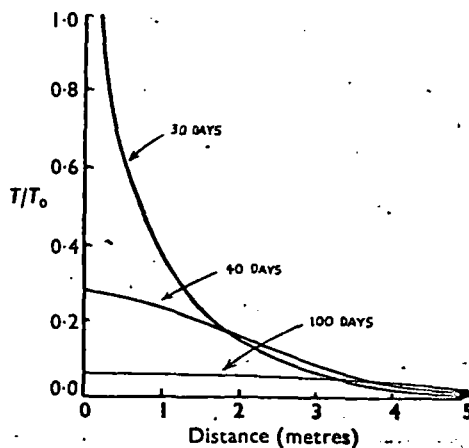


FIG. 1.—Radial distribution of temperature after 30, 40 and 100 days from the start of drilling.

* L. K. Wenzel, U.S. Geol. Surv. Water Supply Paper, No. 887, p. 89, 1942.

The extreme values of $a^2/4k$ likely to be encountered in practice are given by a hole 5 cm. in diameter in quartzite of diffusivity 0.027 cm.²/sec. and by one 60 cm. in diameter in shales of diffusivity 0.006 cm.²/sec., $a^2/4k$ therefore lies between 58 and 38,000.

A typical case ($a = 20$ cm., $k = 0.01$, $t_1 = 30$ days) has been worked out in detail. Fig. 1 gives the radial distribution of temperature after 30, 40 and 100 days from the start of boring. This shows the small spread of the cooling referred to above. Fig. 2 gives the variation with time of the temperature at the wall of the hole, plotted on a logarithmic scale.

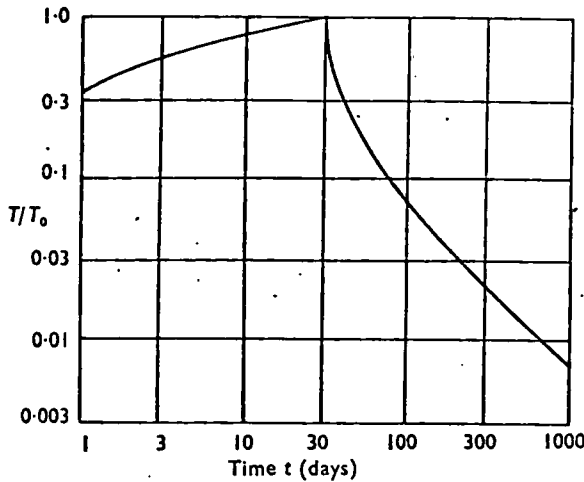


FIG. 2.—Temperature at the wall of the hole.

The disturbance will not reverse the normal geothermal gradient though it may be great enough to halve it.* Thus if enough time is allowed for the disturbance to fall to 1 per cent. of its value at the end of drilling the gradient will not be seriously falsified.

As the denominator in (1) varies slowly it is best used to calculate, as a function of t_1 , the value of t_2/t_1 needed to reduce the disturbance to 1 per cent. of its initial value. This has been done for the extreme values of $a^2/4k$. The results are

t_1	0.1	1	10	100 days	
t_2/t_1	14	11	8.8	7.4	for $a^2/4k = 58$
t_2/t_1	51	28	18	13	for $a^2/4k = 38,000$

t_2/t_1 is the time that it is necessary to leave the hole after drilling has stopped, expressed as a multiple of the time between the hole reaching the point and the end of drilling. For the whole hole to get within 1 per cent. of equilibrium it will therefore be necessary to leave it for 10 or 20 times the time taken to drill. Equilibrium near the bottom, where the disturbance has not lasted so long, will naturally be attained more rapidly. An exact calculation would be difficult but Fig. 1 suggests that the cooling will not start till the bore is within 5 metres of the bottom, and that equilibrium will be attained in 10 or 20 times the time elapsing between reaching that point and the final stopping of the circulation of fluid.

* E. G. Leonardon, *Geophysics*, 1, 115-126, 1936.

These considerations make it likely that many months must elapse before the whole depth of a bore recovers from the effects of drilling but that the bottom hole temperatures may, when drilling has been fast, be taken after as little as a day from the end of drilling. Recovery from the temperature disturbance caused by prolonged production may take many years.

In order to make the calculation possible it has been necessary to depart rather far from the actual state of affairs. The expressions given above should therefore only be used for calculating a limit to the magnitude of the disturbance and not for correcting observed temperatures.

A series of measurements taken at varying periods after the end of drilling would be of interest.

*Department of Geodesy and Geophysics,
Downing Place, Cambridge:
1946 June 11.*

terr
of h
geol
char
disc
10,0
0.31
influ
eight
agrec
Grea

1. *Intr*
flow have b
been made
paper deals
complicated
In the y
the Anglo-
The data hi
and L. A. P.
made by lo
Thermomet
meters is les
The Mas
strike. The
by the Fars
divisions. /
Masjid-i-Sul
of the anticli
have been re
region has be
The temj
behaviour of

SUBJ
GPHYS
Log
TSG

TEMPERATURE SURVEYS IN GAS PRODUCING WELLS

K. S. KUNZ

Schlumberger Well Surveying Corp.
Ridgefield, Conn.

M. P. TIXIER

Schlumberger Well Surveying Corp.
Houston, Texas

**UNIVERSITY OF UTAH
RESEARCH INSTITUTE
EARTH SCIENCE LAB.**

Reprinted From
July, 1955, Issue

~~JOURNAL OF PETROLEUM TECHNOLOGY~~

Schlumberger K-2

permit in general a correct estimation of their possible productions. This is because the formations encountered in those wells are consolidated with low permeabilities, and, as a rule, are artificially treated by shooting or hydraulic fracturing to stimulate the production.

In the following, the principles of the interpretation of the temperature logs will be explained first. Next, the practical applications of the temperature curves, combined with the other logs, will be discussed using actual field examples. Finally, an outline of the mathematical treatment of the problem will be given.

PRINCIPLES OF INTERPRETATION OF TEMPERATURE CURVES

Gas escaping from a high pressure producing bed into a dry hole undergoes a considerable cooling. This cool gas-mixes eventually with warmer gas coming from below and produces a drop in the temperature log opposite a gas zone, which may attain 20° F or more* (see field examples). The amount of cooling is determined by several factors:

1. The radial distribution of pressure in the bed, which in turn depends on the permeability and porosity of the formation and the length of time the bed has been producing.
2. The thickness of the bed.
3. The thermal conductivity of the formation.
4. The amount of gas produced compared to the amount coming from below (for the case of a producing zone located above one or several other producing beds).

DETERMINATION OF THE BOUNDARIES OF THE GAS PRODUCING ZONES.

Determination of the boundaries of the gas producing zones is based on the knowledge of the shape of the temperature log at the various levels of the gas-producing zones. The shape of the curve is different according to whether the producing zone is the closest to the bottom of the hole or is located above.

Fig. 1 shows the typical shapes of the temperature log computed in the case of two beds which are supposed to produce about the same amount of gas, the lower bed being the first producing zone from the bottom. The graph traced on the figure should be considered as being somewhat schematic because several simplifying assumptions have been involved in the computation. The geothermal gradient, in particular, has been neglected and it has been assumed that all the cooling takes place substantially at the wall of the hole. It has been also supposed for the computation that there was no vertical heat exchange: in practice therefore the sharp breaks indicated on the theoretical curve will not be observed in actual surveys but will be rather rounded as shown qualitatively by the dashed line. Despite those approximations, the essential difference in shape between the lower and the upper bed is clearly indicated: at the level of the lower bed the temperature curve shows a plateau *AB*, *A* and *B* being located respectively at each boundary of the bed. At the level of the upper

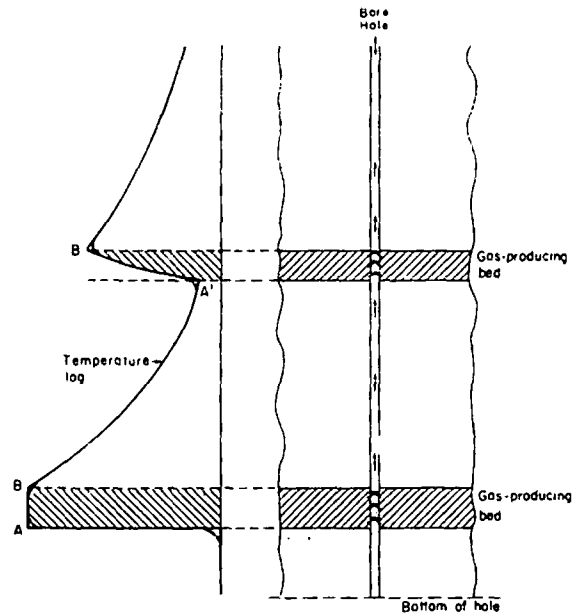


FIG. 1—COMPARATIVE SHAPES OF THE TEMPERATURE LOG OPPOSITE A GAS-PRODUCING BED FIRST FROM BOTTOM OF HOLE, AND A GAS-PRODUCING BED LOCATED ABOVE. (DERIVED FROM APPROXIMATE COMPUTATIONS WITH GEOTHERMAL GRADIENT NEGLECTED.)

bed, a continuous decrease of temperature is observed from *A'* opposite the bottom boundary to *B'* opposite the top boundary.

TEMPERATURE CURVE ABOVE A PRODUCING ZONE

It is supposed that the thermal conductivity of the formation above the bed is sensibly uniform, which seems to be the case in general, and that there is no other producing zone at a short distance above. The corresponding theoretical derivations will be given later on. Results of interest for the practical interpretation of the temperature logs are explained below (Fig. 2)*^o

1. At the level of the producing bed, the gas undergoes cooling and, therefore, immediately above the bed it will be gaining heat from the formation; its temperature is lower than that of the formation. But at a great distance above the producing bed (assuming that there is no other gas zone or other temperature disturbance), the temperature *T'* of the formations remote from the wall has become so much lower, in conformity with the geothermal gradient, that now the gas will be losing heat to the formations. In between, there is some point *I* which will be called the inversion point, where there is no heat exchange between the gas and the formation. There, obviously, the temperature *T* of the gas should equal that of the formation *T'*; in other words, at the point *I*, the temperature log crosses the geothermal gradient. This inversion point should correspond to a maximum of the temperature curve. Above *I*, the temperature in the borehole decreases as the depth decreases, until an asymptotic line is reached. The asymptotic line is parallel to the geothermal gradient.
2. The asymptotic line may be found by going up the temperature log until it is essentially straight and draw-

*In the conventional conditions of wells filled with mud, the temperature logs are run at a time when the gas is prevented from flowing by the mud column. The distribution of the temperature along the borehole is different in that case from that existing in gas producing wells. The discussion of the present paper, therefore, cannot be extended without change to the case of wells filled with mud.

^{oo}In Fig. 2 the curve is represented above a bed such as the upper bed in Fig. 1; the same discussion, of course, would be valid for a bed such as the lower one.

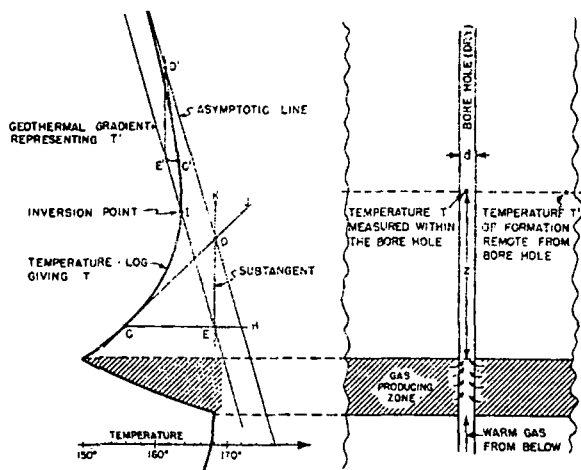


FIG. 2 — TEMPERATURE LOG ABOVE A GAS-PRODUCING ZONE, DETERMINED BY COMPUTATION.

ing a straight line approximating this portion of the log. It is necessary to go far enough above the gas zone to obtain a nearly straight portion of the log — but not too far, however, because the theory assumes that the thermal conductivity of the formation does not change. In practice, the log can be expected to become nearly straight a few hundred feet above the producing zone.

3. The amount of gas produced by a given bed can be derived theoretically from the slope of the curve above the bed. A convenient way for this derivation consists in tracing the *sub-tangent* to the curve. Through any point *C* on the curve above the producing bed, a tangent *CJ* and a horizontal line *CH* can be traced. The vertical line through the intersection at *D* of the tangent *CJ* and of the asymptotic line crosses *CH* in a point *E* which is located on the geothermal gradient line. The line *DE* is the sub-tangent to the curve at a point *C*. The length of the sub-tangent is constant whatever the location of the point *C* above the producing zone (this is illustrated on Fig. 2 where the sub-tangents *DE* and *D'E'* at two different points *C* and *C'* are traced).

The length *L* of the sub-tangent is proportional to the total amount of gas produced by all the beds located below. For practical purposes, a relationship $M = CL$ can be used, where *M* is the production of gas in thousands of cubic feet per day, at atmospheric pressure, and *L* is the length of the sub-tangent in feet. The proportionality coefficient *C* depends on the time elapsed between the beginning of production and the measurements. Its value also depends on the thermal conductivity of the formation, the hole diameter... and on the presence or the absence of a casing. The curve of Fig. 3 is a plot of *C* vs time. The curve was computed for an open hole, 6 in diameter, taking for the thermal conductivity of the formation a value of .0041 cal./degree cm*. This curve can be used, as a first approximation, for the analysis of the temperature logs.

APPLICATION OF TEMPERATURE CURVES — FIELD EXAMPLES

The application of the temperature curves will be discussed on field examples, coming from the San Juan Basin, N. Mex.

*This is the value of *K* for freshly cut sandstone as given in the Smithsonian Physical Tables, 8th Revised Edition, page 275.

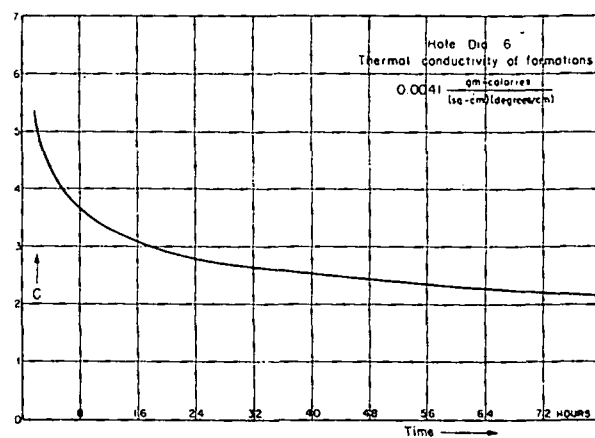


FIG. 3 — PLOT OF *C* VS TIME IN THE GAS PRODUCTION FORMULA $M = CL$.

M — gas production in thousands of cubic feet per day at atmospheric pressure.
L — sub-tangent in the temperature log measured in feet.

The wells in that region are drilled with water base mud until the top of the gas producing series is reached. The conventional electrical log and the MicroLog then are run and the casing is set. Next, the wells are drilled deeper with dry gas. The temperature log, radioactivity logs, the Induction Log, and eventually the Section Gauge log are recorded while the gas is flowing from the formations. While in the initial period of exploitation most of the wells were shot with nitroglycerine, this procedure is being replaced more and more frequently with hydraulic fracturing.

The producing series includes two main reservoirs referred to in the following as A and B. Reservoir A is usually indicated by the radioactivity and Induction Logs. Reservoir B (the lower one), does not always appear as clearly on the logs. The porosities of the reservoir formations are shown by core analysis to vary between 10 and 15 per cent, the permeabilities are very low — around 1 md.

EXAMPLE 1

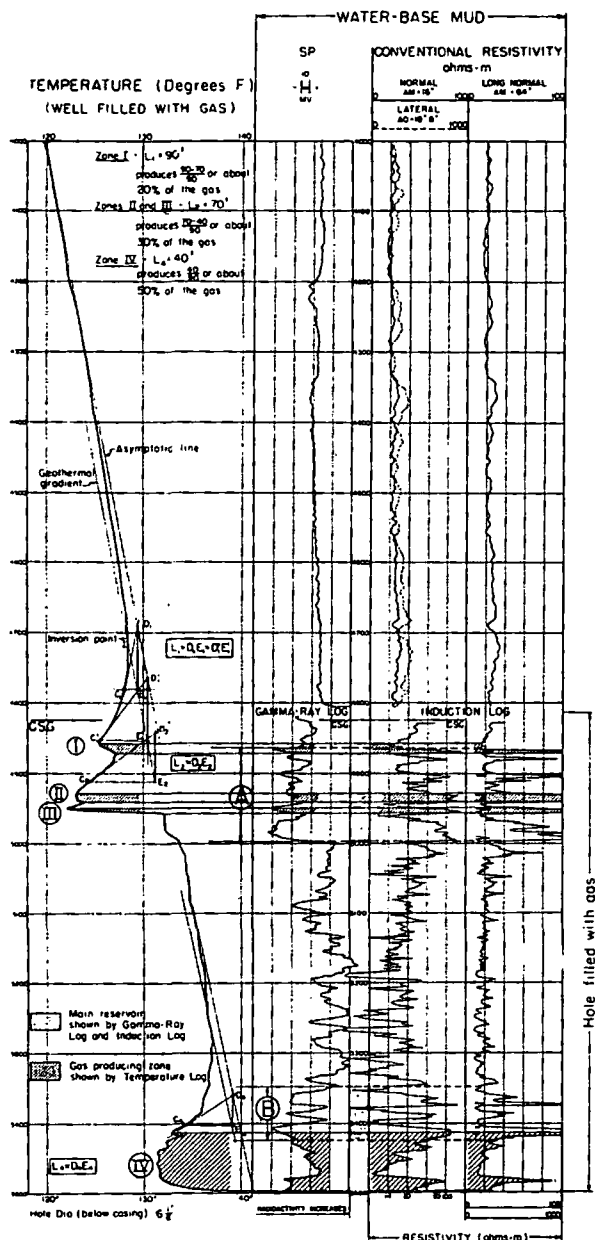
The left-hand track shows the temperature curve recorded in the well while flowing gas and before hydraulic fracturing.

The conventional resistivity curves and the SP curve recorded in water base mud prior to running the casing are traced in the upper right-hand portion of the drawing.

The Gamma Ray Log and the Induction Log, run in the hole filled with gas, are represented at the bottom part. Two Induction Logging curves are traced, which are the reproductions of the same measurements with a hyperbolic and a linear resistivity scale**, respectively.

The part of the well where these two logs were run corresponds to the producing series. The formations are a sequence of sandstones and shales interbedded. Over sections A and B, the proportion of sandstones is greater than in the other portions of the well (the average radioactivity is lower). The resistivities of the sandstones observed on the Induction Log are comparatively high, which suggests the presence of gas. Sections A and B correspond approximately to the two main reservoirs.

**In fact, the Induction Log is primarily a "conductivity log" recorded with a linear conductivity scale, counted from the right to the left. This conductivity scale, when numbered in terms of resistivity, gives the hyperbolic resistivity scale. The curve with the linear resistivity scale is the reciprocal of the conductivity curve.



EXAMPLE 1 — TEMPERATURE SURVEY IN GAS-PRODUCING WELL BEFORE FRACTURING, SAN JUAN BASIN, N. MEX., 1953.

Four main cooling effects, corresponding to four gas producing zones, numbered I to IV are observed on the temperature log.

Zone IV is the closest to the bottom of the hole. If the minor fluctuations are neglected, the curve opposite this section has roughly the shape of a plateau, as described in the theoretical analysis illustrated in Fig. 1. Zones I and III show the characteristic shape defined in Fig. 1 for beds overlying other gas producing zones. Zone II is a very short distance above zone III, and accordingly does not give rise to a large relative deflection.

The comparison of the temperature, the gamma ray, and the Induction Logs shows that zone I straddles the top boundary of section A and includes a part of the overlying shales. Zone II apparently is a shaly sandstone, zone III a sandstone, both located within section

A. Zone IV is mostly shaly, and is located almost entirely below section B.

The asymptotic line has been traced above zone I. Also two sub-tangents D , E , and D' , E' , have been constructed at two points C , and C' , of the curve, and have been found to be substantially equal.

The line drawn through the extremities E , E' , of the sub-tangents is, of course, parallel to the asymptotic line and furthermore crosses the temperature curve approximately at the inversion point I . This line is the geothermal gradient. These results tend to confirm the theory.

It is not possible to trace the asymptotic line above zone II, because the distance from I to II is too short. The sub-tangent D , E , can nevertheless be determined, using the geothermal gradient line.

No such construction is possible for zone III, because the portion of curve between III and II is so short that a tangent cannot be well defined.

An asymptotic line, and a sub-tangent D , E , are also traced for zone IV.

The respective lengths L_1 , L_2 , L_4 of the sub-tangents opposite zones I, II and IV are 90 ft, 70 ft and 40 ft.

The proportions of the total production contributed by each zone are therefore:

Zone I	$\frac{90-70}{90}$	or about 20 per cent
Zones II and III	$\frac{70-40}{90}$	or about 30 per cent
Zone IV	$\frac{40}{90}$	or about 50 per cent.

Taking for the C coefficient a value of 3.5, which corresponds to about eight hours elapsed between the beginning of the production and the time of the logging operation (see Fig. 3), the total production of the well is found to be equal to $3.5 \times 90 = 280$ Mcf/D.

This figure can be compared to the value of 412 Mcf/D measured at the well. The difference is reasonably small, if one considers the various sources of error inherent in the computation (in particular the value of C is obtained from a curve computed for open hole, whereas the well above zone I is cased. Perhaps also, the measurement of the amount of gas produced is not entirely accurate either.)

EXAMPLE 2

In the present instance, after setting the casing the well was drilled with gas to 4,962 ft and a first temperature log was recorded down to the bottom (solid line on the drawing). A first cooling effect can be observed below the casing (zone I), and another one at some distance below (zone II)*. Following this survey, this section was fractured with 10,000 gal of oil and 10,000 lb of sand. The measured production increased from 300 Mcf to 1,850 Mcf/D.

After fracturing, the well was deepened to 5,479 ft and a second temperature survey was made. This second temperature survey shows the effect of hydraulic fracturing in the section from casing to 4,962 ft (dotted line). The lower section, from 4,962 ft to bottom had not been fractured at the time of the second survey (line in dash-dots).

*Zone II is very thin, which explains why the curve does not show a sizeable plateau.

The cool anomalies observed on the second temperature log are located in the same places as zones I and II respectively. The curves opposite and above zone II are little different, which indicates that the production from this zone has not changed appreciably. On the contrary, the slopes of the two curves above zone I are markedly different, and their comparison shows that the production from zone I has considerably increased after fracturing.

The comparative productions of zone I before and after treatment can be roughly estimated in the present case, using the construction of the sub-tangents DE and $D'E$.

The ratio $D'E/DE = 300 \text{ ft}/65 \text{ ft} = 4.5$, compared to $1,850/300$ or about 6, as measured.

It can be said also that, if C is again taken to be 3.5, the respective productions calculated before and after fracturing would be equal to 230 Mcf and 1,000 Mcf/D, against 300 and 1,850 measured.

It is furthermore noticed that the amplitude of the cooling anomaly at the level of zone I is much smaller after fracturing than before. An explanation can be tentatively suggested for this somewhat surprising effect: after the process of fracturing, the permeability of the formation, on the average, becomes large around the borehole; beyond this the formation is not affected and the permeability remains small. Accordingly, when the gas is flowing, the radial pressure gradient is comparatively small near the borehole and becomes great only where the formation is untouched. In other words, the greatest part of the cooling occurs far enough from the borehole that the temperature in the borehole is comparatively little influenced.

EXAMPLE 3

A first temperature survey was made in this well down to the bottom at 5,475 ft before fracturing. One main cooling effect (zone I) is shown, at the level of a sandstone within reservoir A. The second temperature curve, recorded after fracturing, shows this productive zone widely extended upward, throughout the top part of reservoir A and the overlying shaly interval (zone I').

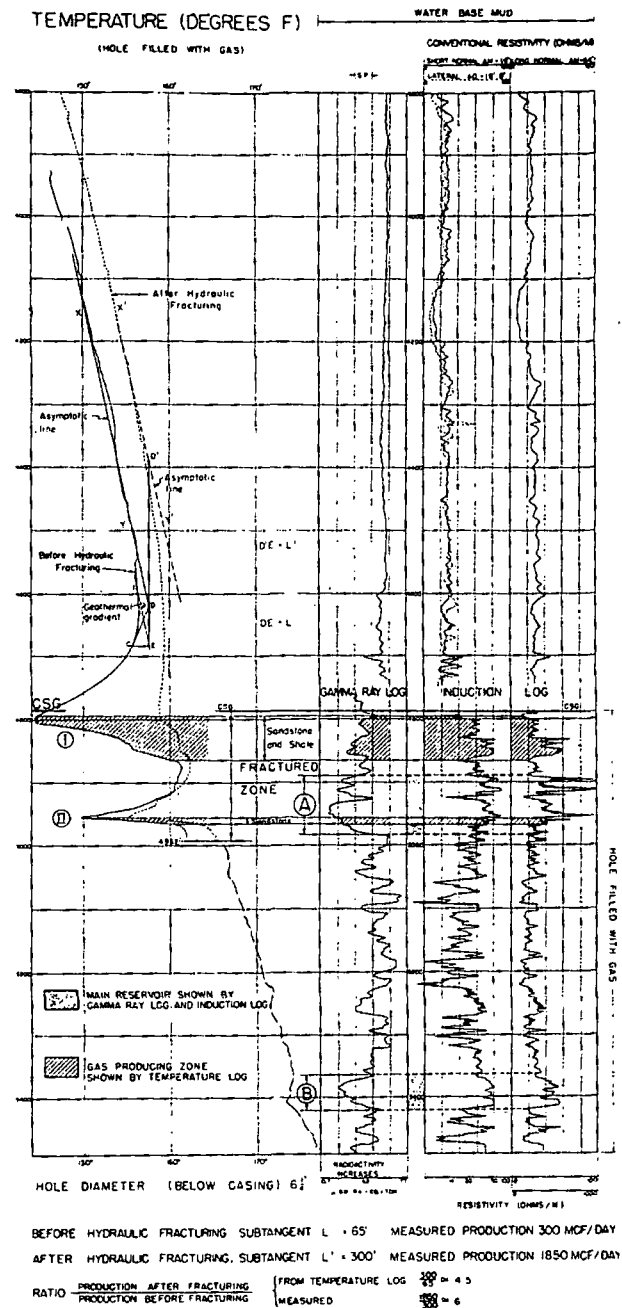
The comparison of the slopes of the two curves, above zones I and I' respectively, brings to the light the important increase of production after treatment. No sub-tangents are traced for comparison in the present example, because the curve after fracturing was not recorded high enough to make possible the construction of an asymptotic line.

The log also shows several other zones, which produce small amounts of gas (sharp breaks in the curve): Zone II and zone II' are sandstones. Zone III' is a shale, zone IV' is at the boundary of a shale and a sandstone, and zone V' includes both sandstones and shales.

EXAMPLE 4

This survey was also made under conditions identical to the ones described in the preceding examples. The first temperature log shows two gas producing sandstones I and II, within reservoir A. After fracturing, the second curve shows a large cooling anomaly at I', just below the casing. (Actually, the upper boundary of the gas producing zone is the casing shoe itself.) A comparatively small deflection of the curve is still observed in the vicinity of beds I and II.

The curves, therefore, show that the bulk of the production after fracturing comes from a new zone I',



EXAMPLE 2 — TEMPERATURE SURVEYS IN GAS-PRODUCING WELLS BEFORE AND AFTER HYDRAULIC FRACTURING, SAN JUAN BASIN, N. MEX., 1954.

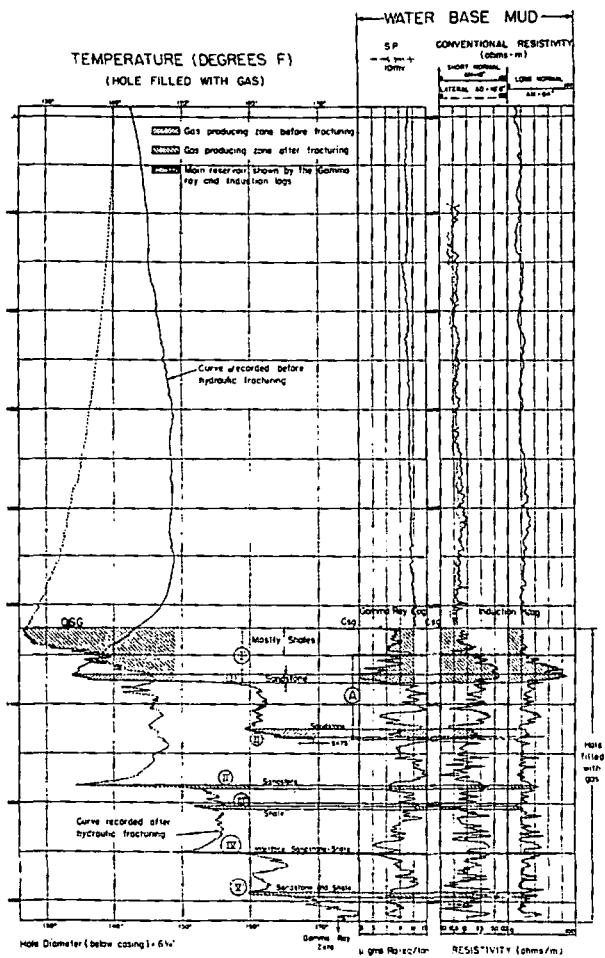
which was not producing before fracturing. This zone is located within a shaly interval at some distance above the main reservoir.

DISCUSSION

OBSERVATIONS

The observations made on the logs and illustrated by the above typical examples can be summarized as follows:

1. The production of gas may come from intervals different from the main reservoir rocks, and this particularly after hydraulic fracturing.
2. The gas producing intervals are often located within those zones where shales are predominant, or near



EXAMPLE 3 — TEMPERATURE SURVEY IN GAS-PRODUCING WELL SHOWING THE EXTENSION UPWARD OF THE MAIN GAS-PRODUCING ZONE AFTER HYDRAULIC FRACTURING (I, BEFORE FRACTURING — I', AFTER FRACTURING).

the boundaries between comparatively thick shales and sandstones.

3. The gas producing zones after fracturing very often are not at the same depths as before treatment.

When the logging operations were started in this basin, the wells were not yet treated by hydraulic fracturing, and the observation that the gas would escape preferentially across the shaly sections seemed rather surprising. Later on, this tendency has become more conspicuous and systematic in the wells surveyed after fracturing.

It has been, therefore, tentatively concluded that the gas may be produced from secondary reservoirs, such as sequences of thin sandstones within shaly intervals, and/or that it may migrate from the main reservoirs along fractures, either natural or induced, connecting those reservoirs with shaly sections.

One point of particular interest is that in many instances the temperature logs show the gas coming out from the boundaries between sandstones and shales. Furthermore, those shaly zones which are the main gas producers are actually sequences of numerous thin shales and sandstones. In other words, they contain a large number of sand-shale interfaces, which, in the

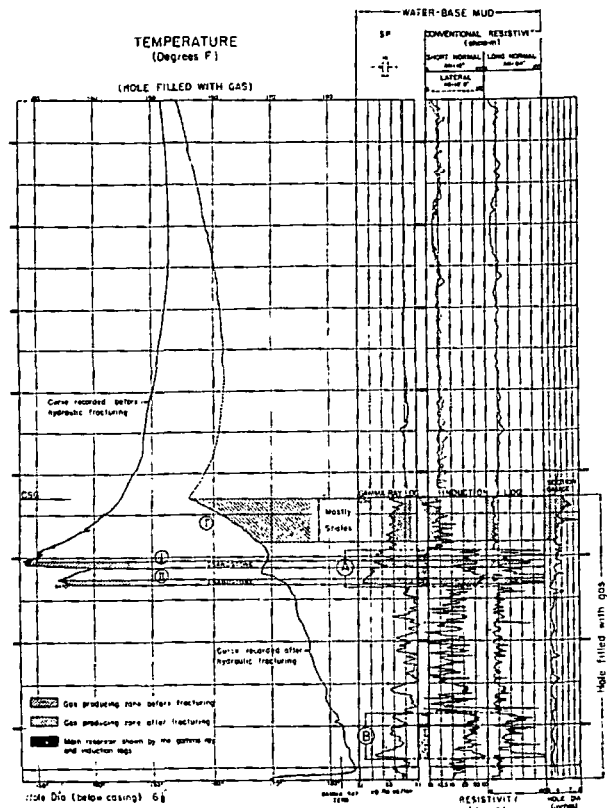
case of low permeability formations, may constitute the easiest way for the gas to flow into the borehole.

It is likely that the capacity of the interfaces to drain gas does exist in the natural conditions of production. It has been recognized, for example, that section B, before fracturing, usually produces more gas than section A, although the total thickness of reservoir rock is greater in A than in B. This comes from the fact that the beds in section B are on the average thinner and more numerous, and therefore, the interfaces are more frequent than in section A. This capacity of the interfaces is appreciably increased by the hydraulic fracturing, since apparently the interfaces constitute zones of least resistance.

It may be suggested, therefore, that the hydraulic fracturing in general, when operated throughout a large interval which includes other formations besides the reservoir rocks, may result in creating channels at depths which are not necessarily favorable for the most efficient drainage, as for example sand-shale interfaces located at a great distance from the reservoir rocks. It may thus be possible that the initial production obtained after fracturing, although very important, may not keep up because the fracturing operation has opened only some intervals with comparatively small reserves, whereas the main reservoirs may be essentially unaffected by the treatment.

GRAPHICAL CONSTRUCTION

The graphical construction used to determine L is certainly a convenient way to estimate the amount of



EXAMPLE 4 — TEMPERATURE SURVEYS IN GAS-PRODUCING WELL BEFORE AND AFTER HYDRAULIC FRACTURING SHOWING THE DISPLACEMENT OF THE MAIN PRODUCING ZONE FROM SANDSTONES I AND II TO THE OVERLYING SHALES I', SAN JUAN BASIN, N. MEX., 1954.

gas produced by each zone. It should be emphasized, however, that the accuracy of this procedure chiefly relies on the determination of the asymptotic line, which is not always obtained with enough precision. One difficulty in this respect is that the temperature logs usually are not recorded high enough above the upper producing zone.

Should the value of the geothermal gradient for the region under investigation be known, the value of L could be also obtained by tracing the geothermal gradient through the inversion point I . But here again, uncertainty will arise as to the location of the point I because of the small curvature of the log around its maximum.

Furthermore, the value of the coefficient C in formula $M = CL$ involves several factors which are not always sufficiently well defined.

The procedure described above cannot, therefore, be considered as applicable in all cases for a determination of the absolute production. It may nevertheless be valuable in assessing the relative productions of each of the zones producing at the same time, or to compare the productions before and after fracturing.

THEORETICAL DERIVATIONS

As stated above, the essential rules for the interpretation of the temperature log have been determined by mathematical analysis and confirmed by field experience.

The essential derivations are explained below.

BASIC COMPUTATIONS

Let z be the distance measured upward along the axis of the borehole from some convenient reference point, and $M(z)$ be the amount of gas flowing per unit time along the borehole. If $m(z)$ is the amount of gas produced per unit height and per unit time, then clearly

$$\frac{dM(z)}{dz} = m(z) \quad \dots \quad (1)$$

The following assumptions will be made:

1. There is sufficient turbulence in the flow of gas in the borehole that it is essentially homogeneous in temperature and pressure across any section of the borehole.
2. The gas is at the same temperature as the wall of the borehole.
3. Due to its expansion, the gas being produced has been cooled a certain amount δT below the temperature $T'(z)$ of the formation remote from the borehole. This amount, of course, will depend on the nature of the bed. Any effect on the cooling caused by changes in the borehole gas temperature T should be small and is neglected.
4. The effect of heat conduction in the formation parallel to the borehole may be ignored.
5. The pressure in the borehole is effectively atmospheric pressure.
6. Convection of heat in the formation may be neglected.

Consider a small length Δz of the borehole lying between z and $z + \Delta z$. The amount of gas entering this volume from below at a temperature $T(z)$ is $M(z)$ and the amount entering from the formation at a temperature $T'(z) - \delta T$ is $m(z) \Delta z$: see assumption 3. These two streams of gas are mixed together and leave the top of this element of volume at a temperature $T(z + \Delta z)$.

The heat absorbed by the first stream per unit time is

$$M(z) C_p [T(z + \Delta z) - T(z)] \quad \dots \quad (2)$$

While that for the second stream is

$$m(z) \Delta z C_p [T(z + \Delta z) - T'(z) + \delta T] \quad (3)$$

with C_p being the specific heat of the gas at constant pressure. The sum of these heats is assumed supplied by conduction of heat from the formation and is therefore given by the expression

$$(2\pi a \Delta z) K \left(\frac{\partial T}{\partial r} \right)_{r=a} \quad \dots \quad (4)$$

where

K : conductivity of the formation

a : radius of the borehole

$\left(\frac{\partial T}{\partial r} \right)_{r=a}$: radial component of the temperature gradient at the wall of the borehole.

It is convenient to write in place of Equation 4:

$$2\pi a \Delta z k [T'(z) - T(z)] \quad \dots \quad (5)$$

where

$$k = K \frac{\left(\frac{\partial T}{\partial r} \right)_{r=a}}{T'(z) - T(z)} \quad \dots \quad (6)$$

is a proportionality constant which, however, is dependent somewhat on the length of time the well has been flowing.

Equating the sum of the expressions in 2 and 3 to that in 5 and dividing by $C_p \Delta z$ one has:

$$M(z) \left[\frac{T(z + \Delta z) - T(z)}{\Delta z} \right] + m(z) [T(z + \Delta z) - T'(z) + \delta T] = \frac{2\pi a k}{C_p} [T'(z) - T(z)]$$

Letting Δz approach zero and rearranging terms, we have the differential equation:

$$M(z) \frac{dT}{dz} + \left[m(z) + \frac{2\pi a k}{C_p} \right] [T(z) - T'(z)] = -m\delta T \quad \dots \quad (7)$$

Since the temperature of the formation $T'(z)$ remote from the borehole may be assumed to be given by:

$$T'(z) = T'_0 - \frac{z}{g} \quad \dots \quad (8)$$

where T'_0 is the formation temperature at $z = 0$ and g is the geothermal gradient, one may write in place of Equation 7 the differential equation:

$$M(z) \frac{d}{dz} [T'(z) - T(z)] + \left[m(z) + \frac{2\pi a k}{C_p} \right] [T'(z) - T(z)] = m\delta T - \frac{M}{g} \quad \dots \quad (9)$$

CHARACTERISTICS OF THE CURVE AT THE LEVEL OF THE GAS PRODUCING ZONES

Assuming a uniform gas producing bed, $m(z)$ is a constant, which will be referred to as m , and if we take $z = 0$ at the bottom of the bed

$$M(z) = M_0 + mz \quad \dots \quad (10)$$

where M_0 is the quantity of gas coming from the beds below. The differential Equation 9 thus becomes

$$(z + e_1) \frac{d}{dz} [T'(z) - T(z)] + \alpha [T'(z) - T(z)] = \delta T - \frac{1}{g} (z + e_2) \quad \dots \quad (11)$$

where

$$e_0 = \frac{M_0}{m}$$

$$\alpha = 1 + \frac{2\pi ak}{m C_p} = 1 + \frac{C}{m} \quad (12)$$

A general solution of Equation 11 is seen to be:

$$T'(z) - T(z) = \frac{\delta T}{\alpha} - \frac{z + e_0}{g(1 + \alpha)} - \frac{B}{(z + e_0)^\alpha} \quad (13)$$

where B is an arbitrary constant. Assuming that the bed is sufficiently thin so that the change in $T'(z)$ across it can be neglected (this amounts to taking $\frac{1}{g} = 0$), one has:

$$T(z) = T'_0 - \frac{\delta T}{\alpha} + \frac{B}{(z + e_0)^\alpha} \quad (14)$$

Solving for B in term of the temperature T_0 at the bottom of bed, one then has:

$$T(z) = T'_0 - \frac{\delta T}{\alpha} + \left(\frac{z}{e_0} + 1\right)^{-\alpha} \left[T_0 - T'_0 + \frac{\delta T}{\alpha}\right] \quad (15)$$

When the producing zone is the closest to the bottom of the hole, there is no gas coming from below the bottom boundary; then $e_0 = 0$ and in Equation 15

$\left(\frac{z}{e_0} + 1\right)^{-\alpha}$ is also equal to zero.

Equation 15 reduces to:

$$T(z) = T'_0 + \frac{\delta T}{\alpha} \quad (16)$$

which shows that, if the producing formation is homogeneous, $T(z)$ is constant: in other words, the curve should exhibit a plateau.

For the bed above the bottom beds e_0 is no longer equal to zero, and Equations 14 and 15 show that the temperature decreases as z increases.

At the top of a gas producing bed, whether it be the bottom bed or not, the entry of the cool gas from the formation ceases and one has left only the warming due to conduction of heat from the formation. Thus the temperature of the gas will start to rise once the top of the bed is passed, and one has a very distinct indication of the upper and lower limits of a gas producing bed.

TEMPERATURE CURVE ABOVE A PRODUCING ZONE

We will now take $z = 0$ at the top of the bed.

Above a gas producing zone, $m(z)$ is zero and $M(z)$ is constant. The differential Equation 9 therefore becomes:

$$\frac{d}{dz}[T'(z) - T(z)] + \frac{2\pi ak}{M C_p}[T'(z) - T(z)] = -\frac{1}{g} \quad (17)$$

The general solution of this differential equation is seen to be:

$$T(z) = T'(z) + \frac{L}{g} - A e^{-\frac{z}{L}} \quad (18)$$

where A is an arbitrary constant and

$$L = \frac{M C_p}{2\pi ak} \quad (19)$$

The last term in Equation 18 becomes small as z becomes large and thus T approaches the asymptotic line shown in Fig. 2 whose temperature is given by

$$T'(z) + \frac{L}{g} = T'_0 - \frac{z - L}{g} \quad (20)$$

where T'_0 is the formation temperature at the depth of the top of the bed.

This line corresponds to a temperature L/g degrees greater than that of the geothermal gradient, T' . As seen from Equations 8 and 20, it represents the same temperature at z as that for the geothermal gradient T' at $z - L$. Thus it may be looked upon as a vertical displacement of L feet of the geothermal gradient in the direction of shallower depth (see Fig. 2).

This displacement L is equal to the sub-tangent DE at any point C of the curve above the producing zone.

It has been explained qualitatively in the section of this paper entitled "Temperature Curve above a Producing Zone" that the temperature log crosses the true geothermal gradient, at the inversion point I , which corresponds to a maximum of the temperature log. This feature can be proved as follows:

The maximum of the temperature log is obtained by differentiating $T(z)$, given by Equation 18, with respect to z and setting this derivative equal to zero. Thus z_1 , the value of z at the maximum, is found from the equation:

$$\frac{dT}{dz} = -\frac{1}{g} + \frac{A}{L} e^{-\frac{z}{L}} = 0 \quad (21)$$

or

$$z_1 = -L \ln \frac{L}{gA} \quad (22)$$

For this value of z from Equations 18 and 20:

$$T(z_1) = T'_0 - \frac{z_1}{g} + \frac{L}{g} - A e^{-\frac{z_1}{L}}$$

which by Equation 21 is

$$T(z_1) = T'_0 - \frac{z_1}{g} = T'(z_1) \quad (23)$$

Thus the gas temperature log crosses the geothermal gradient at this point.

DETERMINATION OF AMOUNT OF GAS PRODUCED

As shown by Equations 12 and 19 the amount of gas produced M is related to the length L of the sub-tangent, obtained as in Fig. 2, by the equation

$$M = CL \quad (24)$$

The magnitude of C is therefore seen to depend on the length of time the well had been flowing before the temperature log was run. This arises from the fact that the temperature gradient about the hole will decrease with time and less heat will be conducted to the gas for the same temperature difference $T' - T$.

According to Equations 6, 19 and 24, the constant C is given by

$$C = \frac{2\pi Ka}{C_p} \left[\left(\frac{\partial T}{\partial r} \right)_{r=r_1} \right] [T'(z) - T(z)] \quad (25)$$

For the computation of the second factor in Equation 25, we will consider the case where the temperatures T of the borehole and T' of the formation are independent of z .

The temperature $T(r)$ in the formation just outside the borehole should be very nearly logarithmic with r and given by

$$T(r) = T + (T'_0 - T) \frac{\log \frac{r}{r_1}}{\log 2} \quad (26)$$

where T_a is the temperature at $r = 2a$ and T is the temperature at the wall of the borehole. From this equation

$$\left(\frac{\partial T}{\partial r}\right)_{r=a} = \frac{T_a - T}{a \log 2} \dots \dots \dots (27)$$

which substituted in Equation 25 gives:

$$C = \frac{2 \pi K}{C_p \log 2} \frac{T_a - T}{T' - T} = 0.0626 \frac{T_a - T}{T' - T} \quad (28)$$

Here we have taken

$$K = 0.0041 \text{ calories/degree-cm}^*$$

$$C_p = 0.593 \text{ calories/degree-gm (methane).}$$

Changing the system of units so that M is measured in thousands of cubic feet per day and L is measured in feet, the expression for C becomes:

$$C = 8.17 \left[\frac{T_a - T}{T' - T} \right] \dots \dots \dots (29)$$

The ratio of temperatures $(T_a - T)/(T' - T)$ as a function of time was obtained numerically by using a finite difference approximation to the heat flow equation. The graph of C vs time as given in Fig. 3 then results.

CONCLUSIONS

A method for the investigation of gas producing wells has been described, which essentially involves the recording of detailed temperature logs by means of a special high speed thermometer, and wherein the radioactivity and Induction Logs constitute the auxiliary documents.

With this method, the temperature logs determine the exact location of the gas producing zones. In favorable cases, they also give an approximate estimation of the amount of gas produced by each separate zone. The other logs give an approximate delineation of the reservoir formations.

The application of the method has shown that the gas producing zones are not always located at the

same depths as the main reservoir formations, but rather within shaly intervals, which contain a great number of sand-shale interfaces. This tendency is emphasized after hydraulic fracturing.

It has also been observed that the gas very often does not enter the wells at the same depths before and after hydraulic fracturing.

On the basis of these observations, a tentative conclusion has been reached that the ways opened by hydraulic fracturing are not necessarily at the right place for the most efficient drainage.

A mathematical study has provided the basis for the interpretation of the temperature logs, by determining the characteristic shape and significant features of the temperature curve opposite and above a gas producing zone.

ACKNOWLEDGMENTS

The authors wish to acknowledge the cooperation of the El Paso Natural Gas Co. in the field tests, and particularly of R. E. Houser who provided data helpful in the interpretation of the logs. They are also indebted to M. Ferre' for his help in defining the theoretical aspects of the problem and to J. Bricaud for his valuable theoretical suggestions. They would also like to thank M. Martin for his efficient assistance in the preparation of the manuscript.

REFERENCES

1. Schlumberger, M., Doll, H. G., and Perebinossoff, A. A.: "Temperature Measurements in Oil Wells," presented at the 172nd Meeting of the Institute of Petroleum Technologists (Nov. 10, 1936).
2. Guyod, H.: "Temperature Well Logging," *Oil Weekly* (Oct. 21, 28; Nov. 4, 11; Dec. 2, 9 and 16, 1946).
3. Bird, J. M.: "Interpretation of Temperature Logs in Water and Gas System Wells and Gas Producing Wells," *Producers Monthly* (Aug. 1954) 18, No. 10.

*See first Footnote page 113.

★★★